New insights into the *in vivo* and *in vitro* functions of mammalian TOR complex 2

Inauguraldissertation

zur
Erlangung der Würde eines Doktors der Philosophie
vorgelegt der
Philosophisch-Naturwissenschaftlichen Fakultät
der Universität Basel

von

Nadine Cybulski

aus Andermatt (UR)

Basel, 2010

Genehmigt von der Philosophisch-Naturwissenschaftlichen Fakultät auf Antrag von Prof. Dr. Michael N. Hall *und* Prof. Dr. Markus A. Rüegg.

Basel, den 28. April 2009

Prof. Dr. Eberhard Parlow
Dekan

Table of Contents

Summary

Target of rapamycin (TOR) is the main controller of cell growth and metabolism in response to nutrients, growth factors and the cellular energy status. TOR is a serine/threonine kinase conserved from yeast to mammals and is found in two functionally and structurally distinct multi-protein complexes named TOR complex 1 (TORC1) and TORC2. Mammalian TORC1 (mTORC1) contains mTOR, mLST8, raptor and PRAS40, while mTORC2 contains mTOR, mLST8, rictor, mSin1, and PRR5. mTORC2 is activated in response to growth factors, such as insulin and insulin-like growth factor 1 (IGF1), and its main functions involve the regulation of actin cytoskeleton dynamics and phosphorylation of several AGC kinases in their hydrophobic motif. TORC1 is directly inhibited by the immunosuppressant and anti-cancer drug rapamycin, whereas TORC2 is not. Thus, use of rapamycin provides a simple and straightforward method to specifically study the TORC1 signaling branch. There is no known TORC2-specific inhibitor, so genetic manipulation is required to study its biological function(s).

This thesis describes new *in vivo* and *in vitro* functions of mTORC2. The first part deals with the *in vivo* function of mTORC2 in adipose tissue. The adipose tissue, in addition to its function as a long-term fat storage depot, also has endocrine functions, plays an important role in the regulation of whole body glucose and lipid metabolism and is one of the most insulin-responsive tissues in the body. To study mTORC2 function in adipose tissue, we have generated mice that lack the mTORC2-essential component rictor specifically in adipose tissue. Phenotypic characterization revealed the unexpected finding that these mice were larger due to an increase in lean tissue mass and that they had elevated serum IGF1 levels. Furthermore, the knockout mice were hyperinsulinemic, but glucose tolerant. Overall, these findings suggest an important role for adipose mTORC2 in controlling full body growth and whole body glucose metabolism.

The second part of this thesis describes a new *in vitro* function of mTORC2 in fibroblasts. We have taken advantage of the *raptor* and *rictor* floxed mice to isolate mouse embryonic fibroblasts (MEFs), which were then used to establish inducible *raptor* and *rictor* knockout MEF cell lines. After initial characterization of these two cell lines, a deeper analysis of the role of mTORC2 in the actin-mediated process of cell migration was performed. We have found that mTORC2 is required for cell migration and for regulating the activity of the Rho GTPases Rac1, Cdc42, and RhoA. We have extended this study by

showing that mTORC2-dependent cell migration is also required in oncogenic cells, which suggests that mTORC2 could have an important function in the development of cancer and metastasis.

Introduction

The TOR signaling pathway

Rapamycin is an antifungal metabolite that was initially isolated from soil samples from the Easter Island (locally known as Rapa Nui) in the 1970s and that was found to have inhibitory effects on cell proliferation of mammalian cells. Further studies led to the identification of the TOR (target of rapamycin) kinase in the budding yeast *Saccharomyces cerevisiae* (Heitman et al., 1991). Yeast cells bearing mutations in the *TOR* genes were resistant to rapamycin, which normally forms a complex with the peptidyl-prolyl *cis/trans* isomerase FKBP12 to bind to and inhibit the TOR kinase. TOR is a Ser/Thr kinase and is conserved in every eukaryote examined so far, including yeasts, algae, slime mold, plants, worms, flies and mammals (Wullschleger et al., 2006). Recently, TOR was also identified in the protozoan parasite *Trypanosoma brucei* (Barquilla et al., 2008). The main function of TOR is the regulation of cell growth, and its function is critical for a cell or organism since disruption of the gene is lethal in all eukaryotes (Kunz et al., 1993; Long et al., 2002; Menand et al., 2002; Oldham et al., 2000). For example, mice deficient for mammalian TOR (mTOR) die very early during embryonic development (Gangloff et al., 2004; Murakami et al., 2004). The importance of a functional TOR signaling pathway is further underscored by the high incidence of the TOR pathway being involved in human diseases. Dysfunctional TOR signaling is associated with many forms of cancer, and is linked to diseases such as tuberous sclerosis complex (TSC) or diabetes.

TOR is a central controller of cell growth and is regulated in response to nutrients, growth factors and cellular energy status. To fulfill its function within the cell TOR is found in two structurally and functionally distinct multiprotein complexes, TOR complex 1 (TORC1) and TORC2. In mammals, rapamycin-sensitive TORC1 (mTORC1) contains mTOR, mLST8, and its specific components raptor and PRAS40 (Fonseca et al., 2007; Hara et al., 2002; Kim et al., 2002; Kim et al., 2003a; Loewith et al., 2002; Oshiro et al., 2007; Sancak et al., 2007; Thedieck et al., 2007; Vander Haar et al., 2007; Wang et al., 2007). mTORC2 is rapamycin insensitive and contains mTOR, mLST8 and the specific components rictor, mSin1, and PRR5 (Frias et al., 2006; Jacinto et al., 2006; Jacinto et al., 2004; Pearce et al., 2007; Sarbassov et al., 2004; Thedieck et al., 2007; Woo et al., 2007; Yang et al., 2006).

In the following, TOR itself and the individual complexes, along with their upstream regulators and downstream substrates, will be described in more detail.

The TOR kinase

The TOR genes, *TOR1* and *TOR2*, were initially identified in the budding yeast *S. cerevisiae* (Heitman et al., 1991), where they share 67% primary sequence identity. While some yeasts and the protozoan parasite *T. brucei* have two *TOR* genes, higher eukaryotes only have a single TOR gene, but they all encode for a very large protein of ~ 280 kDa in size. The TOR proteins share high sequence homology among all eukaryotes and they belong to the same kinase family known as phosphatidylinositol kinase-related kinase (PIKK) family (Abraham, 2001; Keith and Schreiber, 1995). Although the TOR kinase domain resembles the catalytic domain of the lipid kinases phosphatidylinositol 3-kinases, TOR is a serine/threonine protein kinase and is the founding member of the PIKK family that includes the ATM, ATR, TOR, SMG-1, TRRAP and DNA-PK subfamilies of PIKKs (Abraham, 2004).

The TOR proteins are composed of numerous highly conserved domains (Figure I-1). The amino-terminal part contains a large stretch of tandem HEAT repeats. This motif is common among Huntingtin, Elongation factor 3, the A subunit of PP2A and TOR. The HEAT repeats are composed of 40-50 amino acids and form a structure of two tandem anti-parallel α-helices that are thought to mediate protein-protein interactions (Perry and Kleckner, 2003). Towards the carboxy-terminal domain the HEAT repeats are followed by a moderately conserved FAT (FRAP, ATM and TRRAP) domain, which is a shared domain of the PIKK family and is always found together with the highly conserved FATC (FAT C-terminus) domain at the very carboxy-terminal end of the protein. The FAT and FATC domains are believed to interact with each other to modulate kinase activity. Next to the FAT domain is the FRB (FKBP-Rapamycin Binding) domain that allows binding of the FKBP-rapamycin complex, thereby leading to allosteric inhibition of the kinase. The kinase domain of the protein lies next to the FRB domain. Furthermore, a repressor domain was identified in mTOR and comprises a region of 20 amino acids (2430-2450) located directly upstream of the FATC domain. Deletion of this region results in increased TOR kinase activity (Sekulic et al., 2000). This repressor domain also contains two phosphorylation sites: Thr2446 is phosphorylated by AMP-dependent kinase (AMPK) (Cheng et al., 2004) and Ser2448 is phosphorylated by the TOR substrate S6K1 (Chiang and Abraham, 2005; Holz and Blenis, 2005). However, the physiological meaning of these phosphorylation sites is not well understood. Additionally, an autophosphorylation site was identified at Ser2481, but the physiological relevance is also not well defined (Peterson et al., 2000). Only recently, it was suggested that this phosphorylation is specific to only one of the two complexes and resembles the kinase activity of the complex (Copp et al., 2009). A schematic summary of the various domains within the TOR kinase is depicted in Figure I-1.

The abundance of several putative protein-protein interaction domains clearly suggested that TOR might associate with many cellular proteins. This assumption was also supported by gel filtration experiments demonstrating that TOR consistently migrated in a 2 MDa complex (Kim et al., 2002; Loewith et al., 2002). These ideas led to the identification of several binding partners of TOR that were subsequently found to define the two functionally distinct multiprotein complexes, TOR complex 1 (TORC1) and TORC2. The complexes will be described in more detail in the next part.

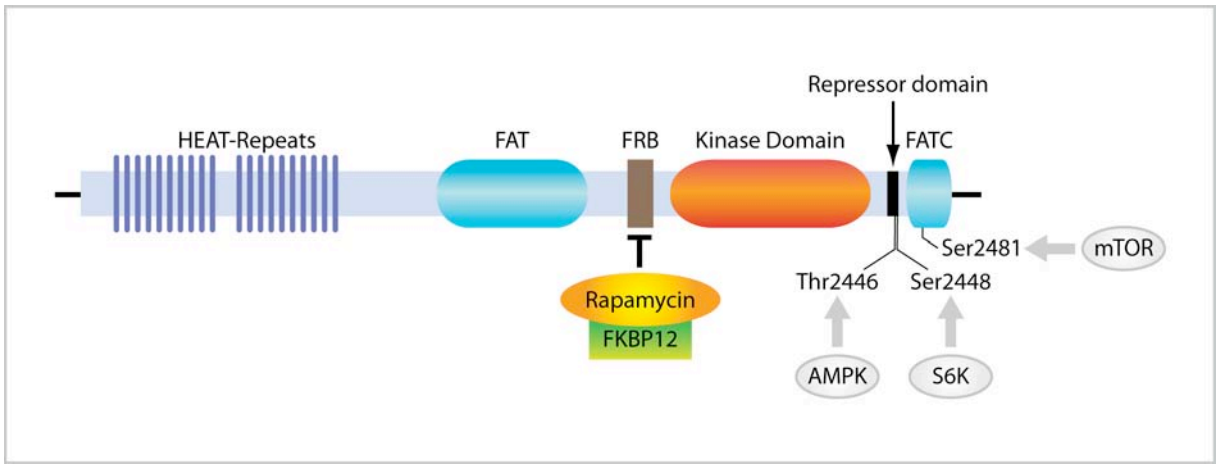

Figure I-1. Illustration of the domain structure of mammalian TOR.
For more details see text.

TOR complex 1

Composition and localization

In yeast, TORC1 is comprised of either TOR1 or TOR2, LST8 (lethal with sec thirteen), KOG1 (kontroller of growth), and TCO89 (89-kDa subunit of TOR complex one) (Loewith et al., 2002; Reinke et al., 2004). TCO89 is the only non-essential component of yeast TORC1 and no homologue was found in higher eukaryotes. Deletion of any other member of the complex is lethal in yeast (Heitman et al., 1991; Loewith et al., 2002). Interestingly, only when assembled with the TORC1 components, the FKBP12-rapamycin inhibitory complex can bind to the FRB domain and block the activity of TOR.

Mammalian TORC1 (mTORC1) consists of mTOR, mLST8 and the KOG1 homologue raptor (Hara et al., 2002; Kim et al., 2002; Kim et al., 2003a; Loewith et al., 2002). A full body knockout of any component of mTORC1 in mice results in early embryonic lethality (Gangloff et al., 2004; Guertin et al., 2006). mLST8 (previously also known as GβL) is a 36 kDa protein that consists entirely of seven WD40 repeats (about 40 amino acids with

conserved W and D forming four anti-parallel β strands) allowing protein-protein interaction (Kim et al., 2003a). The molecular function of mLST8 within mTORC1 is still ambiguous. Initial studies suggested that the constitutive binding of mLST8 to mTOR was important for the activity of mTORC1 (Kim et al., 2003a). However, more recent findings in mLST8$^{-/-}$ mouse embryonic fibroblasts (MEFs) revealed that mLST8 is dispensable for mTORC1 function (Guertin et al., 2006). Also, in *S. cerevisiae* no clear data could be obtained on the role of LST8 in regulating TORC1. raptor is a 150 kDa protein and contains a highly conserved amino-terminal region followed by three HEAT repeats and seven WD40 repeats. raptor is a positive regulator of mTOR activity and functions as a scaffold protein to couple mTOR to its substrates (Hara et al., 2002; Kim et al., 2003a; Schalm et al., 2003). Inhibition of mTORC1 by rapamycin results in the disruption of raptor binding to mTOR (Kim et al., 2002; Oshiro et al., 2004).

Despite several approaches in various labs, the localization of TORC1/mTORC1 within the cell is not clearly defined. However, a common finding of all studies in yeast suggests that TORC1 associates with membranes. Binding of TORC1 to the plasma membrane, vacuolar membrane and also endosomal membranes was demonstrated (Araki et al., 2005; Cardenas and Heitman, 1995; Chen and Kaiser, 2003; Kunz et al., 2000; Reinke et al., 2004; Sturgill et al., 2008; Wedaman et al., 2003), but the physiological significance of TORC1 association to distinct membranes is not understood, as well as the question whether TORC1 localization is a regulated and dynamic process. In mammalian cells the localization of mTOR to endomembranes is consistent with the findings in yeast. But mTOR localization also remains ambiguous as individual studies proposed different compartmental localization of mTOR, including mitochondrial, endoplasmic reticulum and Golgi apparatus membranes (Desai et al., 2002; Drenan et al., 2004). One study even suggests a nuclear localization of mTOR (Bachmann et al., 2006). Recently, new findings propose a regulated localization of mTOR to specific endomembranes upon activation by amino acids (Sancak et al., 2008).

Upstream regulators of mTORC1

mTORC1 integrates three major inputs to regulate catabolic and anabolic processes that collectively determine cell growth and metabolism. Growth factors (insulin/insulin-like growth factor) and nutrients (amino acids) activate mTORC1, while a low cellular energy status inhibits mTORC1 (also see Figure I-2).

Activation by insulin occurs via the well-established insulin/PI3K/Akt pathway. Insulin binding to its receptor activates a cascade of phosphorylation and recruitment events leading to the phosphorylation and activation of Akt (also known as PKB), which then can activate

mTORC1 via two pathways. The main pathway involves an inhibitory phosphorylation of the TSC1/TSC2 (tuberous sclerosis complex 1 and 2) complex, a GTPase activating protein (GAP) towards the Rheb GTPase (Garami et al., 2003; Inoki et al., 2003a; Inoki et al., 2002; Manning et al., 2002; Potter et al., 2002; Tee et al., 2003; Zhang et al., 2003). When the TSC1/TSC2 complex is inactive Rheb is in its active GTP-bound form and can directly bind and activate mTORC1 (Long et al., 2005a; Long et al., 2005b; Smith et al., 2005). However, the molecular mechanism of how Rheb activates mTORC1 is not clear. Akt can further activate mTORC1 by an inhibitory phosphorylation of the protein PRAS40 (Proline-rich Akt substrate) that otherwise binds raptor and thereby inhibits mTORC1 (Fonseca et al., 2007; Oshiro et al., 2007; Sancak et al., 2007; Thedieck et al., 2007; Vander Haar et al., 2007; Wang et al., 2007).

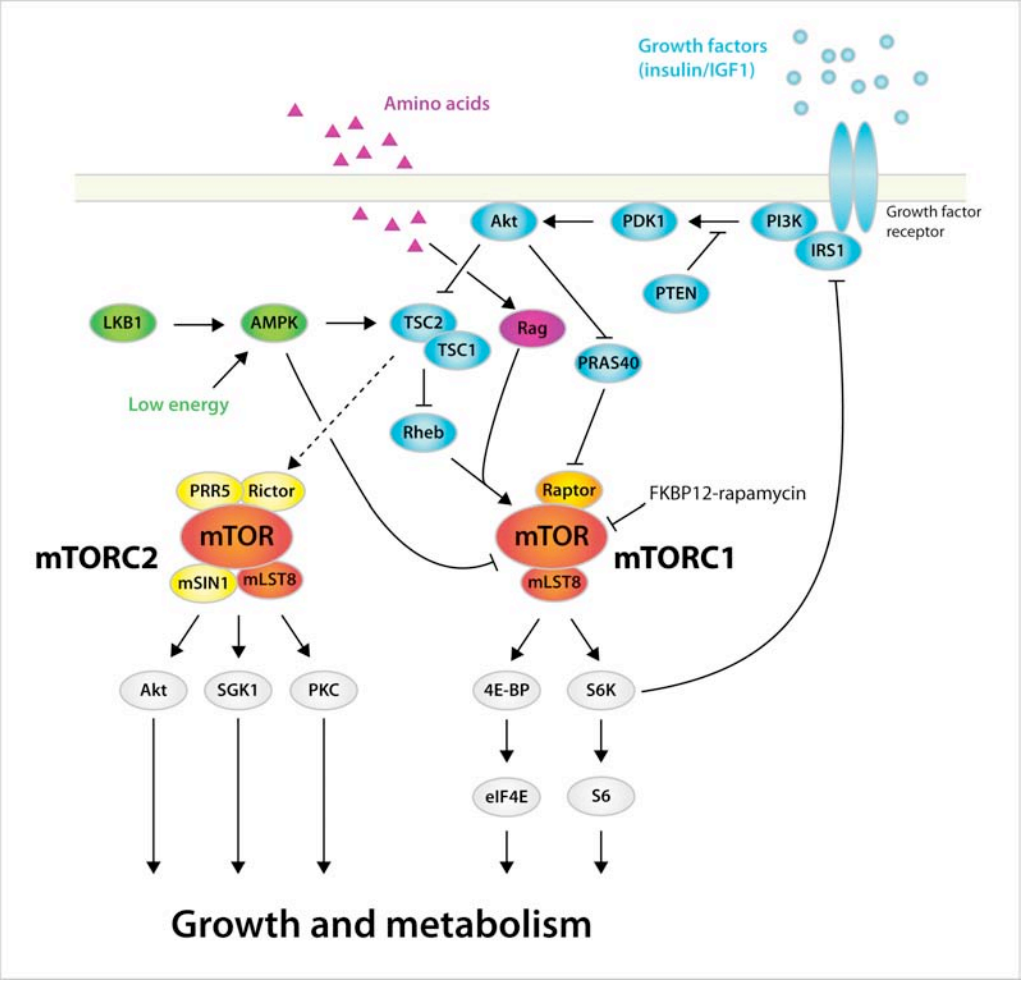

Figure I-2: Overview of the mTOR signaling pathway. *For more details see text.*

Regulation of mTORC1 by the cellular energy status also involves the TSC1/TSC2 complex. If energy levels (glucose availability) are low within the cell, the AMP/ATP ratio is increased and sensed by AMPK. AMP directly binds to and allosterically activates AMPK to allow full activation of AMPK by the tumor suppressor LKB1 (Shaw et al., 2004b). LKB1

phosphorylates and activates AMPK, which in turn phosphorylates TSC2 and activates the TSC1/TSC2 complex causing inhibition of mTORC1 (Corradetti et al., 2004; Inoki et al., 2003b; Shaw et al., 2004a). Overall, active AMPK turns on ATP-generating catabolic pathways, such as fatty acid oxidation and glycolysis, and shuts off ATP-consuming anabolic processes, such as translation and fatty acid synthesis.

The major nutritional input that regulates mTORC1 activity is the supply of amino acids. Amino acids, in particular leucine and arginine, are essential for mTORC1 activation, since insulin alone is not sufficient to activate mTORC1 (Hara et al., 1998). The molecular mechanism how amino acids activate mTORC1 is not fully understood, however, several studies investigated single steps of mTORC1 activation to narrow down the proteins involved in amino acid activation of mTORC1. In cells lacking either TSC1 or TSC2 the mTORC1 pathway remains sensitive to amino acid starvation, suggesting that amino acids activate mTORC1 downstream of the TSC1/TSC2 complex (Smith et al., 2005). Further studies suggested that amino acids regulate Rheb binding to mTORC1 (Long et al., 2005b). Only recently, a new regulator of the mTORC1 signaling branch was identified. The Rag proteins belong to the family of small GTPases and were shown to regulate mTORC1 activity in the presence of amino acids (Kim et al., 2008; Sancak et al., 2008). Amino acids increase the binding of active Rag to mTORC1 thereby promoting the intracellular localization of mTOR to the proximity of its activator Rheb. Overexpression of a constitutively active mutant of Rag rendered the mTORC1 branch insensitive to amino acids.

Several other studies proposed another mechanism how amino acids signal to mTORC1 independent of the TSC1/TSC2-Rheb-Rag branch and they include the positive mTORC1 regulators hVps34 (vacuolar protein sorting 34) (Byfield et al., 2005; Nobukuni et al., 2005), a class III PI3 kinase, and MAP4K3 (mitogen-activated protein kinase kinase kinase kinase 3) (Findlay et al., 2007).

Besides the three major inputs – nutrients, growth factors and cellular energy status – that regulate mTORC1 activity, additional pathways can influence mTORC1 signaling. These include positive regulation via the Wnt signaling pathway (Inoki et al., 2006), mitogenic activation by the lipid second messenger phosphatidic acid (PA) (Fang et al., 2003; Fang et al., 2001; Ha et al., 2006; Kam and Exton, 2004; Sun et al., 2008) and negative regulation via cellular stresses such as hypoxia through REDD1 and 2 (Regulated in Development and DNA Damage Response genes 1 and 2) (Brugarolas et al., 2004; DeYoung et al., 2008; Reiling and Hafen, 2004).

Downstream effectors of mTORC1

In mammals, mTORC1 regulates various cellular processes including ribosome biogenesis, translation, transcription, autophagy, and mitochondrial metabolism (Soulard and Hall, 2007). Despite influencing a broad range of cellular processes only two direct substrates for mTORC1 have been identified so far: S6K (p70 S6 kinase) and 4E-BP1 (eIF4E-binding protein 1, also known as PHAS-I) (Brunn et al., 1997; Burnett et al., 1998). Both proteins contain a TOS (TOR signaling) motif, a five amino acid sequence that allows binding of the substrates to raptor, and which is crucial for mTOR-dependent phosphorylation (Nojima et al., 2003; Schalm and Blenis, 2002; Schalm et al., 2003).

S6K belongs to the family of AGC kinases (protein kinases A, G and C) and once activated phosphorylates the ribosomal protein S6 to activate translation. S6K contains several mTOR phosphorylation sites, but the main site required for S6K activation is Thr389, which is located in the hydrophobic motif (Pearson et al., 1995). Phosphorylation in the hydrophobic motif is required for interaction of S6K with phosphoinostide-dependent kinase 1 (PDK1) and subsequent phosphorylation and full activation by PDK1 at Thr229 in the activation loop (Alessi et al., 1998; Pullen et al., 1998). The hydrophobic motif and the activation loop, along with the mode of activation, are common to all AGC kinases. Several other rapamycin-sensitive phosphorylation sites in S6K were also described (Isotani et al., 1999; Pearson et al., 1995; Saitoh et al., 2002).

In addition to being a downstream effector of mTORC1 signaling S6K also has an important regulatory function on the upstream insulin signaling pathway, which is defined as the negative feedback loop. Upon activation of mTORC1, activated S6K phosphorylates IRS1 at multiple inhibitory sites thereby promoting degradation of IRS (Harrington et al., 2004; Haruta et al., 2000; Shah et al., 2004; Tremblay et al., 2007; Ueno et al., 2005; Um et al., 2004). As a consequence, further Akt signaling by insulin is attenuated and cells are in an insulin-resistant state.

4E-BP1 is a small protein (12 kDa) and negatively regulates translation initiation. Hypophosphorylated 4E-BP1 binds to and sequesters eIF4E (eukaryotic initiation factor 4E). mTORC1 phosphorylates 4E-BP1 at multiple sites and thereby causes the dissociation from eIF4E (Gingras et al., 1999; Gingras et al., 2001; Mothe-Satney et al., 2000). Upon release from 4E-BP1, eIF4E recruits additional factors, which will finally result in the assembly of the small ribosomal subunit and the recruitment to the mRNA to initiate translation.

Overall, upon activation mTORC1 positively regulates translation initiation via activating phosphorylation of S6K and inhibitory phosphorylation of 4E-BP1.

TOR complex 2

The following part on TOR complex 2 is part of a manuscript prepared for an invited review for publication in TiBS (Trends in Biological Sciences). It covers the major findings on TOR complex 2 in budding yeast, fission yeast, slime mold, worm, flies and mammals.

TORC2 in budding yeast

TOR was initially identified in the budding yeast *Saccharomyces cerevisiae,* in a genetic selection for spontaneous rapamycin resistant mutants (Heitman et al., 1991). In contrast to other eukaryotes, yeast (budding and fission yeast) contains two TOR genes, *TOR1* and *TOR2*. The existence of two TORs in yeast facilitated the study of TOR signaling as it initially helped to identify two separate TOR signaling branches. Biochemical studies later demonstrated the existence of two functionally distinct TOR complexes that correspond to and thereby confirm the two previously identified branches. Whereas rapamycin-sensitive TORC1 contains either TOR1 or TOR2, rapamycin-insensitive TORC2 contains only TOR2 of the two TORs. TORC2 consists also of AVO1, AVO2, AVO3, LST8 and BIT61 (Loewith et al., 2002; Reinke et al., 2004) (Figure I-3a). AVO1, AVO3 and LST8 are essential, conserved proteins required for kinase activity. In contrast, AVO2 and BIT61 are not essential, and no clear homologous counterparts have been identified so far in higher eukaryotes, although BIT61 and the mammalian TORC2 (mTORC2) component proline-rich protein 5 (PRR5) share low sequence similarity (Hayashi et al., 2007; Woo et al., 2007). Studies investigating the molecular organization of TORC2 in yeast revealed that TORC2 is oligomeric, likely a TORC2-TORC2 dimer (Wullschleger et al., 2005).

Even before the two TOR complexes were identified, TOR2, but not TOR1, was known to regulate the cell cycle-dependent polarization of the actin cytoskeleton (Schmidt et al., 1996), thereby implicating TOR2, and hence later on TORC2, in the spatial control of yeast cell growth. Further studies showed that the aberrant depolarization of the actin cytoskeleton in TORC2 temperature sensitive mutants could be suppressed by hyperactivation of the cell wall integrity pathway, which involves Protein Kinase C1 (PKC1). In fact, several genetic studies revealed that PKC1, via the Rho-like GTPases RHO1 and RHO2 and their GDP/GTP exchange factor ROM2, mediates TORC2 signaling to actin organization (Bickle et al., 1998; Helliwell et al., 1998a; Helliwell et al., 1998b; Loewith et al., 2002; Schmidt et al., 1997). However, further molecular details on the activation of this pathway required the identification of TORC2 substrates. In 2005, Kamada et al. identified the first yeast TORC2 substrate, Yeast Protein Kinase 2 (YPK2) (Kamada et al., 2005).

YPK2 is an AGC kinase and closely related to mammalian serum and glucocorticoid induced protein kinase-1 (SGK1). TORC2 activates YPK2 by directly phosphorylating Ser641 and Thr659 in the turn and hydophobic motifs, respectively (Figure I-3a). Recent results showed that TORC2 activity is also required for the phosphorylation of the turn motif in PKC1 (Facchinetti et al., 2008), although it is unclear whether TORC2 phosphorylates PKC1 directly. In addition to YPK2, Slm proteins, which bind phosphatidylinositol-4,5-bisphosphate (PIP2), have been characterized as direct TORC2 substrates. Slm1 and Slm2 can regulate actin organization independently of YPK2 (Fadri et al., 2005). However, a constitutively active mutant of YPK2 suppresses the lethality provoked by the complete loss of TORC2 (Kamada et al., 2005), suggesting that YPK2 is the main TORC2 effector. Most TORC2 mediated functions, including actin remodeling, are now believed to be mediated via YPK2.

Aronova et al. (Aronova et al., 2008) recently described a new function for TORC2. They showed that TORC2, via YPK2, controls the sphingolipid biosynthetic pathway and hence mediates *de novo* ceramide biosynthesis. Other studies have shown that YPK2 and its homologue YPK1 are also involved in regulating eisosome assembly and turnover in a sphingolipid-dependent manner (Luo et al., 2008). Eisosomes are protein complexes near the plasma membrane involved in the early steps of endocytosis. Whether TORC2 is also directly involved in the regulation of endocytosis remains to be confirmed. Interestingly, GFP-tagged TOR2 localizes to punctate structures in the proximity of the plasma membrane, which resemble eisosomes (Sturgill et al., 2008).

Thus, the downstream effectors and functions of TORC2 in *S. cerevisiae* are coming into focus, the upstream regulators of TORC2 remain completely unknown.

TORC2 in fission yeast

Schizosaccharomyces pombe, like *S. cerevisiae*, has two TOR homologues, Tor1 and Tor2. However, and this easily leads to confusion, fission and budding yeast TOR proteins are numbered in the opposite way, as the *S. pombe* proteins were named based on order of discovery rather than based on function. Budding yeast TOR2 is the sole TOR protein found in TORC2, whereas in fission yeast Tor1 is the main determinant of TORC2 (Matsuo et al., 2007), suggesting that *S. pombe* Tor1 is functionally equivalent to *S. cerevisiae* TOR2. *S. pombe* TORC2 is composed of Tor1, Sin1, Ste20, Wat1 (also known as Pop3) and Bit61 (Figure I-3b). *S. pombe* Tor1 is not essential for normal growth but is required for survival under stress conditions, proper G1 arrest, and sexual development (Kawai et al., 2001; Weisman and Choder, 2001). Surprisingly, in contrast to other organisms, rapamycin has no effect on normal growth in *S. pombe*. Initially, rapamycin was found to affect sexual development; later experiments showed that Tor1-mediated amino acid uptake in fission

yeast is also rapamycin sensitive (Weisman et al., 1997; Weisman et al., 2001; Weisman et al., 2005). As rapamycin blocks Tor1-mediated functions, it was believed that rapamycin in fission yeast inhibits TORC2 function. However, Petersen and Nurse recently showed that rapamycin can also inhibit Tor2, and hence TORC1, but in a nutrient-dependent manner (Petersen and Nurse, 2007). Currently, it remains unclear why rapamycin does not arrest fission yeast growth as in other eukaryotes. Furthermore, the molecular details on how rapamycin inhibits TORC2 and possibly TORC1 are not well understood.

To identify potential substrates of fission yeast Tor1, Matsuo et al. performed a high-copy suppressor screen of a *Tor1* sterility mutant and isolated Gad8 as a potential candidate (Matsuo et al., 2003). Gad8 is a Ser/Thr kinase belonging to the AGC kinase family and is the fission yeast homologue of YPK2 in budding yeast and SGK1 in other organisms. Matsuo et al. demonstrated that the activity and phosphorylation status of Gad8 depend on Tor1 activity. On a molecular level, they showed that the critical Tor1 phosphorylation sites in Gad8 are Ser527 and Ser546, the turn and hydrophobic motif sites, respectively (Figure I-3b). These findings contributed very early to the idea that TOR complexes regulate many AGC kinases.

TORC2 in Dictyostelium

Dictyostelium discoideum is a powerful model organism to study mechanisms of cell movement and chemotaxis. This slime mold is a unicellular eukaryotic organism that, upon starvation, forms multicellular aggregates. This developmental program depends on chemotaxis toward a high extracellular level of cyclic AMP secreted by neighboring cells. Lee et al. showed that the underlying mechanism of cell movement and aggregate formation depends on TORC2 (Lee et al., 2005). TORC2 in *D. discoideum* comprises Tor, Lst8, Rip3 (AVO1 in *S. cerevisiae*) and Pia (AVO3 in *S. cerevisiae*) (Figure I-3c), and cells deficient for any of these components lose speed, cell polarity and directionality, i.e., they display an overall defect in chemotaxis. Furthermore, Lee et al. demonstrated that cells lacking any TORC2 component exhibit reduced PKBA and PKBR1 activity, two Akt (also known as protein kinase B) homologues and AGC kinase family members that are required to fully activate the chemotactic response.

Chemoattractant signaling triggers several cellular responses. One well characterized response is the production of phosphatidylinositol 3,4,5-triphosphate (PIP3) at the leading edge of motile cells. It is well established that PIP3 production is an important step in regulating chemotaxis; however, chemotaxis still occurs in the absence of PIP3 (Chen et al., 2003; Hoeller and Kay, 2007), and a recent study provided insight on the molecular pathway regulating PIP3-independent chemotaxis. Kamimura et al. (Kamimura et al., 2008)

showed that TORC2 is activated in a PIP3-independent manner by a heterotrimeric G protein and by cytosolic Ras GTPases. This signaling leads to activation of the PKBs, mainly PKBR1, which in turn phosphorylate several downstream targets to ultimately regulate directed cell movement. These findings suggest a possibly direct regulation of TORC2 by Ras. This idea is further supported by the presence of a Ras-binding domain in Rip3 (Ras-interacting protein-3), the mSin1 homologue in *D. discoideum*, which, when mutated, causes an impaired chemotactic response (Lee et al., 2005). Kamimura et al. also confirmed that TORC2 activity is required to phosphorylate the hydrophobic motif in PKBA and PKBR1 and thus to activate these AGC kinases (Lee et al., 2005). Overall, these studies in *D. discoideum* underscore the importance of TORC2 in actin remodeling and cell movement, and could provide insight on the role of TORC2 in actin organization in other organisms. *D. discoideum* might also be a particularly valuable system for unraveling the upstream regulation of TORC2. So far, only very little is known about the upstream regulation of TORC2 in other organisms, and it would be of interest to know whether Ras-mediated activation of TORC2 is conserved in other organisms.

TORC2 in worms and flies

Recently, two independent studies have demonstrated that TORC2 is also present in the nematode *Caenorhabditis elegans* (Jones et al., 2009; Soukas et al., 2009). Both studies identified *CeRictor* in a screen for mutants with altered lipid storage and showed that loss-of-function mutants in *CeRictor* are viable, but developmentally delayed with a reduced overall body size (Figure I-3d). Increased fat storage in the mutant worms suggests an important role for TORC2 in regulating fat metabolism. Interestingly, an *sgk1* null mutant, but not a mutant with impaired AKT signaling, phenocopies a *CeRictor* mutant, and a constitutively active SGK1 suppresses a *CeRictor* mutation. Thus, TORC2 in worms appears to signal mainly through SGK1. This, combined with findings in yeast suggesting that the SGK1 homolog YPK2 is the main TORC2 effector, lends doubt to whether Akt is the primary effector of TORC2 in other eukaryotes. Loss of mTORC2 in mammals has only little effect on Akt activity (see below).

Similar to TORC2 mutants in worms, *rictor* and *sin1* mutants of the fly *Drosophila melanogaster* are viable, but reduced in body size (Hietakangas and Cohen, 2007; Lee and Chung, 2007). Also in flies, TORC2 is the main kinase phosphorylating Akt at the hydrophobic motif (Figure I-3e). Although loss of TORC2 normally causes only a mild growth

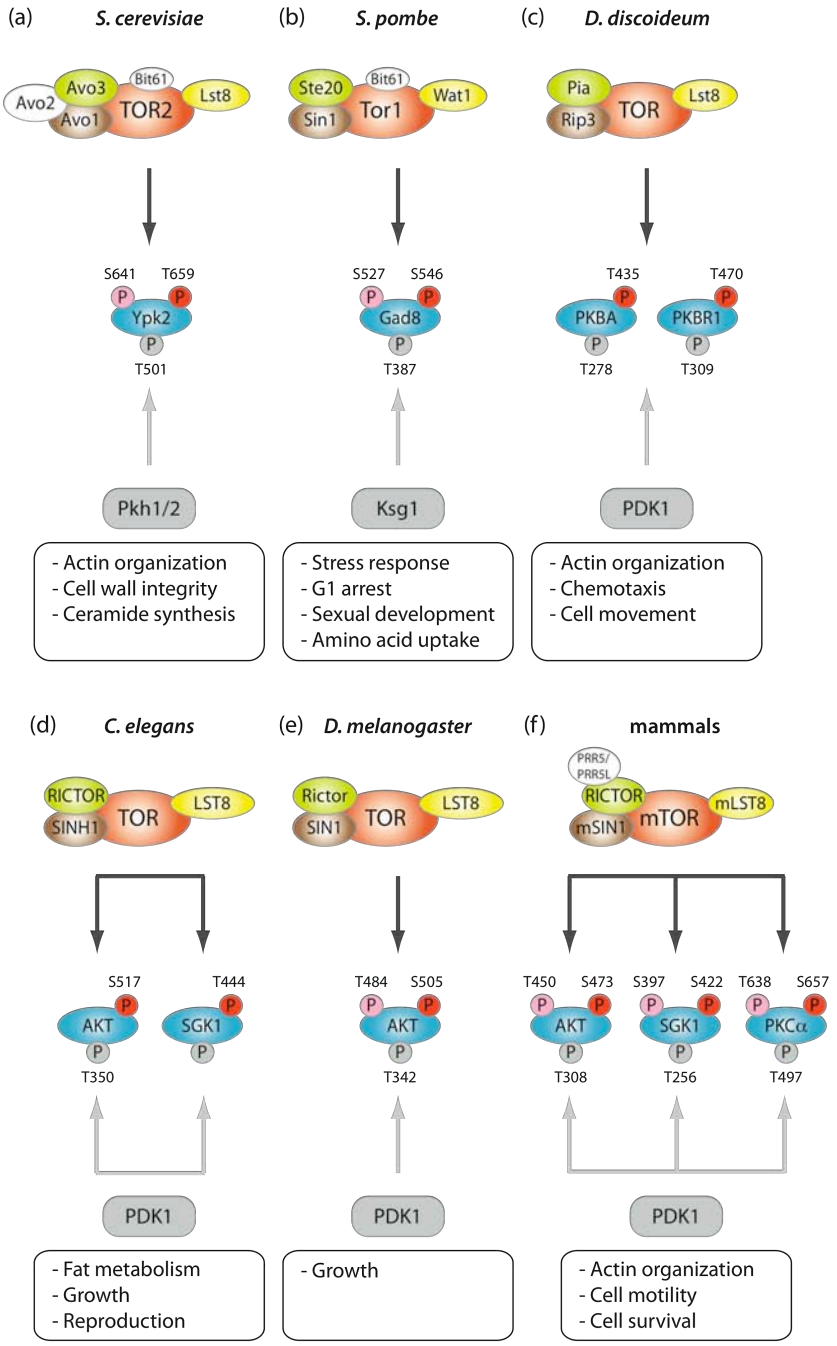

Figure I-3: The conserved TORC2 pathway. *TORC2 structure and function are conserved in (a) budding yeast (S. cerevisiae), (b) fission yeast (S. pombe), (c) slime mold (D. discoideum), (d) worms (C. elegans), (e) flies (D. melanogaster) and (f) mammals. In all organisms, TORC2 is composed of the TOR kinase (orange), LST8 (yellow), AVO3 or its homologue (green), and AVO1 or its homologue (brown). In S. cerevisiae, S. pombe and mammals, additional TORC2 components were identified (white). All shown TORC2 substrates (blue) are members of the AGC kinase family. The AGC kinases share a conserved mode of regulation involving phosphorylation of their hydrophobic motif (red), turn motif (pink), and activation loop (gray). TORC2 phosphorylates the hydrophobic motif in all shown kinases. TORC2 has so far been shown to phosphorylate the turn motif, directly or indirectly, in YPK2, Gad8, and mammalian Akt and PKCα. PDK1, which is also conserved in all organisms shown, phosphorylates the activation loop.*

defect in flies, Hietakangas and Cohen (Hietakangas and Cohen, 2007; Lee and Chung, 2007) made the interesting observation that loss of TORC2 strongly inhibits hyperplasia caused by elevated phosphatidylinositol-3-kinase (PI3K) signaling, suggesting that TORC2-regulated Akt activity might be more important in conditions of elevated Akt signaling.

TORC2 in mammals

Mammalian TORC2 was identified in 2004. At that time, TORC2 was known to consist of mTOR, mLST8 and the TORC2-specific component rictor (Jacinto et al., 2004; Sarbassov et al., 2004). More recently, two additional complex-specific components were identified - the AVO1 homologue mSin1 (Frias et al., 2006; Jacinto et al., 2006; Yang et al., 2006), and the BIT61 family members PRR5 and PRR5L (also known as Protor1 and Protor2) (Pearce et al., 2007; Thedieck et al., 2007; Woo et al., 2007). Except for PRR5 and PRR5L, all mTORC2 components are essential and knockout of any one of them in mice results in developmentally delayed embryos that die in midgestation around embryonic day E10.5 (Guertin et al., 2006; Jacinto et al., 2006; Shiota et al., 2006; Yang et al., 2006).

Similar to TORC2 in *S. cerevisiae*, mTORC2 cannot be directly inhibited by rapamycin. However, in a few cell lines, prolonged rapamycin treatment can inhibit mTORC2 activity indirectly (Sarbassov et al., 2006). In their study, Sarbassov et al. showed that long-term rapamycin treatment prevents *de novo* mTORC2 assembly and thereby inhibits mTORC2 activity, but only in a few of the many cell lines examined. The effect of rapamycin on mTORC2 assembly appears to be due to rapamycin binding free mTOR and to an indirect consequence of rapamycin's inhibition of protein synthesis and thus the synthesis of new mTOR.

A recent study by Copp et al. (Copp et al., 2009) showed that mTOR is phosphorylated in an mTORC-specific manner. mTOR phosphorylation at Ser2448 is predominantly, but not exclusively, associated with mTORC1 whereas mTOR in mTORC2 is specifically phosphorylated at Ser2481. Copp et al. suggest that the mTORC2 specific phosphorylation at Ser2481 could be used as a biomarker for mTORC2 sensitivity to rapamycin. However, to date, the functional importance of these phosphorylation sites is completely unknown, and it is important to point out that these sites should always be used along with other complex-specific readouts to definitively specify complex activation.

The first function ascribed to mTORC2, based on the previously known function of TORC2 in yeast, is the regulation of the actin cytoskeleton. Knockdown of mTORC2-specific components in cultured cells results in alteration of the actin cytoskeleton. Furthermore, also as in yeast, it was suggested that mTORC2 signals to the actin cytoskeleton via

RhoGTPases and PKC (Jacinto et al., 2004; Sarbassov et al., 2004). However, while two research groups have independently observed an altered actin cytoskeleton upon knockdown of mTORC2-specific components, opposite phenotypes were observed. Jacinto et al. observed that mTORC2 is required for cell spreading and actin fiber assembly. In contrast, the findings by Sarbassov et al. suggest that loss of mTORC2 promotes actin fiber assembly. More recently, a role for mTORC2 in regulating the actin cytoskeleton was questioned when no obvious alterations in the actin cytoskeleton were observed in embryonic fibroblasts derived from *rictor* knockout mice (Guertin et al., 2006; Shiota et al., 2006). The apparent discrepancies on mTORC2-mediated actin regulation could possibly be related to the different systems studied. The early knockdown studies looked at actin changes immediately after loss of mTORC2, but used different cell lines, whereas the subsequent studies looked at knockout cells permanently deficient for mTORC2. One possible explanation could be that cells constitutively lacking mTORC2 might adapt by using other mechanisms to regulate actin cytoskeletal organization. Several other studies using different approaches have supported a role for mTORC2 in actin-regulated processes. Misregulated mTORC2 activity results in altered cell motility in various cell types, including different cancer cells where migration plays an important role in metastasis (Dada et al., 2008; Liu et al., 2006; Masri et al., 2007). Overall, the molecular mechanism by which mTORC2 regulates the actin cytoskeleton remains unclear.

In 2005, the first direct substrate of mTORC2, Akt, was identified. mTORC2 was found to be a long sought-after kinase phosphorylating Ser473 in the hydrophobic motif of Akt (Figure I-3f) (Hresko and Mueckler, 2005; Sarbassov et al., 2005). Although earlier knockdown studies of rictor showed decreased phosphorylation also of Thr308 in the activation loop, further studies in knockout mice suggested that phosphorylation of Thr308, by phosphoinositide-dependent kinase 1 (PDK1), does not depend on prior Ser473 phosphorylation (Frias et al., 2006; Guertin et al., 2006; Jacinto et al., 2006; Shiota et al., 2006). The independent phosphorylation of Thr308 and Ser473 contrasts with the hierarchical phosphorylation of Thr229 and Thr389 in S6K; phosphorylation by mTORC1 (Thr389) is required for subsequent phosphorylation by PDK1 (Thr229) (reviewed in (Mora et al., 2004)). Furthermore, rather than being inactive, Akt without Ser473 phosphorylation appears to remain largely active as determined by the phosphorylation state of the Akt substrates glycogen synthase kinase 3 (GSK3), Tuberous Sclerosis Complex protein 2 (TSC2), Bad and the forkhead class O transcription factors 1/3a (FoxO1/3a). Only FoxO1/3a and possibly Bad show decreased phosphorylation upon loss of Ser473 phosphorylation (Guertin et al., 2006; Jacinto et al., 2006; Yang et al., 2006). Thus, mTORC2-mediated Akt phosphorylation does not seem to determine absolute activity, but rather appears to

determine substrate specificity. It is also possible that under conditions of low Akt activity, some Akt substrates can be phosphorylated by another kinase. For example, under conditions of insulin resistance when Akt is no longer active, GSK3 is phosphorylated by S6K (Zhang et al., 2006). Furthermore, it has been shown that FoxO can also be phosphorylated by SGK1 (Brunet et al., 2001), another mTORC2 substrate, providing a possible explanation for why cells with reduced mTORC2 activity show reduced FoxO phosphorylation but not reduced GSK3 phosphorylation.

Following the identification of Akt as an mTORC2 substrate, other AGC kinases were identified as additional substrates. In particular, many groups focused on the phosphorylation of PKC. Sarbassov et al. showed that PKCα phosphorylation (at the hydrophobic motif) and activity depend on mTORC2 (Sarbassov et al., 2004). However, this study suggested that the control of PKCα by mTORC2 is indirect. Ikenoue et al. (Ikenoue et al., 2008) and Facchinetti et al. (Facchinetti et al., 2008) later showed that mTORC2 is required for phosphorylation of all conventional PKCs and the novel PKCε at their hydrophobic motif and, in addition, at their turn motif, thereby controlling post-translational processing and stability of PKC (Figure I-3f). Loss of mTORC2 activity results in a reduction in total protein levels of PKC. Ikenoue et al. and Facchinetti et al., also showed that mTORC2 directly phosphorylates the turn motif in Akt. Interestingly, only phosphorylation of the hydrophobic motif, but not the turn motif, of PKC and Akt occurs in a growth-factor dependent manner. Overall, whether mTORC2 is the direct kinase of PKC remains an open question, as no study to date has been able to demonstrate direct *in vitro* phosphorylation of either site on any PKC isoform by mTORC2. Furthermore, it remains unclear how strongly mTORC2 activity influences PKC-mediated signaling events.

As discussed above, YPK2 and Gad8 were identified early on as TORC2 substrates, in budding and fission yeast, respectively. Both AGC kinases have close homology to the mammalian SGK kinase family. However, SGK1 was identified in mammals as an mTORC2 substrate only very recently (Garcia-Martinez and Alessi, 2008). mTORC2 phosphorylates SGK1 at its hydrophobic motif site (Figure I-3f) and thereby regulates SGK1's activity toward its physiological substrate n-myc downstream regulated 1 (NDRG1). Given the very modest reduction in Akt activity upon loss of mTORC2, as discussed above, is Akt a major mTORC2 effector? Studies in both yeast and worms suggest that SGK is the main TORC2 effector in these organisms. Whether SGK1 is also the most important physiological substrate of TORC2 in mammals is not clear. SGK1-SGK3 double knockout (DKO) mice have a mild phenotype, including a defect in renal function that does not affect embryonic development (Grahammer et al., 2006). In contrast, Akt1-Akt2 DKO mice and Akt1-Akt3 DKO mice are

impaired in development, and the latter display a phenotype similar to that of rictor knockout mice (Guertin et al., 2006; Peng et al., 2003; Shiota et al., 2006; Yang et al., 2005). Furthermore, loss of either rictor (Guertin et al., 2009) or Akt1 (Chen et al., 2006) suppresses the development of prostate neoplasia in *Pten* (phosphatase and tensin homolg) deficient mice. These findings are similar to those in *D. melanogaster* where tissue hyperplasia and increased Akt activity induced by *Pten* loss are reduced upon loss of rictor. Curiously, loss of rictor in the *Pten* prostate cancer mouse model reduces Akt phosphorylation at both Thr308 and Ser473. Overall, Akt still seems to be an important mTORC2 effector, at least upon enhanced signalling through the PI3K pathway.

While the processes downstream of TORC2 are coming into focus, knowledge on TORC2's upstream regulators is almost completely lacking. In yeast, absolutely nothing is known about extracellular or intracellular signals controlling TORC2. In mammalian cells, mTORC2 phosphorylates Akt upon serum stimulation, in particular growth factors such as insulin and insulin-like growth factor 1 (IGF1), suggesting that mTORC2 is regulated by the PI3K pathway (Frias et al., 2006; Ikenoue et al., 2008; Jacinto et al., 2006; Yang et al., 2006). This observation alone does not indicate that intrinsic mTORC2 kinase activity is stimulated by the PI3K pathway. Activation of PI3K leads to the production of phosphatidylinositol 3,4,5 trisphosphate (PIP3) and recruitment of Akt to the plasma membrane where it is phosphorylated by PDK1 and a possibly constitutively active, membrane-bound mTORC2. Thus, mTORC2 could be constitutively active and its regulated phosphorylation of Akt is controlled at the level of Akt localization. However, arguing against this possibility and in favor of a model in which the PI3K pathway stimulates intrinsic mTORC2 kinase activity are the observations that mTORC2-dependent mTOR autophosphorylation at Ser2481 (Copp et al., 2009) and *in vitro* mTORC2 activity are stimulated by growth factors (Frias et al., 2006; Yang et al., 2006). Furthermore, mTORC2 appears to phosphorylate SGK1 in response to growth factors even though SGK1 lacks a PH domain and is activated independently of membrane recruitment. Taken together, these latter findings suggest that growth factors, via the PI3K pathway, stimulate intrinsic mTORC2 kinase activity.

How might growth factors activate mTORC2 kinase activity? Despite several indications that growth factors stimulate mTORC2 activity, it remains a mystery how the growth factor signal is relayed within the cell to activate mTORC2. A recent report suggests that growth factors could signal to mTORC2 via the TSC1-TSC2 complex (a complex of the two tuberous sclerosis complex proteins 1 and 2). Huang et al. (Huang et al., 2008) have proposed that the TSC1-TSC2 complex, a GTPase activating protein (GAP) that lies upstream of and negatively regulates mTORC1, also regulates mTORC2 function by binding directly to mTORC2. In contrast to the negative regulation of mTORC1 by TSC1-TSC2,

TSC1-TSC2 is proposed to positively regulate mTORC2 activity in a GAP-independent manner. The GTPase Rheb, which lies directly downstream of TSC1-TSC2 and activates mTORC1 (Manning and Cantley, 2003), does not appear to lie upstream of mTORC2. The observation that TSC1-TSC2 GAP-activity is not required for mTORC2 activation suggests that the mechanism is not via mTORC1 and the negative feedback loop, which is a hallmark of activated mTORC1 signaling. The mTORC1 substrate S6K directly phosphorylates insulin receptor substrate (IRS) thereby promoting degradation of IRS (Tremblay et al., 2007). As a consequence, further Akt signaling by insulin is attenuated and cells are in an insulin-resistant state. Indeed, Huang et al. argue that TSC-mediated activation of mTORC2 is not via the negative feedback loop. The way in which TSC1-TSC2 binding to mTORC2 regulates mTORC2 activity as well as potential GAP-independent activities for TSC1-TSC2 remain poorly understood.

Is mTORC2 found at the plasma membrane and is mTORC2 localization regulated? In the *Pten* prostate cancer mouse model, where PI3K signaling is increased, rictor and Ser473-phosphorylated Akt are enriched at the plasma membrane. Furthermore, Partovian et al. (Partovian et al., 2008) demonstrated that a Syndecan-4 deficiency reduces mTORC2 localization to detergent-insoluble membrane fractions (rafts) in endothelial cells. Interestingly, Syndecan-4, which is a single-pass transmembrane proteoglycan, recruits PKCα to the plasma membrane and thereby regulated PKCα activity; this, in turn, is required for proper mTORC2 localization to the rafts and subsequent Akt activation. However, the mechanism by which PKCα regulates mTORC2 recruitment is not known, and is further complicated by the fact that PKCα is known to be a downstream target of mTORC2.

Although we have some insights into how mTORC2 might be regulated, it will be a major breakthrough to identify upstream regulators of the TORC2 signaling branch, in both yeast and mammals.

Concluding remarks and future perspectives

We have summarized and highlighted the major recent findings on TORC2 in various organisms. The sum of all studies clearly shows conserved functions of TORC2 across organisms (Figure I-1). In plants and algae, many components of the TOR signaling pathway have been elucidated and *Arabidopsis Thaliana* TOR (AtTOR) is important in the control of plant growth (Anderson et al., 2005; Deprost et al., 2007; Diaz-Troya et al., 2008; Mahfouz et al., 2006). However, no rictor or Sin1 homologue has been identified in *A. thaliana* or the green alga *Chlamydomonas reinhardtii* questioning the existence of TORC2 in photosynthetic organisms. Interestingly, TORC2 was recently identified in the protozoan parasite *Trypanosoma brucei*, which causes sleeping sickness in humans (Barquilla et al.,

2008). In contrast to other eukaryotes, rapamycin treatment of *T. brucei* inhibits cell growth by exclusively preventing TORC2 assembly, without affecting TORC1.

TORC2, together with its sibling complex TORC1, is the main kinase that phosphorylates and thereby regulates the activity of several AGC kinases. TORC2 also regulates actin cytoskeletal organization in most systems studied. However, it remains unclear how TORC2 specifically regulates this process in the context of diverse physiological processes that involve motility, such as embryogenesis, inflammation, metastasis, or wound healing.

Several studies have shown that a full body knockout of any mTORC2 component is embryonic lethal. As a next step, it would be highly interesting to determine how mTORC2 in individual organs influences whole body growth and metabolism. Conditional knockout studies of the mTORC2-specific component rictor in skeletal muscle display minimal phenotypes (Bentzinger et al., 2008; Kumar et al., 2008), suggesting that the role of mTORC2 in muscle is less important. Loss of rictor in adipose tissue, however, results in a more dramatic phenotype. Adipose mTORC2 negatively controls whole-body growth and also influences glucose metabolism by influencing IGF1 and insulin levels, respectively (work of this thesis: Cybulski et al., 2009).

Does mTORC2 have a role in diseases such as cancer or metabolic disorders? Guertin et al. (Guertin et al., 2009) made the interesting observation that mTORC2 is important for the development of prostate cancer induced by *Pten* loss, but is not important for non-cancerous prostate epithelial cells. Moreover, as conditional knockout studies show a role for mTORC2 in regulating glucose metabolism, mTORC2 could play a role in the development of type 2 diabetes (work of this thesis: Cybulski et al., 2009; Kumar et al., 2008). The involvement of mTORC2 in diseases is only starting to be considered. Future studies might reveal the need for drugs that specifically inhibit mTORC2, such as rapamycin for mTORC1.

mTOR associated diseases

Dysregulated mTOR signaling is often linked to tumor formation (Guertin and Sabatini, 2007). mTOR itself is not mutated in tumors or cancers, but many upstream regulators and downstream effectors that are functionally linked to the mTOR signaling pathway are well-known proto-oncogenes or tumor suppressors. The most evident link between aberrant mTOR signaling and tumor formation is found in patients with tuberous sclerosis complex, a disease characterized by hamartomas (begin tumors) caused by inactivating mutations of the

tumor suppressors TSC1 and TSC2 (Inoki et al., 2005). Hamartomas are also found in patients with Peutz-Jeghers syndrome (PJS). In PJS mTOR signaling is increased due to a loss of function mutation in the negative upstream regulator LKB1. Further proto-oncogenes that are commonly activated in cancers and that result in increased mTOR signaling are PI3K, Akt/PKB, Rheb and S6K1, while inactivating mutations in the tumor suppressors PTEN and 4E-BP1 have the same effect (Wullschleger et al., 2006). So far, the direct link between cancer and mTOR is limited to the mTORC1 signaling branch and rapamycin and its derivatives have already been tested in clinical studies for cancer treatment. However, little is known about the role of the mTORC2 signaling branch in cancer. First indications that mTORC2 signaling can be misregulated in cancers come from studies that show that mTORC2 is required for the development of prostate cancer caused by PTEN deletion (Guertin et al., 2009).

Several studies in mice have shown that mTORC1 signaling in various metabolic tissues plays an important role in regulating whole body energy metabolism (Polak and Hall, 2009) and dysregulation of mTOR signaling is associated with metabolic disorders such as obesity and diabetes. As described above, constitutive activated mTORC1 signaling inhibits IRS via the negative feedback loop from mTOR-S6K resulting in a strong inhibition of the insulin-mediated PI3K pathway. As a consequence, cells become desensitized to insulin, causing insulin resistance.

Far less is known about mTORC2 and its role in regulating whole body energy metabolism. First knockout studies revealed that, at least in muscle, loss of mTORC2 results in little-to-no phenotype. Muscle-specific *rictor* knockout mice are slightly glucose tolerant but don't show any further metabolic abnormalities (Bentzinger et al., 2008; Kumar et al., 2008).

Adipose tissue

It was believed for a long time that the adipose tissue solely functions as a fat storage compartment within the body. However, during the last few years intensive research has replaced this view by the notion that adipose tissue also has a central role in lipid and glucose metabolism and functions as an endocrine organ. Adipose tissue is an important player in the regulation of energy homeostasis (Figure I-4).

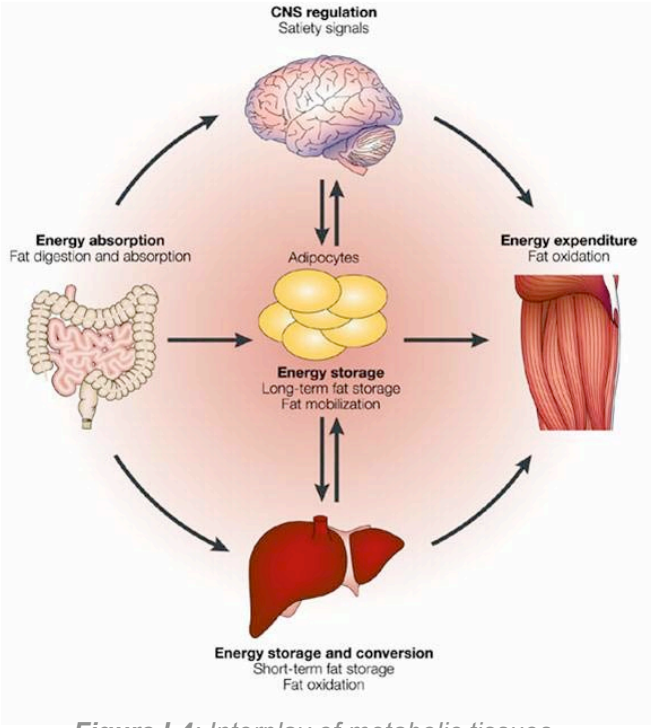

***Figure I-4**: Interplay of metabolic tissues. Adapted from Shi and Burn, 2004.*

Adipose tissue is considered to be a vital organ, is unique to vertebrates and is found in most mammals, birds, reptiles and amphibians. It is mainly composed of the fat-storing adipocytes, which can determine up to 85% of the white adipose tissue mass, but adipose tissue also comprises other cell types, such as macrophages, fibroblasts, preadipoyctes, nerve and endothelial cells. Adipocytes have a great capacity to store fat and can expand to a size larger than most other cell types. The fat is stored within a single large lipid droplet that can represent approximately 90% of the cell volume of an adipocyte (Haugen and Drevon, 2007). In addition to white adipose tissue, also brown adipose tissue exists. Brown adipocytes store fat in multiple lipid droplets and they contain a large number of mitochondria, which give them their brown appearance. In contrast to the fat storage function of white adipose tissue, brown adipose tissue has a primary function in heat generation and adaptive thermogenesis by means of uncoupling of the proton gradient from ATP production. Due to this function brown adipose tissue has an important role in the thermoregulation of small, hibernating rodents. In humans, brown adipose tissue is found in newborns but is largely replaced by white adipose tissue in adults (Cannon and Nedergaard, 2004).

In the following part the role of white adipose tissue in fat storage, fat release, its function as an endocrine organ, as well as associated diseases will be described in more detail.

Fat storage and release

The primary role of adipose tissue, in particular of the adipocyte cell, is to store energy in the form of triacylglycerol (TAG) during times when input exceeds expenditure and to break down this stored lipid into free fatty acids (FFA) when energy is required (Haugen and Drevon, 2007). TAGs are lipid molecules composed of three fatty acids attached to a glycerol backbone. Fatty acids can be saturated or unsaturated. The main source of FFAs comes from the diet, but upon shortage, FFAs can also be synthesized by the body from glucose in a process called *de novo* lipogenesis. In the diet, fat is mainly stored as TAGs, and many fats that originate from animals are mainly composed of saturated fatty acids, whereas vegetable-derived fats often contain a high percentage of unsaturated fatty acids.

Upon food intake, dietary fats are first digested in the stomach and upper small intestine through the action of stomach acids, bile salts, and digestive enzymes, such as lipases. In the intestinal cells, the absorbed fat is re-assembled into TAGs and packaged together with cholesterol, fat-soluble vitamins and carrier lipoproteins into small particles called chylomicrons that are then secreted into the blood stream. Except for the liver, most organs are able to extract the lipids from the chylomicrons with the help of lipoprotein lipases, which are secreted by the individual organs and are found in the capillaries of mainly heart, skeletal muscle and adipose tissue, but also other non-liver organs. Lipoprotein lipases break the TAGs down into free fatty acids. While the heart and skeletal muscle metabolize the fatty acids for energy production, the adipose tissue stores the fatty acids by forming new TAGs. Once the chylomicrons are depleted of TAGs and remain loaded with cholesterol, they are known as chylomicron remnants that are taken up by the liver (Shi and Burn, 2004).

Between meals, the liver can also synthesize TAGs from glucose, which are then distributed to the body in the form of very low density lipoproteins (VLDL). VLDLs provide fatty acids mainly to the heart and skeletal muscle for oxidation and as more and more TAGs are removed, the composition of the VLDL changes and it becomes an intermediate-density lipoprotein (IDL). Further loss of TAGs results in smaller and denser particles called low density lipoproteins (LDL), that are then enriched in cholesterol. LDLs provide cholesterol to peripheral tissues. LDL is often referred to as the ‘bad’ cholesterol fraction, since an excess of LDL in the blood stream is a major cause of atherosclerosis. The ‘good’ cholesterol fraction is known as high density lipoprotein (HDL). HDL is assembled in the blood and transports excess cholesterol away from or out of tissues back to the liver for eventual disposal.

As mentioned before, the adipose tissue stores dietary fat as TAG. FFAs that are released from lipoproteins (mainly chylomicrons) by lipoprotein lipase enter the adipocytes

through both passive diffusion and active transport. FFAs are toxic to cells, so once inside the cell they are transported via fatty acid-binding proteins and converted to acyl coenzyme A (acyl-CoA). This activated form of FFA can then be either oxidized by mitochondria for energy generation (more common in other cells), or be transported to the endoplasmic reticulum for esterification with glycerol 3-phosphate that is generated by glucose metabolism. The formation of TAGs requires several enzymatic steps and once synthesized the TAGs are stored away into lipid droplets.

During fasting or exercise, fatty acids and glycerol are released from the adipose tissue into the blood stream in order to supply peripheral tissues with sufficient energy. The process of lipid mobilization by releasing FFAs is called lipolysis. In the fed state, lipolysis is inhibited by insulin, while in the starved state epinephrine and other lipolytic hormones promote the breakdown of stored TAGs. At least three adipocyte lipases are required to release the three fatty acids bound to one glycerol backbone. Adipose TAG lipase (ATGL) removes the first fatty acid, followed by hormone-sensitive lipase (HSL) that degrades the diacylglycerols into monoacylglycerols. The last step requires monoglyceride lipase.
Activation of lypolysis through lipolytic hormones causes an increase in intracellular cyclic AMP (cAMP) levels and activation of cAMP-dependent protein kinase A (PKA). Activated PKA phosphorylates and activates HSL, which regulates the rate-limiting step of lipolysis. PKA also phosphorylates perilipin, a lipid-droplet-coating protein, that when phosphorylated, facilitates access of HSL to the lipid droplet, and hence lipolysis. Once released into the blood, FFAs are transported in an albumin-bound form to different tissues that can oxidize them, mainly liver, heart, kidney and muscle (Shi and Burn, 2004).

Endocrine functions

Adipose tissue has long been believed to be solely a fat storage depot, but it is now clear that adipose tissue is a complex and highly active metabolic and endocrine organ. It has the capacity to actively communicate by sending and receiving different types of signals. Adipose tissue expresses many receptors that allow it to respond to endocrine and autocrine signals, such as insulin, glucagon, catecholamines, insulin like growth factor 1 (IGF1) and many others. On the other hand, it also secretes a variety of factors, including metabolites and proteins that derive from both adipocyte and nonadipocyte fractions. These metabolically active adipose-derived factors are commonly known as “adipokines” and they affect whole body energy metabolism and the function of many organs and tissues including

muscle, liver, vasculature, and brain. Adipokines act in an autocrine, paracrine and/or endocrine manner and are involved in glucose and lipid metabolism, inflammation, coagulation, blood pressure and feeding behavior (Kershaw and Flier, 2004; Wang et al., 2008).

The two best-characterized and most studied adipokines are leptin and adiponectin. Leptin is a small protein secreted from adipocytes and its serum levels correlate with adipose tissue mass as well as the nutritional status (Friedman, 2009). However, leptin levels are not directly influenced by short-term nutritional status (food intake) but rather reflect the long-term nutritional status. Leptin acts through the sympathetic nervous system to negatively regulate appetite and food intake. Its binding to the leptin receptor in the hypothalamus results in the reduction of neuropeptide-Y (NPY) and agouti regulated protein (AgRP) activity, two orexigenic neuropeptides, while increasing the activity of the anorexigenic neuropeptides pro-opiomelanocortin (POMC) and cocaine- and amphetamine related protein (CART). Leptin was discovered in 1994 as the product of the *obese* (*ob*) gene. Mice with a mutation in the *ob* gene are extremely obese due to the lack of functional leptin, resulting in a reduced feedback signal to stop eating. Besides its central role in regulating food intake and energy expenditure, leptin also influences lipid metabolism by increasing hepatic lipid oxidation and lipolysis in skeletal muscle and adipocytes (Hajer et al., 2008).

Adiponectin is another protein hormone that is produced exclusively by adipocytes and is regarded as an insulin sensitizer that plays an important role in the development of insulin resistance. In contrast to most other adipokines, serum adiponectin levels negatively correlate with adipose tissue mass (Garaulet et al., 2007). Adiponectin improves insulin sensitivity by reducing hepatic glucose production and enhancing insulin action in the liver and skeletal muscle.

Many additional adipokines and their associated role in regulating whole body energy metabolism have been identified (Kershaw and Flier, 2004; Wang et al., 2008). The following table gives an overview of the functional groups of adipokines and the major factors involved:

Functional category	**Factors**
Lipid metabolism	Cholesteryl ester transfer protein (CETP), Lipoportein lipase (LPL), Retinol binding protein 4, Apolipoprotein E, Steroid hormones
Glucose metabolism and insulin resistance	Adiponectin, Resistin, Visfatin, Omentin, Vaspin, Leptin, TNFα
Food intake	Leptin
Inflammation	Tumor necrosis factor α (TNFα), Interleukin-6 (IL-6), Adiponectin, Resistin, C-reactive protein (CRP), Adipsin
Vasculature	Angiotensin, Vascular endothelial growth factor (VEGF), Adrenomedullin, Plasminogen activator inhibitor-1 (PAI-1)

Adipose tissue associated diseases

Body fat has the very important function of storing fatty acids for times of low energy availability. However, the right amount of body fat is very important as too much or too little fat are a serious health risk.

Obesity, an excess of body fat results from an imbalance of caloric intake and energy expenditure, but also genetic factors can influence the progression of obesity. Obesity is strongly associated with many diseases, in particular diabetes and cardiovascular diseases (Hajer et al., 2008). As mentioned before, adipose tissue has an important function as an endocrine organ to control whole body energy homeostasis and obesity is often associated with marked changes in the secretory function of the adipose tissue that promotes the development of diseases.

Obesity-linked type 2 diabetes is due to a combination of insulin resistance and dysfunction of the insulin-secreting pancreatic β-cells (Guilherme et al., 2008; Lingohr et al., 2002). Insulin resistance results from an impaired insulin responsiveness of skeletal muscle resulting in diminished glucose uptake. In a first step, normal glucose levels can be maintained by increased insulin production/secretion by pancreatic β-cells. However, when the pancreatic β-cells fail to secrete enough insulin to compensate for insulin resistance, blood glucose levels rise and diabetes will ensue. Several adipose-derived factors, such as adiponectin, TNFα, leptin, IL6 and FFAs, are known to affect insulin sensitivity of peripheral tissues, and they furthermore have effects in the pancreas leading to β-cell failure (Hajer et al., 2008).

Obesity is also a major risk factor for hypertension and cardiovascular diseases, in particular coronary heart disease (Bays, 2009). High blood glucose levels (resulting from type 2 diabetes), elevated blood pressure, elevated TAGs, low plasma HDL and high plasma LDL are associated with obesity and are all known to increase the risk for coronary heart disease.

Cell migration

Cell migration is involved in many physiological and pathophysiological processes including embryogenesis, angiogenesis, nerve growth, tissue repair, inflammation, invasion or metastasis (Franz et al., 2002), and normally requires the orchestrated movement of cells in a particular direction to a specific location.

Cell migration is a very dynamic and highly coordinated process, which involves rapid changes in the dynamics of actin filaments, together with the formation and disassembly of cell adhesion sites. The migration process can be divided into five different steps (Ridley et al., 2003). Directed cell movement is initiated by protrusion of the leading edge and formation of new actin filaments followed by adhesion to the matrix. The third step in the migratory process is cell-body contraction resulting from forces generated through actomyosin interactions. The next event involves the release of cell contacts at the rear of the cell and the cycle ends with the recycling of membrane receptors from the rear to the front, which relies mainly on protein trafficking. Each step of the cycle requires a highly coordinated restructuring of the actin cytoskeleton. The protrusive structures at the leading edge of a motile cell are called lamellipodia and filopodia. A lamellipodium is a thin, flat and sheet-like protrusion that is filled with a branched network of actin filaments, while filopodia are thin, spike-like structures that are filled with tight parallel bundles of filamentous actin. The main regulators of the actin cytoskeleton, and hence important regulators of direct cell migration, are the Rho GTPases (Hall, 1998; Heasman and Ridley, 2008).

Rho GTPases belong to the family of small GTPases and are mainly known for their role in controlling actin cytoskeletal assembly and contraction, but RhoGTPases are also involved in other important processes including regulation of cell polarity, microtubule dynamics, vesicular transport pathways and gene transcription (Jaffe and Hall, 2005). RhoGTPases function as molecular switches that cycle between an active GTP-bound form and an inactive GDP-bound form. The cycling of Rho GTPases between these two states is regulated by three sets of proteins. (1) Guanine nucleotide exchange factors (GEFs) facilitate the exchange process, (2) GTPase-activating proteins (GAPs) facilitate inactivation of GTP-bound Rho by increasing GTPase activity, and (3) guanine nucleotide dissociation inhibitors (GDI) prevent dissociation of GDP and thereby prevent activation. Upon activation, Rho proteins interact with and activate downstream effector proteins to stimulate a variety of processes.

Mammalian RhoGTPases comprise a family of 20 members, but the most highly conserved and most extensively studied Rho GTPases are RhoA, Rac1 and Cdc42. RhoA is implicated in the formation of stress fibers and focal adhesions, Rac1 promotes

lamellipodium formation and Cdc42 functions in the formation of filopodia (Ladwein and Rottner, 2008; Mattila and Lappalainen, 2008).

Fibroblasts are commonly used to study the basic mechanisms of cell migration because they contain the fundamental machinery for cell migration.

Aims of the Thesis

Full body knockout of any mTORC2-component in mice results in embryonic lethality emphasizing the importance of this complex at least in embryogenesis. However, very little is known about mTORC2 function in individual tissues and its role in whole body metabolism. Furthermore, compared to the mTORC1 signaling branch, the mTORC2 signaling branch is less characterized and little is known about its upstream regulators and downstream functions. Therefore, the aim of this thesis was to gain new insights into the *in vivo* and *in vitro* functions of mTORC2.

The first part focuses on the *in vivo* function of mTORC2 and describes the phenotypic characterization of adipose-specific knockout mice of the mTORC2-specific component *rictor*. mTORC2 signaling is activated upon insulin stimulation and adipose tissue is one of the most insulin-sensitive tissues in the body strongly suggesting a role for mTORC2 in this tissue.

The second part of this thesis focuses on the *in vitro* function of mTORC2 and analyses its role in cell migration. Using an inducible knockout mouse embryonic fibroblast (MEF) cell line for *rictor*, the effects of loss of mTORC2 were investigated.

Results

Part 1: Phenotypic characterization of rictor adipose-specific knockout mice

Manuscript accepted for publication in PNAS.

Cybulski N., Polak P., Auwerx J., Rüegg M.A., Hall M.H. mTOR complex 2 in adipose tissue negatively controls whole body growth.

mTOR complex 2 in adipose tissue negatively controls whole body growth

Nadine Cybulski*‡, Pazit Polak*‡, Johan Auwerx†§,

Markus A. Rüegg*, and Michael N. Hall*¶

* Biozentrum, University of Basel, 4056 Basel, Switzerland

†Insitut de Génétique et de Biologie Moléculaire et Cellulaire

& Institut Clinique de la Souris

CNRS/INSERM/Université Louis Pasteur

67404 Illkirch, France

Key words: mTORC2, adipose tissue, growth, genetics, signal transduction

‡N.C. and P.P. contributed equally to this work.

§ Current address: École polytechnique fédérale de Lausanne, 1015 Lausanne, Switzerland

¶To whom correspondence should be addressed:

E-mail: m.hall@unibas.ch

Tel: 0041 61 267 2150, Fax: 0041 61 267 21 49

Abstract

Mammalian Target Of Rapamycin (mTOR), a highly conserved protein kinase that controls cell growth and metabolism in response to nutrients and growth factors, is found in two structurally and functionally distinct multiprotein complexes termed mTOR complex 1 (mTORC1) and mTORC2. mTORC2, which consists of rictor, mSIN1, mLST8, and mTOR, is activated by insulin/IGF1 and phosphorylates Ser473 in the hydrophobic motif of Akt/PKB. While the role of mTOR in single cells is relatively well characterized, the role of mTOR signaling in specific tissues and how this may contribute to overall body growth are poorly understood. To examine the role of mTORC2 in an individual tissue, we generated adipose-specific *rictor* knockout mice (*rictor*$^{ad-/-}$). *rictor*$^{ad-/-}$ mice are increased in body size due to an increase in size of non-adipose organs including heart, kidney, spleen, and bone. Furthermore, *rictor*$^{ad-/-}$ mice have a disproportionately enlarged pancreas and are hyperinsulinemic, but glucose tolerant, and display elevated levels of insulin-like growth factor 1 (IGF1) and IGF1 binding protein 3 (IGFBP3). These effects are observed in mice on either a high fat or a normal diet, but are generally more pronounced in mice on a high fat diet (HFD). Our findings suggest that adipose tissue, in particular mTORC2 in adipose tissue, plays an unexpectedly central role in controlling whole body growth.

Introduction

Mammalian Target Of Rapamycin (mTOR), a highly conserved protein kinase that controls cell growth and metabolism in response to nutrients and growth factors, is found in two structurally and functionally distinct multiprotein complexes termed mTOR complex 1 (mTORC1) and mTORC2 (Wullschleger et al., 2006). mTORC1 contains raptor, mLST8, PRAS40 and mTOR, and is sensitive to the immunosuppressant and anti-cancer drug rapamycin (Hara et al., 2002; Kim et al., 2002; Loewith et al., 2002; Vander Haar et al., 2007). mTORC2 consists of rictor, mSIN1, mLST8 and mTOR, and is insensitive to rapamycin although long-term rapamycin treatment can indirectly inhibit mTORC2 in some cell types (Jacinto et al., 2006; Jacinto et al., 2004; Sarbassov et al., 2004; Sarbassov et al., 2006; Yang et al., 2006). The best-characterized substrates of mTOR are S6K and 4E-BP via which mTORC1 controls translation, and Akt/PKB via which mTORC2 may control cell survival and possibly other processes (Hresko and Mueckler, 2005; Polak and Hall, 2009; Sarbassov et al., 2005). mTORC2 also phosphorylates and activates SGK1, and

phosphorylates and stabilizes PKCα (Facchinetti et al., 2008; Garcia-Martinez and Alessi, 2008; Ikenoue et al., 2008; Sarbassov et al., 2004). As mTORC1 can be pharmacologically inhibited with rapamycin, it is relatively well characterized and has been implicated in various disorders including cancer, cardiovascular disease, obesity and diabetes (Wullschleger et al., 2006). In contrast, as there is no specific inhibitor of mTORC2, mTORC2 signaling is less well characterized and its physiological role is unclear. Knockout studies have underscored the importance of both complexes as full body deletion of any component of either mTOR complex results in embryonic lethality (Guertin et al., 2006; Jacinto et al., 2006; Shiota et al., 2006; Yang et al., 2006). *rictor*-deficient embryos fail to develop beyond day E10.5 and arrest as slightly smaller and developmentally delayed embryos compared to littermate controls (Guertin et al., 2006; Shiota et al., 2006).

While the general role of mTOR in single cells is relatively well characterized, the role of mTOR signaling in specific tissues and how this may contribute to overall body growth and whole body metabolism are poorly understood (Polak and Hall, 2009). Adipose-specific *raptor* knockout mice are resistant to diet-induced obesity and have improved glucose metabolism (Polak et al., 2008). Conditional knockout of *raptor* in skeletal muscle results in slight glucose intolerance, muscle dystrophy, and death by the age of 6 months (Bentzinger et al., 2008). Knockout of *rictor* specifically in skeletal muscle results in little-to-no phenotype and thus provided little insight on the physiological role of mTORC2 at least in muscle (Bentzinger et al., 2008; Kumar et al., 2008).

Adipose tissue is a fat storage depot and an endocrine organ that controls energy metabolism, appetite and fertility in response to nutrients and insulin (Haugen and Drevon, 2007; Shi and Burn, 2004). Interestingly, the equivalent tissue in *Drosophila*, the fat body, controls full body growth in response to nutrients. Colombani et al (Colombani et al., 2003) have demonstrated that down regulation of TOR signaling, most likely mTORC1, specifically in the fat body results in a reduction in overall body size. Excess adipose tissue (obesity) leads to many metabolic disorders including type 2 diabetes, cardiovascular diseases and cancer. Given the central role of mTOR as a nutrient sensor and the increasing prevalence of obesity, it is important to understand the role of adipose mTOR in controlling whole body growth and metabolism. In this study, we examined the role of mTORC2 in adipose tissue. To circumvent the embryonic lethality caused by full body ablation of any component of mTORC2, we used the Cre/LoxP system to knock out *rictor* specifically in adipose tissue. Strikingly, *rictor*$^{ad-/-}$ mice are enlarged due to an increase in lean tissue mass resulting from elevated levels of IGF1. Furthermore, the knockout mice are hyperinsulinemic yet glucose tolerant. These results suggest the existence of an mTORC2-dependent adipose to liver/pancreas signaling axis that controls full body growth and metabolism.

Results

Generation and confirmation of adipose-specific *rictor* knockout mice.

To delete *rictor* in adipose tissue, we generated mice in which exons four and five of the *rictor* gene were flanked by *loxP* sites (*rictor*$^{fl/fl}$). The *rictor*$^{fl/fl}$ mice were crossed with mice expressing cre recombinase under control of the adipose-specific, *fabp4/aP2* gene promoter (He et al., 2003) (Fig. II-1*A*). Adipose-specific *rictor* knockout mice (*rictor*$^{ad-/-}$) lacked rictor protein in adipose tissue but not in liver, heart, kidney, spleen, brain or macrophages (Fig. II-1*B* and II-S1), indicating that *rictor* was indeed deleted specifically in adipocytes. Adipose tissue of *rictor*$^{ad-/-}$ mice exhibited reduced Akt Ser473 phosphorylation and reduced PKCα levels, indicating that mTORC2 signaling was defective (Fig. II-1*B*). As expected, Akt Thr308 phosphorylation and phosphorylation of the Akt substrate GSK3 were not affected in adipose tissue.

***rictor*$^{ad-/-}$ mice are enlarged due to an increase in lean mass.**

Body weight of *rictor*$^{ad-/-}$ and control wild type littermates (*rictor*$^{fl/fl}$) was monitored during a 10 week time course in mice 8 to 18 weeks of age. At 8 weeks of age, knockout and control mice were of similar weight. On a normal diet (chow), *rictor*$^{ad-/-}$ mice gained weight at a slightly higher rate than control mice such that they were 4% heavier at the end of the time course (Fig. II-1*C*). The increased body weight of *rictor*$^{ad-/-}$ mice compared to control mice was more pronounced on a HFD (Fig. II-1*D*). After ten weeks on a HFD (started at 8 weeks of age), the *rictor*$^{ad-/-}$ mice were 17% heavier than control *rictor*$^{fl/fl}$ mice, but were already significantly heavier after only 5-6 weeks on the HFD. Body length of the *rictor*$^{ad-/-}$ mice was also increased (Fig. II-1*E*), suggesting that the increase in weight was due to an overall increase in body size rather than an increase only in fat mass. Indeed, whole body dexa scan analysis of mice after 6 weeks on a HFD revealed an increase specifically in lean tissue mass (Fig. II-2*A*); no difference was observed in the total amount of fat mass after 6 weeks on a HFD (Fig. II-2*B*).

To investigate further the increase specifically in lean tissue mass, individual organs of *rictor*$^{ad-/-}$ and *rictor*$^{fl/fl}$ mice, fed either a chow or high fat diet for 10 weeks, were excised and weighed (Fig, II-2*C-J*). On a chow diet, the heart, kidneys, spleen, and pancreas were 40%, 28%, 38%, and 41% heavier, respectively, in *rictor*$^{ad-/-}$ mice compared to *rictor*$^{fl/fl}$ control mice. On a HFD, the heart, kidneys, spleen and pancreas were 40%, 47%, 62%, and 129% heavier, respectively, in *rictor*$^{ad-/-}$ mice (Fig. II-2*C-F*). Interestingly, the pancreas was heavier in the *rictor*$^{ad-/-}$ mice on both diets but was disproportionately heavier (129%) on the HFD, compared to other organs (Fig. II-2*F*). The liver was also heavier (75%) in *rictor*$^{ad-/-}$ mice, but

only on the HFD (Fig. II-2*G*). Furthermore, as revealed by whole body dexa scan analysis, *rictor*$^{ad-/-}$ mice exhibited a 15% increase in bone mineral content with no change in bone mineral density, indicating that overall bone size was also increased (Fig. II-2*H*). Thus, all lean tissues examined were enlarged as a result of an mTORC2 deficiency in adipose tissue.

After ten weeks on a HFD, the inguinal fat pad was not significantly increased in *rictor*$^{ad-/-}$ mice compared to control *rictor*$^{fl/fl}$ mice (Fig. II-2*I*), although the epididymal fat pad was increased 30% (Fig. II-2*J*). This is consistent with the dexa scan analysis described above which detected no increase in overall fat mass after six weeks on a HFD. Thus, *rictor*$^{ad-/-}$ mice are larger than control mice due to an increase mainly, if not exclusively, in lean tissue mass. Surprisingly, this effect was particularly evident in mice on a HFD. Furthermore, given the increase in lean mass with little-to-no increase in overall fat mass, *rictor*$^{ad-/-}$ mice are leaner than control mice. This leanness could account for the relatively mild increase in full body weight (17%) compared to the observed increases in weights of individual organs.

rictor$^{ad-/-}$ mice exhibit normal WAT morphology and have increased liver steatosis.

To investigate further the effect of *rictor*$^{ad-/-}$ on adipose tissue, we performed histology on the epididymal fat pad. The epididymal fat pads from *rictor*$^{ad-/-}$ and control *rictor*$^{fl/fl}$ mice were indistinguishable with regard to fat cell size and morphology (Fig. II-3*A*). We also examined histological sections of the liver, a secondary fat storage organ. Hepatic cells from HFD-fed *rictor*$^{ad-/-}$ mice contained particularly enlarged lipid droplets, indicative of more advanced steatosis (Fig. II-3*B*). Quantification of liver triglycerides confirmed the increased fat accumulation in the liver of *rictor*$^{ad-/-}$ mice compared to control *rictor*$^{fl/fl}$ mice (Fig. II-3*C*). The amount of glycogen in the liver was not changed in *rictor*$^{ad-/-}$ mice compared to control mice (Fig. II-S2). Thus, the increase in hepatic fat accumulation likely accounts for the particularly enhanced size (75% increase) of the liver in HFD-fed *rictor*$^{ad-/-}$ mice, as described above.

rictor$^{ad-/-}$ mice have altered levels of cholesterol and adiponectin.

To characterize further the phenotype of *rictor*$^{ad-/-}$ mice, we examined several blood metabolites and hormones that could be affected upon altered adipose function. Free fatty acids and triglyceride levels were unchanged in *rictor*$^{ad-/-}$ mice compared to *rictor*$^{fl/fl}$ mice. Cholesterol levels were increased in *rictor*$^{ad-/-}$ mice, but only on a chow diet. Serum leptin and IL-6 were also unchanged, but serum levels of adiponectin were decreased approximately 30% in *rictor*$^{ad-/-}$ mice, on either a chow or high fat diet (Table II-1).

***rictor*$^{ad-/-}$ mice are hyperinsulinemic but glucose tolerant.**

To assess the role of adipose mTORC2 in whole body glucose metabolism, we first examined blood glucose and insulin levels. On a chow or high fat diet, blood glucose levels were similar or slightly lower in both fasted (overnight) and fed *rictor*$^{ad-/-}$ mice compared to control *rictor*$^{fl/fl}$ mice (Fig. II-4*A*,*B*). However, insulin levels were significantly increased in fasted or fed *rictor*$^{ad-/-}$ mice compared to control mice, on a chow or high fat diet (Fig. II-4*C,D*). To further investigate the effect of mTORC2-deficient adipose tissue on insulin levels, we performed a morphometric analysis on the pancreas. Consistent with an enlarged pancreas, pancreatic islets were at least two-fold larger but otherwise morphologically unchanged in *rictor*$^{ad-/-}$ mice compared to control *rictor*$^{fl/fl}$ mice (Fig. II-4*E,F*). Furthermore, the increase in size of the islets correlated with an increase in total weight of β cells (Fig. II-4*G*) The increase in size of the pancreas and insulin producing islets, even disproportionately increased in HFD-fed knockout mice, likely account for the hyperinsulinemia of *rictor*$^{ad-/-}$mice.

We next performed a glucose tolerance test on *rictor*$^{ad-/-}$ and control *rictor*$^{fl/fl}$ mice, on a chow or high fat diet. Hyperinsulinemia, as observed in the *rictor*$^{ad-/-}$ mice, is normally a response to insulin resistance and generally correlates with glucose intolerance. However, unexpectedly, the hyperinsulinemic *rictor*$^{ad-/-}$ mice were similarly glucose tolerant (chow diet) or even more glucose tolerant (HFD) than *rictor*$^{fl/fl}$ mice on the corresponding diets (Fig. II-5*A,B*). Furthermore, *rictor*$^{ad-/-}$ mice produced higher levels of blood insulin in response to an injected glucose bolus, compared to *rictor*$^{fl/fl}$ control mice (Fig. II-S3). Thus, *rictor*$^{ad-/-}$ mice remain glucose tolerant under conditions (HFD) where wild type mice are unable to do so. In addition, the hyperinsulinemia of *rictor*$^{ad-/-}$ mice does not correlate with glucose intolerance but may rather reflect a primary effect of mTORC2-deficient adipose on the pancreas. Such a primary effect on the pancreas could underlie the disproportionately large size of the pancreas in *rictor*$^{ad-/-}$ mice.

rictor$^{ad-/-}$ mice are more glucose tolerant than control mice. Is this due to increased insulin sensitivity, to the observed elevated levels of insulin, or to both? To distinguish these possibilities, we examined the insulin sensitivity of *rictor*$^{ad-/-}$ and *rictor*$^{fl/fl}$ mice. *rictor*$^{ad-/-}$ mice were slightly insulin resistant compared to the wild type control mice, based on less efficient clearance of blood glucose in response to injected insulin (Fig. II-5*C*). To investigate further this insulin resistance, we examined Akt Thr308 and Ser473 phosphorylation in muscle, adipose tissue and liver of insulin-injected *rictor*$^{ad-/-}$ and *rictor*$^{fl/fl}$ mice. Mice were injected with either saline or insulin and, after 15 minutes, tissues were excised and processed for immunoblotting to detect Akt phosphorylation. Insulin stimulated Thr308 and Ser473 phosphorylation in both the *rictor*$^{ad-/-}$ and control *rictor*$^{fl/fl}$ mice in all three tissues, but this stimulation was less robust in the *rictor*$^{ad-/-}$ mice (Fig. II-5*D*). Thus, *rictor*$^{ad-/-}$ mice are modestly insulin resistant, possibly due to reduced levels of the insulin-sensitizer adiponectin

(Table II-1). Furthermore, these results suggest that the glucose tolerance of *rictor*$^{ad-/-}$ mice is due to an elevated level of insulin that overcomes a weak insulin resistance. Elevated levels of IGF1 (see below) might also contribute to the glucose tolerance of *rictor*$^{ad-/-}$ mice (Liao et al., 2006).

As expected, insulin failed to stimulate mTORC2-dependent Akt Ser473 phosphorylation in adipose tissue of *rictor*$^{ad-/-}$ mice (Fig. II-5*D*). However, insulin stimulated Akt Thr308 and GSK3 phosphorylation in adipose tissue of *rictor*$^{ad-/-}$ mice, suggesting that mTORC2-deficient adipose tissue remains insulin responsive. To further investigate the insulin responsiveness of mTORC2-deficient adipose tissue, we assayed glucose uptake in isolated, insulin-treated adipocytes. While basal and insulin-stimulated glucose uptake were lower in *rictor*-deficient adipocytes, both *rictor*$^{ad-/-}$ and wild type adipocytes displayed a three-fold stimulation in response to insulin (Fig. II-5*E*), confirming that mTORC2-deficient adipocytes remain insulin responsive.

rictor$^{ad-/-}$ mice have elevated serum IGF1.

Organismal growth is controlled largely by growth hormone (GH) and IGF1 (Butler and Le Roith, 2001; Dupont and Holzenberger, 2003). GH is produced in the pituitary gland and acts by stimulating IGF1 production in the liver. To understand further the increased body size of *rictor*$^{ad-/-}$ mice, we measured serum levels of GH and IGF1. IGF1 serum levels were significantly increased in *rictor*$^{ad-/-}$ mice compared to control *rictor*$^{fl/fl}$ mice, on either a chow (21%) or high fat diet (58%) (Fig. II-6*A*). The increase in IGF1 levels correlated with an increase in IGF1 mRNA levels in the liver, the main IGF1 secreting organ, and in adipose tissue (Fig. II-6*B*). In parallel, IGF1 binding protein 3 (IGFBP3) serum levels were also elevated in *rictor*$^{ad-/-}$ mice, on a chow or high fat diet (26% and 39%, respectively) (Fig. II-6*C*). IGFBP3 is the major IGF1 binding protein that together with acid-labile subunit (ALS) stabilizes IGF1 in the serum (Duan and Xu, 2005; Yakar et al., 2005). In contrast, GH serum levels were unchanged (Fig. II-6*D*), suggesting that elevated levels of IGF1 in the blood were not due to altered, GH-mediated signaling from the pituitary gland. The increased levels of IGF1 likely account for the increased body size and furthermore contribute to the glucose tolerance of *rictor*$^{ad-/-}$ mice.

Discussion

Here we describe the generation and characterization of mice lacking rictor specifically in adipose tissue. rictor is an essential and specific subunit of mTORC2. The most striking and unexpected observation was that *rictor*$^{ad-/-}$ mice are increased in body size due to an increase in size of non-adipose tissue. Furthermore, *rictor*$^{ad-/-}$ mice have elevated levels of IGF1 and insulin. The hyperinsulinemia is likely due to a disproportionately increased pancreas and increased β cell mass. The increase in IGF1 levels is due to a GH-independent increase in IGF1 expression in adipose tissue and the liver. Overall, our results suggest that mTORC2 in adipose tissue controls an adipose to pancreas/liver signaling axis that ultimately controls whole body growth and glucose metabolism.

How might mTORC2 in adipose control the pancreas and liver? mTORC2 in adipose tissue may positively control expression and/or secretion of a factor(s) that negatively regulates these organs. Alternatively, adipose mTORC2 could negatively control a factor(s) that positively regulates the pancreas and/or liver. In either case, adipose mTORC2 would negatively regulate the pancreas and liver such that a knockout of adipose mTORC2 results in increased insulin production by the pancreas and increased IGF1 secretion by the liver (Fig. II-6*E*). The physiological significance of this negative regulation of the pancreas and liver by adipose mTORC2 may be related to the fact that mTORC2 is itself stimulated by insulin and IGF1 (Wullschleger et al., 2006). Insulin/IGF1-responsive mTORC2 in adipose tissue may be part of a negative feedback endocrine loop acting on the pancreas and liver to maintain insulin and IGF1 homeostasis (Fig. II-6*E*). Consistent with such a negative feedback loop, an adipose-specific knockout of IGF1 receptor results in elevated levels of IGF1 and larger mice but unchanged levels of GH (Kloting et al., 2008), similar to the adipose-specific mTORC2 knockout described here. Thus, according to this model, insulin and IGF1 activate mTORC2 in adipose tissue and this, in turn, leads to down regulation of insulin and IGF1 production in the pancreas and liver, respectively. It will be of interest to determine if disruption of this putative feedback loop between organs plays a role in metabolic or growth disorders. In this context, it is relevant to note that the feedback loop appears to be particularly important in response to a high fat diet, as suggested by our observation that the growth phenotype of *rictor*$^{ad-/-}$ mice is more pronounced on a high fat diet.

What is the mTORC2-regulated factor(s) that could be signaling from adipose tissue to the pancreas and/or liver? It must be something other than leptin, IL-6, or free fatty acids as these factors are unchanged in *rictor*$^{ad-/-}$ mice (Table II-1). *IGF1* expression is increased in adipose tissue in *rictor*$^{ad-/-}$ mice, suggesting that IGF1 could be a factor by which adipose

mTORC2 signals to other organs. However, IGF1 produced by adipose tissue would likely not be a major factor in signaling to the pancreas and liver because there are few-to-no IGF1 receptors in the liver, and because the liver is the major producer of circulating IGF1. The secreted factor(s) that signals from adipose to the pancreas and liver remains to be determined.

The downstream effectors of mTORC2 that mediate the effects described here are unknown. mTORC2 controls many AGC family kinases (Jacinto and Lorberg, 2008; Polak and Hall, 2009), and we have shown that an mTORC2 deficiency in adipose tissue results in reduced Akt Ser473 phosphorylation and reduced levels of PKCα. It seems unlikely that the phenotype described here is due to loss of Akt Ser473 phosphorylation as loss of Akt Ser473 phosphorylation only mildly affects Akt activity. PKCα is poorly characterized in adipose tissue and it thus remains to be determined whether loss of PKCα plays a significant role. Recent findings suggest that the TORC2 substrate and AGC kinase SGK1 plays an important role in TORC2 downstream signaling and thus possibly in the phenotype described here (Garcia-Martinez and Alessi, 2008; Jones et al., 2009; Soukas et al., 2009). However, SGK1 also remains to be characterized in adipose tissue.

In summary, our results and the recent results of Kloting et al (Kloting et al., 2008) suggest that adipose tissue, and in particular IGF1-mTOR signaling in adipose tissue, plays an unexpectedly central role in controlling whole body growth. This notion is further supported by Colombani et al (Colombani et al., 2003) who demonstrated that TOR in the fly fat body controls whole body growth, via a hormonal mechanism. However, mice and flies do not appear to be completely analogous, as adipose mTORC1 in mice does not control systemic growth positively, as suggested for flies (Polak et al., 2008). In mice, adipose mTORC2 controls systemic growth negatively.

Methods

Mice. *LoxP* sites were introduced into the intron upstream exon 4 and into the intron downstream of exon 5 using a *neo* cassette flanked with *frt* sites as a selectable marker (Fig. 1*A*). Expression of Cre recombinase deletes exons 4 and 5 and causes a frameshift in the *rictor* open reading frame. The vector containing the targeting construct was introduced into embryonic stem cells of the129S1/SvlmJ mouse strain and positive ES cells were selected by G418 resistance. Targeted stem cells were injected into blastocysts of C57BL/6J mice to obtain chimeric mice. Injection of ES cells into blastocysts and subsequent generation of chimeric mice was performed at the Institut Clinique de la Souris (ICS), Strasbourg, France.

After germline transmission, mice were crossed with C57BL/6J mice expressing Flp recombinase to remove the *neo* cassette and subsequently with C57BL/6J Flp deleter mice to obtain *rictor*$^{fl/fl}$mice. The *rictor*$^{fl/fl}$ mice lack the *neo* cassette and behave like wildtype. Mice with an adipose-specific deletion of rictor (*rictor*$^{ad-/-}$) were obtained by crossing *rictor*$^{fl/fl}$ mice with C57BL/6J mice expressing Cre recombinase under the control of the adipocyte-specific *fabp4/aP2* gene promoter (He et al., 2003) (purchased from JAX Laboratories), which is expressed relatively late in adipogenesis (Tontonoz et al., 1994), leading to knockout of *rictor* only in mature adipocytes in neonates. *rictor*$^{ad-/-}$ mice were born at the expected Mendelian ratio. For all experiments, male mice that had been backcrossed at least 5 times with the C57BL/6 strain were used. Littermates with the *lox/lox* genotype (*rictor*$^{fl/fl}$) *were* used as control group in all experiments and are indistinguishable from wildtype mice. . All mouse experiments described were approved by the *Kantonales Veterinaeramt* of *Kanton Basel-Stadt*.

Metabolic studies. At 8 weeks of age male mice were either fed a normal chow diet (4.5% calories from fat, Kliba Nafag) or put on a high fat diet (60% calories from fat, Harlan Research Diets) and monitored for 10 weeks. Body weight was recorded weekly. Quantification of blood metabolites was performed using commercially available kits.

Dual energy x-ray absorptiometry (Dexa) scan analysis. Dexa scan analysis was performed with the ultra high-resolution densitometer PIXImus (GE Medical systems) allowing precise measurement of bone density and body composition (fat and lean mass). Bone mineral content and density and body composition were recorded on anesthetized mice.

Histological analysis. Liver tissues were prepared for cryosectioning and sections were stained with Oil Red O and hematoxylin. Pancreas and adipose tissue were fixed in 4% formaldehyde and paraffin-embedded using a standard protocol. Adipose tissue sections were prepared and stained with hematoxylin and eosin (H&E). For islet size quantification pancreatic sections (8µm) were cut in regular intervals and sequential sections were stained with H&E. All sections were photographed and the area of every islet was quantified using the ImageJ software. In average, 40 islets per pancreas were analyzed. For quantification of β cell mass, β cells were stained using rabbit antibodies against insulin and detected with a secondary antibody conjugated with horseradish peroxidase (Vectastain ABC kit, Vector Labs) followed by incubation in DAB peroxidase substrate solution and subsequent counterstaining with hematoxylin. Images of the entire pancreatic section were obtained using a digital microscope (Coolscope, Nikon) and sections were analyzed using ImageJ

software. The β cell mass was calculated by the percentage of β cell area and pancreas weight. For immunofluorescence, pancreatic sections were stained for insulin and glucagon using rabbit antibodies against insulin and mouse antibodies against glucagon. Immune complexes were detected with secondary antibodies conjugated with TexasRed or FITC, respectively.

Glucose uptake into adipocytes. Adipocytes were isolated from epididymal and inguinal fat pads by 60' digestion in KRBH buffer containing 1% BSA and 1100U/ml collagenase. Cells were starved for an additional 60' in KRBH buffer containing 1% BSA. During the last 30' 100nM insulin was added. To measure glucose uptake, isolated adipocytes were washed once in HBS buffer (140mM NaCl, 20mM Hepes pH7.4, 5mM KCl, 2.5mM $MgSO_4$, 1mM $CaCl_2$) and incubated for 10' in transport solution (HBS containing 10uM 2-deoxy glucose and 0.5uCi/ml ^{3}H 2-deoxy glucose). Cells were washed 3 times in cold PBS and radioactivity was measured by scintillation counter. Glucose uptake was normalized to cell number, which was determined by qPCR on intronic DNA. Primers used were 5'-CTACAGATGTGGTAAAGGTCCGC-3', 5'-GCAATGGTCTTGTAGGCTTCG-3'.

Quantitative PCR. Total RNA was isolated from frozen tissues using TriZOL reagent (Invitrogen). 3μg total RNA was reverse transcribed using Superscript II reverse transcriptase (Invitrogen) and random nonamers. qPCR was performed using the power SYBR green mix (Applied Biosystems) and normalized to Polr2a expression. The following primers were used: Polr2a sense 5'-AATCCGCATCATGAACAGTG-3', Polr2a antisense 5'-CAGCATGTTGGACTCAATGC-3'; IGF1 sense 5'-GCTGCTGAAGCCATTCATTT-3', IGF1 antisense 5'-TTGCTCTTAAGGAGGCCAAA-3'.

Statistical analysis. All data are shown as mean ± s.e.m. Statistical significance between two groups was determined using unpaired, two-tailed Student's t-test. * $P<0.05$; ** $P<0.01$.

Acknowledgements.

We thank A. Hein, K. Beier, I. Ginez, W. Dolci and A. Löschmann for technical assistance, and T. Sorg, X. Warot and M.F. Champy for support in generation and phenotyping of knockout mice. We acknowledge support from the Roche Research Foundation (P.P.) and the Swiss National Science Foundation and the Canton of Basel (M.A.R. and M.N.H.). We declare that no competing interests exist.

Figures and Tables

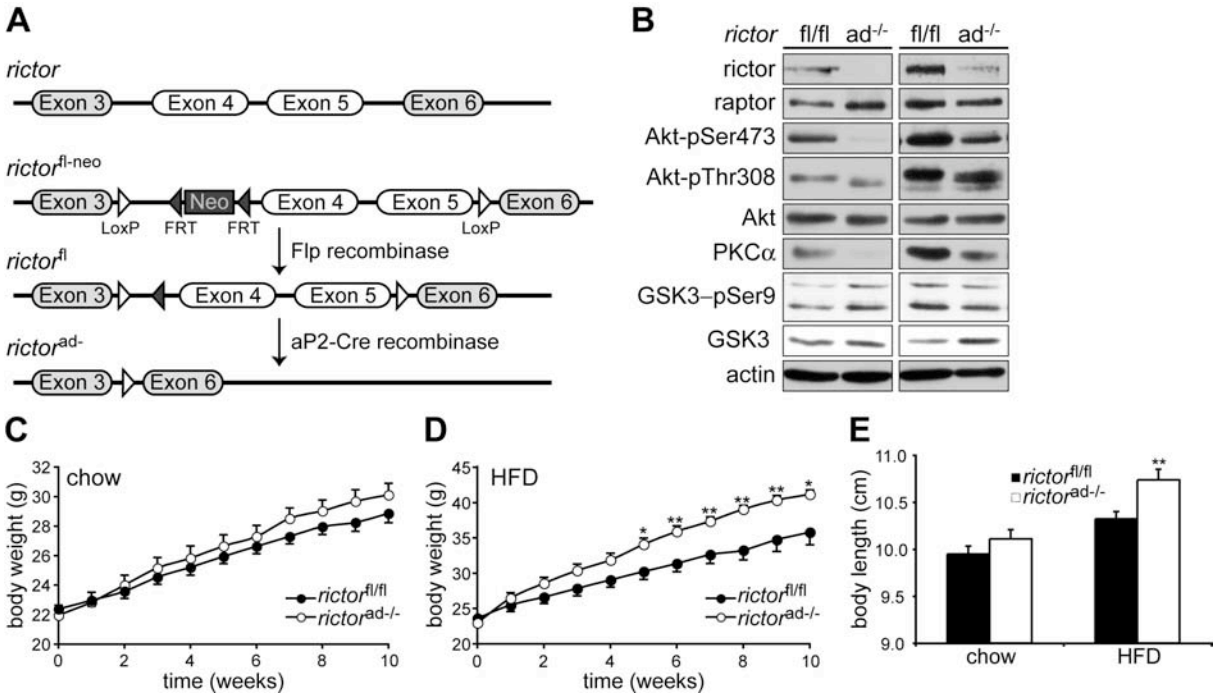

Fig. II-1. *Adipose-specific rictor knockout mice have increased body weight. (A) Adipose-specific rictor knockout mice (rictor$^{ad-/-}$) were generated using the Cre/LoxP system (see Experimental procedures). (B) Immunoblot showing knockout of rictor and impaired mTORC2 signaling in adipose tissue of two littermates. A short (right) and long (left) exposure are shown. Residual rictor protein in rictor$^{ad-/-}$ in the long exposure is likely from stromal vascular cells in the adipose tissue that do not express aP2-Cre. (C) Weight curves of rictor$^{fl/fl}$ (n=16) and rictor$^{ad-/-}$ (n=14) male mice 8 to 18 weeks of age maintained on a chow diet. (D) Weight curves of rictor$^{fl/fl}$ and rictor$^{ad-/-}$ male mice fed a HFD for 10 weeks (n=10 per genotype). (E) Body length determined by measuring nasal-to-anal distance. Mice were put on HFD at the age of 8 weeks. Values in D - F are mean ± s.e.m. *P<0.05; **P<0.01, rictor$^{ad-/-}$ vs. rictor$^{fl/fl}$.*

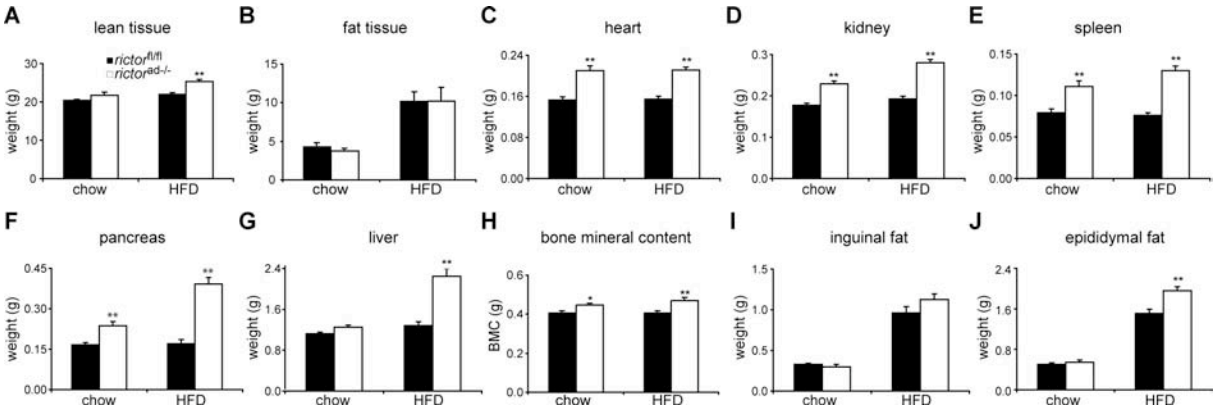

Fig. II-2. rictor$^{ad-/-}$ mice have increased lean mass. *(A and B) Lean mass (A) and fat mass (B) in rictor$^{fl/fl}$ and rictor$^{ad-/-}$ mice was determined by dexa scan analysis. Mice were maintained on a chow diet or fed a HFD for 6 weeks (n=6-8 per group). (C – J), Weight of individual organs. Individual organs were excised and weighed. Mice were maintained on a chow diet or fed a HFD for 10 weeks. Bone mineral content was determined by dexa scan analysis as in (A) and (B). Values in (A – J) are represented as mean ± s.e.m (n=11-27 per genotype; n=5 in (F)). *P<0.05; **P<0.01, rictor$^{ad-/-}$ vs. rictor$^{fl/fl}$.*

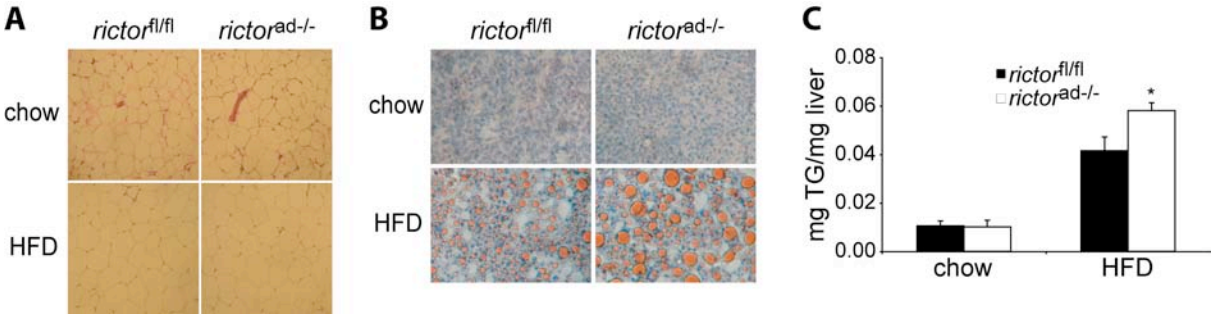

Fig. II-3. rictor$^{ad-/-}$ mice have unaltered adipose tissue morphology and increased hepatic steatosis. *(A) Representative image of H&E stained sections of epididymal fat. (B) rictor$^{ad-/-}$ and rictor$^{fl/fl}$ develop hepatic steatosis after HFD. Representative image of liver sections stained with Oil Red O and hematoxylin. (C) Quantification of liver triglycerides in mice fed a chow diet (n=4 per group) or a HFD for 10 weeks (n=16 per group).*

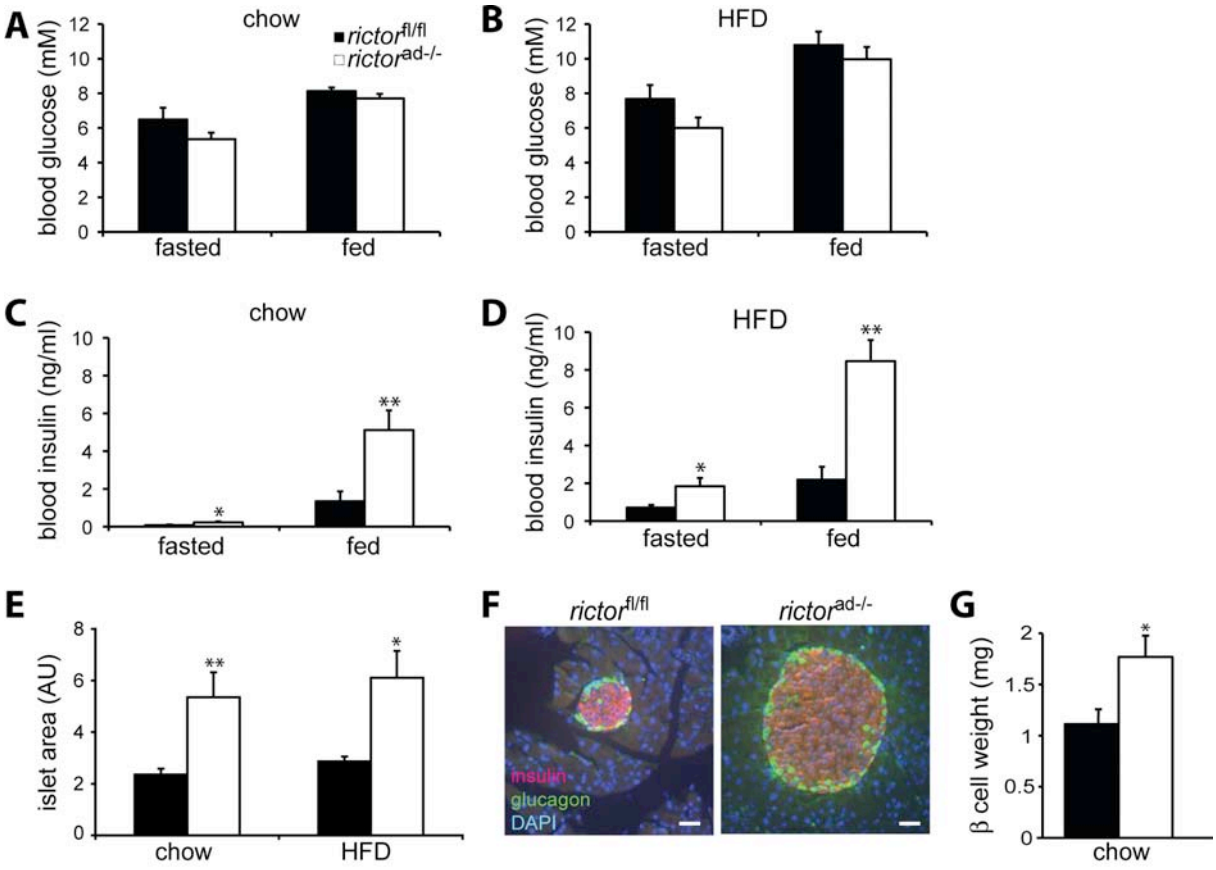

Fig. II-4. rictor$^{ad-/-}$ mice are hyperinsulinemic. *(A and B) Blood glucose from overnight fasted or fed mice either on chow diet (A) or HFD for 10 weeks (B) (n=10-15). (C and D) Blood insulin form overnight fasted or fed mice either on chow diet (C) or HFD for 10 weeks (D) (n=10). (E) Quantification of average islet area represented in arbitrary units (AU). n=3-5 per group. (F) Representative image of an islet in rictor$^{fl/fl}$ and rictor$^{ad-/-}$ mice immunostained for insulin (red) and glucagon (green). Nuclei were stained with DAPI (blue). Images were taken at the same magnification and islets are shown at the same scale. (G) Quantitative analysis of β cell mass of rictor$^{fl/fl}$ and rictor$^{ad-/-}$ mice on chow diet.*

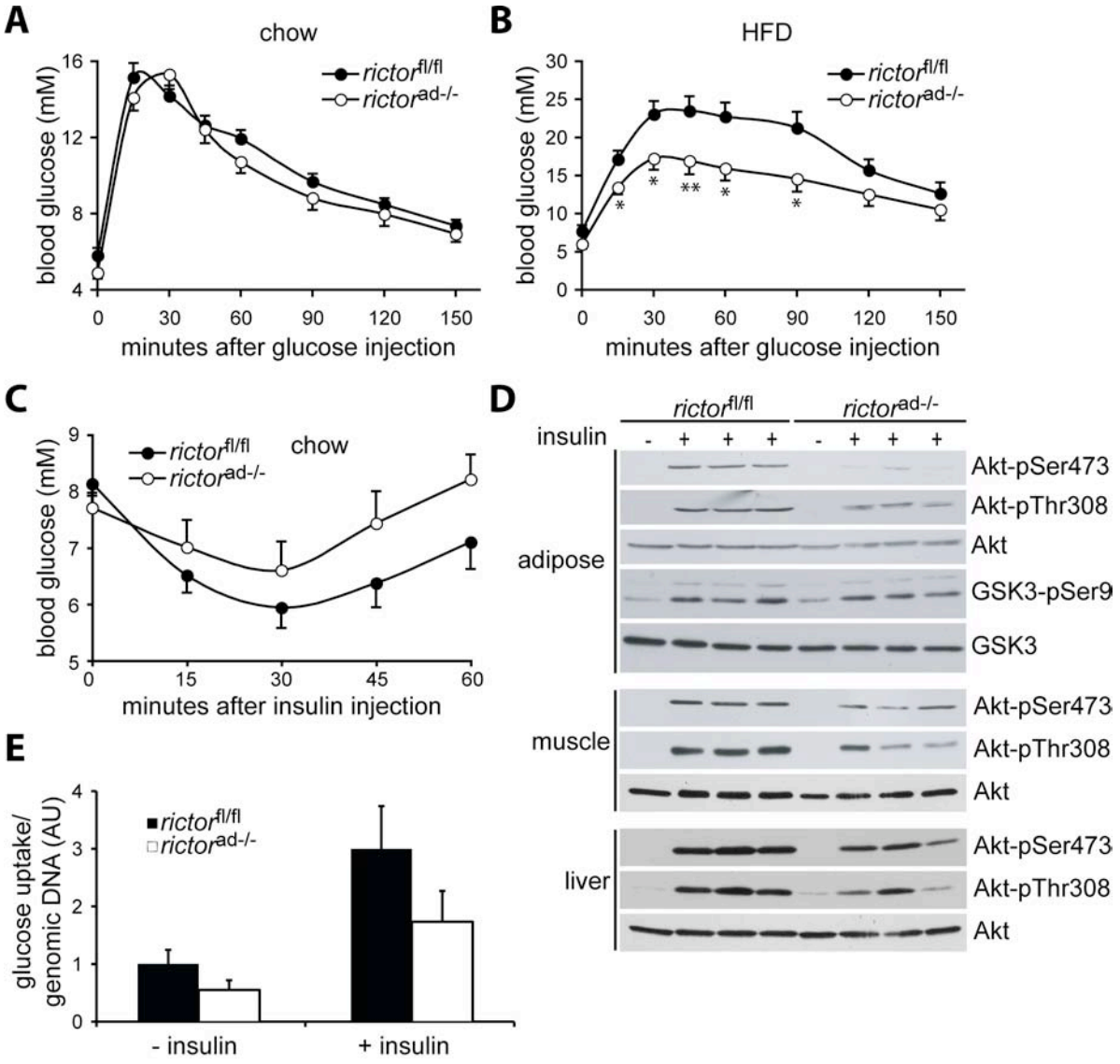

Fig. II-5. rictor$^{ad-/-}$ mice have improved glucose tolerance after HFD. *(A and B) Glucose tolerance tests in overnight-starved mice fed a chow diet (A) or HFD for 10 weeks (B). Mice were injected with glucose (2g/kg, i.p.) and blood glucose was subsequently measured at the indicated time points (n=10-16). *P<0.05, **P<0.01, rictor$^{ad-/-}$ vs. rictor$^{fl/fl}$. n=9-10 per group. (C) Insulin sensitivity test in fed mice on a chow diet. Mice were injected with insulin (0.75IU/kg, i.p.) and blood glucose was subsequently measured at the indicated time points (n=10-11, P>0.05). (D) Immunoblot of in vivo insulin stimulated adipose tissue and muscle. 21-week old mice fed a chow diet were starved over night and aneasthesized, followed by i.p. injection of saline or 150mU/g body weight insulin. After 15 minutes adipose tissue, muscle and liver were removed and snap frozen. Lysates were run on a SDS-PAGE and immunoblotted for phosphorylated and total Akt, and phosphorylated and total GSK3. (E) Basal and insulin-stimulated glucose uptake was measured on isolated adipocytes from rictor$^{fl/fl}$ and rictor$^{ad-/-}$ mice on chow diet. Glucose uptake was normalized to cell number and data are shown in arbitrary units (n=5).*

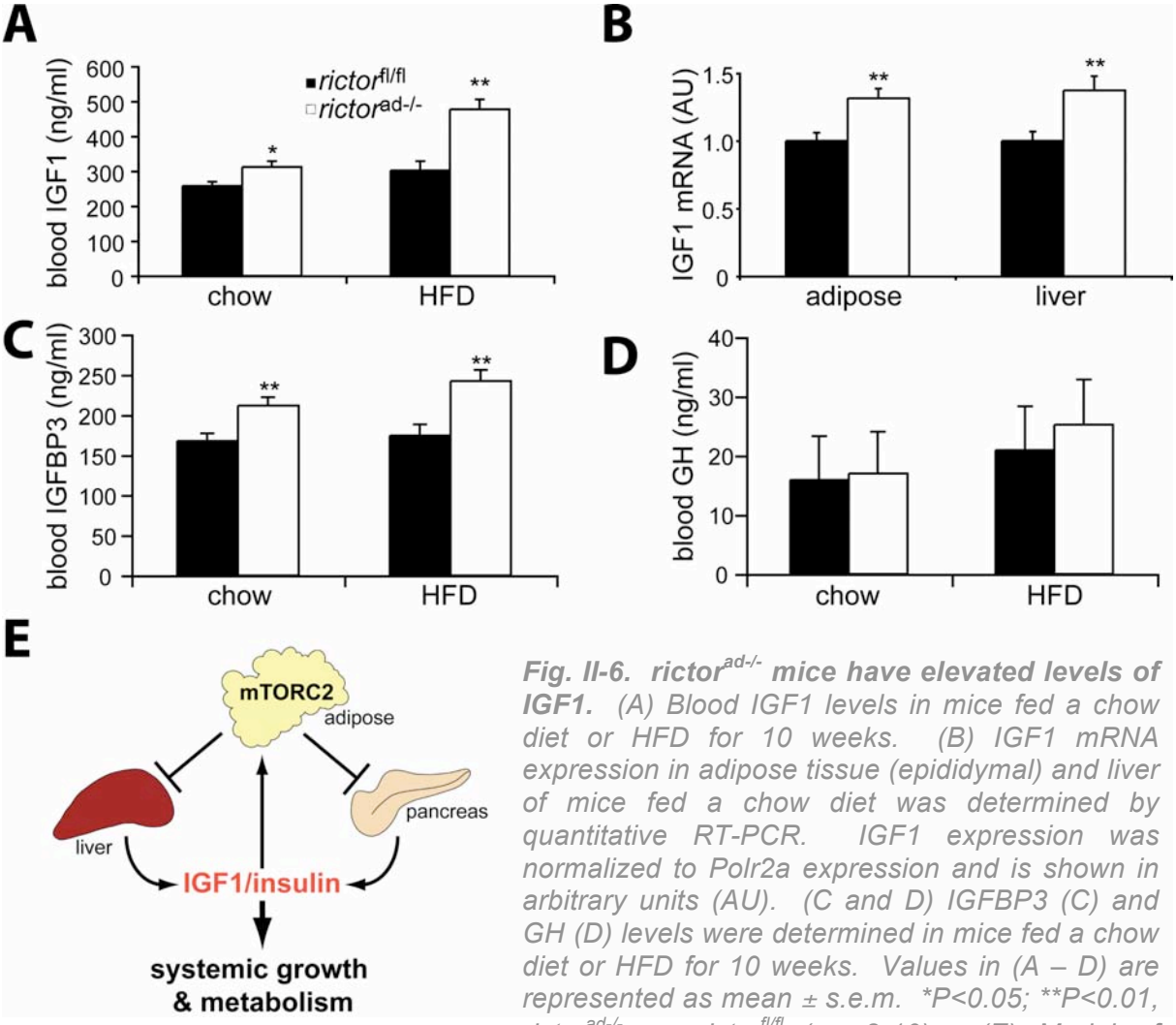

Fig. II-6. rictor$^{ad-/-}$ mice have elevated levels of IGF1. *(A) Blood IGF1 levels in mice fed a chow diet or HFD for 10 weeks. (B) IGF1 mRNA expression in adipose tissue (epididymal) and liver of mice fed a chow diet was determined by quantitative RT-PCR. IGF1 expression was normalized to Polr2a expression and is shown in arbitrary units (AU). (C and D) IGFBP3 (C) and GH (D) levels were determined in mice fed a chow diet or HFD for 10 weeks. Values in (A – D) are represented as mean ± s.e.m. *P<0.05; **P<0.01, rictor$^{ad-/-}$ vs. rictor$^{fl/fl}$ (n= 8-10). (E) Model of adipose mTORC2 regulating whole body growth. Adipose mTORC2 negatively regulates IGF1 and insulin production by liver and pancreas, respectively, and thereby controls systemic growth and metabolism.*

	chow		HFD	
	rictor$^{fl/fl}$	rictor$^{ad-/-}$	rictor$^{fl/fl}$	rictor$^{ad-/-}$
cholesterol (mg/dL)	52.1 (2.7)	88.5 (5.9) **	132.0 (6.8)	141.3 (19.8)
triglycerides (mg/dL)	88 (5.1)	93.5 (7.5)	68.7 (3.4)	69 (5.3)
free fatty acids (mM)	0.363 (0.039)	0.402 (0.026)	0.413 (0.042)	0.476 (0.035)
adiponectin (ug/ml)	59.0 (2.2)	41.6 (2.5) **	60.1 (3.9)	40.0 (2.2) **
leptin (ng/ml)	5.67 (0.87)	4.6 (0.64)	27.37 (3.44)	25.64 (1.79)
IL-6 (pg/ml)	1.95 (0.90)	1.47 (0.58)	2.63 (0.58)	3.58 (0.82)

Table II-1. Blood metabolites. *Clinical chemistry and hormone values of mice fed a chow diet or HFD for 10 weeks. Values are mean ± s.e.m (n=9-10 per group) *P<0.05, **P<0.01.*

Supplementary data

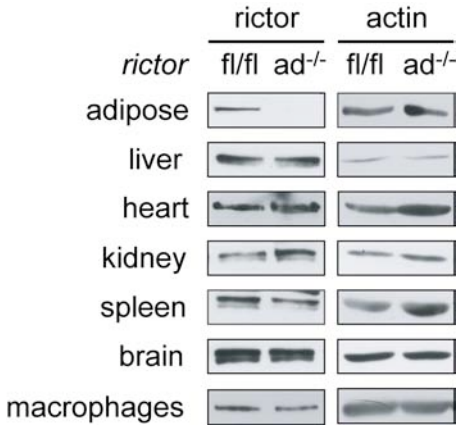

Fig. II-S1. *Immunoblot showing specific knockout of rictor in adipose tissue but not in other tissue examined.*

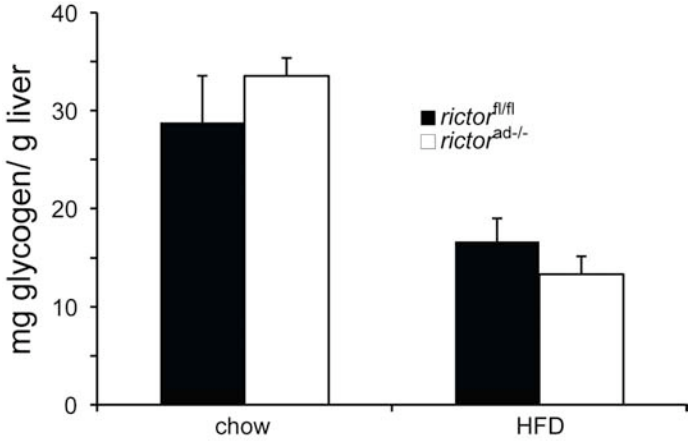

Fig. II-S2. *Quantification of hepatic glycogen content in rictor$^{ad-/-}$ and rictor$^{fl/fl}$ mice fed a chow diet (n=4 per group) or a HFD for 10 weeks (n=10 per group).*
A small piece of frozen liver tissue was dissolved at 95°C for 30 min in 0.3ml 0.5M KOH. 25μl of 6% Na_2SO_4 and 750μl 100% MeOH were added to cooled samples. Samples were incubated for 1h at -80°C and centrifuged at 14 000 rpm at 4°C for 5 min. 200μl of 2mg/ml amyloglucosidase in 0.2M sodium acetate buffer (pH 4.9) was added to the pellet for 60 min of incubation at 37°C. 10μl of sample was used for glucose assays (GAHK-20 kit, Sigma). Glycogen standard curve was prepared using glycogen (G1767, Sigma) dissolved in 0.5M KOH.

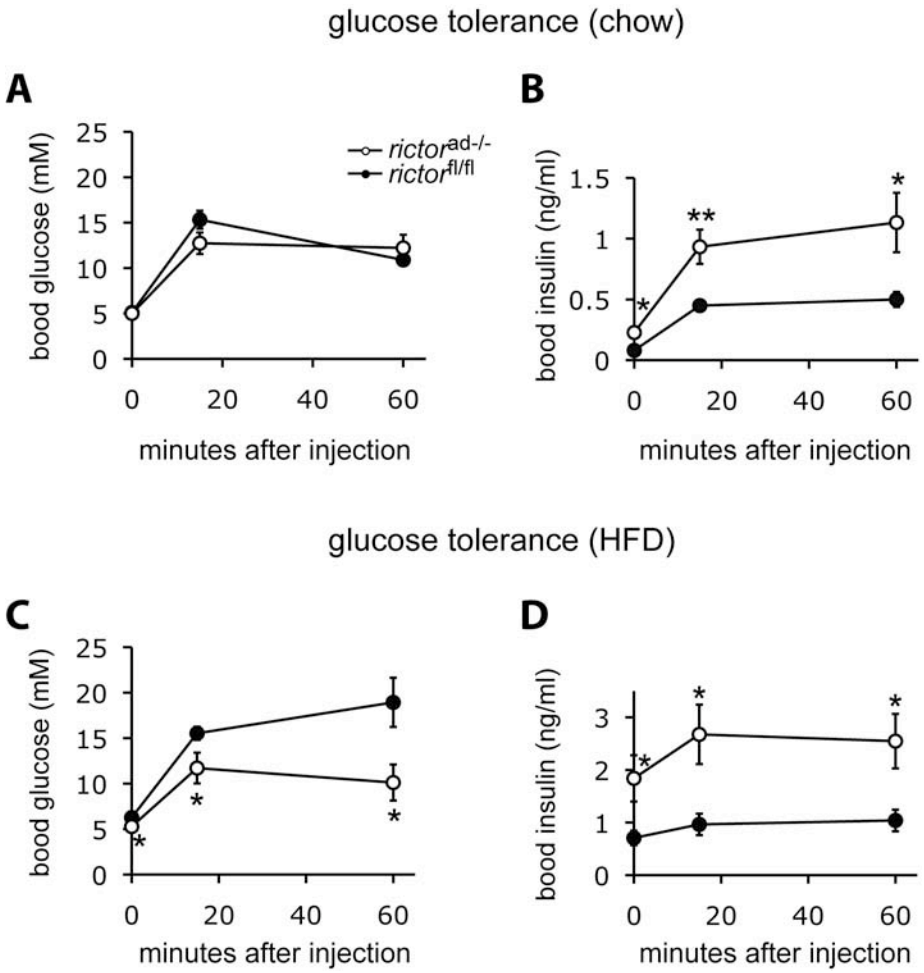

Fig. II-S3. *Glucose tolerance test in mice fed a chow diet (A and B) or HFD for ten weeks (C and D). Mice were injected with glucose (2g/kg, i.p.) and blood glucose (A and C) and insulin (B and D) were simultaneously measured at the indicated time points. *P<0.05, **P<0.01, rictor$^{ad-/-}$ vs. rictor$^{fl/fl}$. n=9-10 per group.*

Additional results

As described in the manuscript above, we suggest that mTORC2 in adipose tissue negatively regulates IGF1 and insulin production by liver and pancreas, respectively. One possibility how this regulation might occur, is that mTORC2 in adipose tissue may control expression and/or secretion of a factor(s) that in turn regulates these organs. To address this point, we undertook global gene expression analysis to identify genes for which expression is altered in adipose tissue deficient for mTORC2. We used the Affymetrix Gene Chip Mouse Gene 1.0 ST Array, which covers more than 28'000 genes. Since the growth phenotype was more pronounced on a HFD, we limited the microarray analyses to epididymal adipose tissue RNA from *rictor*$^{ad-/-}$ and *rictor*$^{fl/fl}$ mice (n=3) that were fed a HFD for 10 weeks.

We identified a set of 194 genes whose mRNA levels were upregulated at least 1.4-fold in *rictor*$^{ad-/-}$ mice compared to *rictor*$^{fl/fl}$ mice and expression of 71 of these genes was increased at least twofold. mRNAs of 217 genes were downregulated at least 1.4-fold in *rictor*$^{ad-/-}$ mice compared to *rictor*$^{fl/fl}$ mice, 33 of them at least twofold. To be of further interest as a possible candidate, genes with altered expression should initially fulfill the following requirements: (1) Altered expression has to be validated by qPCR. (2) Expression has to be altered on both diets since serum IGF1 and insulin levels were increased in *rictor*$^{ad-/-}$ mice compared to *rictor*$^{fl/fl}$ mice on a chow and high fat diet. (3) Genes with altered expression should encode for a secreted protein.

Using the IPA Software we identified at least 12 genes that were upregulated and 5 genes that were downregulated and encode for proteins with a defined location in the extracellular space. Proteins of the extracellular space include proteins that are secreted into the circulation, as well as proteins that are constituents of the extracellular matrix. We decided to validate by qPCR the mRNA levels of adiponectin and several other genes that encode for secreted proteins (Glipr1, Cilp, QPCT, RBP4, Retnla). Independently of the third criteria, we also chose two genes that were shown to be involved in regulating adipose tissue and whole body energy metabolism (Cpe and KLB). In addition, we decided to verify RBP7 gene expression by qPCR, which encodes a cellular protein and is related to RBP4, which in turn contributes to insulin resistance. RBP7 was the most strongly downregulated gene in the microarray data. The selected genes and their function are listed in Table II-S1; information was obtained from the Biobase proteome database.

The microarray data revealed a 1.5-fold decrease in adiponectin mRNA levels. This decrease correlated well with the observed decrease in serum adiponectin levels in *rictor*$^{ad-/-}$ mice compared to *rictor*$^{fl/fl}$ mice described in the manuscript above and, thus, was a good

initial control for the validation of the microarray dataset. The decrease at the transcriptional level could be confirmed by qPCR in *rictor*$^{ad-/-}$ mice compared to *rictor*$^{fl/fl}$ mice on a HFD (Fig. II-S4). However, on a chow diet mRNA levels were not significantly decreased, despite decreased serum levels, indicating that it is more difficult and not as straightforward to predict a correlation between the data obtained by microarray analysis and changes in the level of a secreted factor.

Regarding the other genes that we chose for further validation by qPCR, altered mRNA expression was confirmed for nearly all genes on mice fed a HFD. However, on a chow diet, mRNA expression of only one gene was significantly altered. RBP4 mRNA levels were significantly decreased in *rictor*$^{ad-/-}$ mice compared to *rictor*$^{fl/fl}$ mice on both diets (Fig. II-S4). RBP4 is a retinol binding protein and it is the only specific transport protein for retinol (vitamin A) in the circulation that delivers retinol to tissues (Quadro et al., 1999). More recent findings identified RBP4 as an adipokine that contributes to insulin resistance in obesity and type 2 diabetes (Yang et al., 2005). As suggested by decreased mRNA expression, *rictor*$^{ad-/-}$ mice would likely have decreased serum RBP4 levels and should therefore have enhanced insulin sensitivity. However, *rictor*$^{ad-/-}$ mice are slightly insulin resistant. Furthermore, no growth phenotype was described in mice with a full body knockout of RBP4 (Quadro et al., 1999), making it unlikely that this factor accounts for the elevated IGF1 and insulin serum levels in the *rictor*$^{ad-/-}$ mice.

Initial analysis of the microarray data revealed no promising candidate whose altered expression could account for altered levels of a secreted factor that could regulate IGF1 and insulin secretion. However, a more profound and extended analysis of the data might be required, considering the fact, as mentioned above, that serum adiponectin levels are reduced on both diets, but only on a high fat diet this is manifested also at the transcriptional level. This could also be true for many other genes, which would also not fulfill the requirements set at the beginning.

Even though the initial goal was to search for candidate genes that encode for secreted proteins, other genes appearing in the microarray dataset would also be of potential interest in further understanding the role of mTORC2 in regulating adipose tissue function. The IPA software allows the assignment of individual genes into biological function categories. An mTORC2-deficiency in adipose tissue influenced transcription of genes participating mainly in cellular movement (60 genes), cell morphology (71 genes), lipid metabolism (43 genes) and small molecule biochemistry (66 genes), suggesting that mTORC2 might have further functions in adipose tissue in addition to the ones described in this work. It should also be kept in mind that gene expression of most validated genes was altered only in *rictor*$^{ad-/-}$ mice fed a HFD, but not in *rictor*$^{ad-/-}$ mice fed a chow diet, suggesting

that mTORC2 in adipose tissue might be particularly important after a HFD challenge. This is also supported by the more pronounced growth phenotype of *rictor*$^{ad-/-}$ mice on a HFD.

Table II-S1: *Overview of genes and their function that were further analyzed by qPCR.*

Gene	Description	Fold change	Function
Glipr1	Glioma pathogenesis-related 1	+7.0	Secreted; plays a role in induction of apoptosis, regulates reactive oxygen species level, inhibits angiogenesis and promotes JUN kinase activity
QPCT	Glutaminyl-peptide cyclotransferase	+2.8	Extracellular; binds to zinc ion, may play a role in protein modification process; human QPCT gene is associated with hypertension, pheochromocytoma, and papillary thyroid carcinoma; identified in an insulinoma cell line
Cilp	Cartilage intermediate layer protein nucleotide pyrophosphohydrolase	+2.4	Secreted; human Cilp is a putative phosphoprotein phosphatase and is associated with osteoarthritis and lumbar disc disease
Cpe	Carboxypeptidase E	+2.1	Sorting receptor of the secretory pathway; enzyme responsible for final proteolytic processing step of prohormone intermediates, gene mutation is associated with hyperproinsulinemia; increase in human CPE autoantibody correlates with diabetes mellitus type 1; Cpe knockout mice become obese at app. week 10, have impaired glucose tolerance and are insulin resistant
Adipoq	Adiponectin	-1.5	Secreted; mediates glucose, cholesterol, and lipid metabolism; human ADIPOQ is associated with various cancers, diabetes, HIV infection, acromegaly, obesity, coronary, inflammatory, eating, and metabolic disorders
RBP4	Retinol binding protein 4	-2.1	Secreted; a cofactor transporter that plays a role in vitamin transport and glucose and vitamin metabolism; human RBP4 is associated with obesity and type 2 diabetes; serum levels are elevated in insulin-resistant animals
Retnla	Resistin like alpha	-2.5	Secreted; acts in protein synthesis, activation of MAPKK and PKB, regulates angiogenesis, cell differentiation and proliferation, macrophage activation, and vasoconstriction; reduced expression in adipose tissue of ob/ob and db/db mice
KLB	Klotho beta	-2.9	Transmembrane protein; coreceptor protein that binds Fgfr1 and Fgfr4, plays a role in fibroblast growth factor receptor signaling pathway, Fgf21-mediated glucose uptake, and Slc2a1 expression in adipocytes, acts as a cofactor for Fgf21 activity
RBP7	Retinol binding protein 7	-4.0	Cellular; required for retinoid incorporation into milk, may play a role in maintaining normal retinoic acid homeostasis in the heart and cardiovascular system

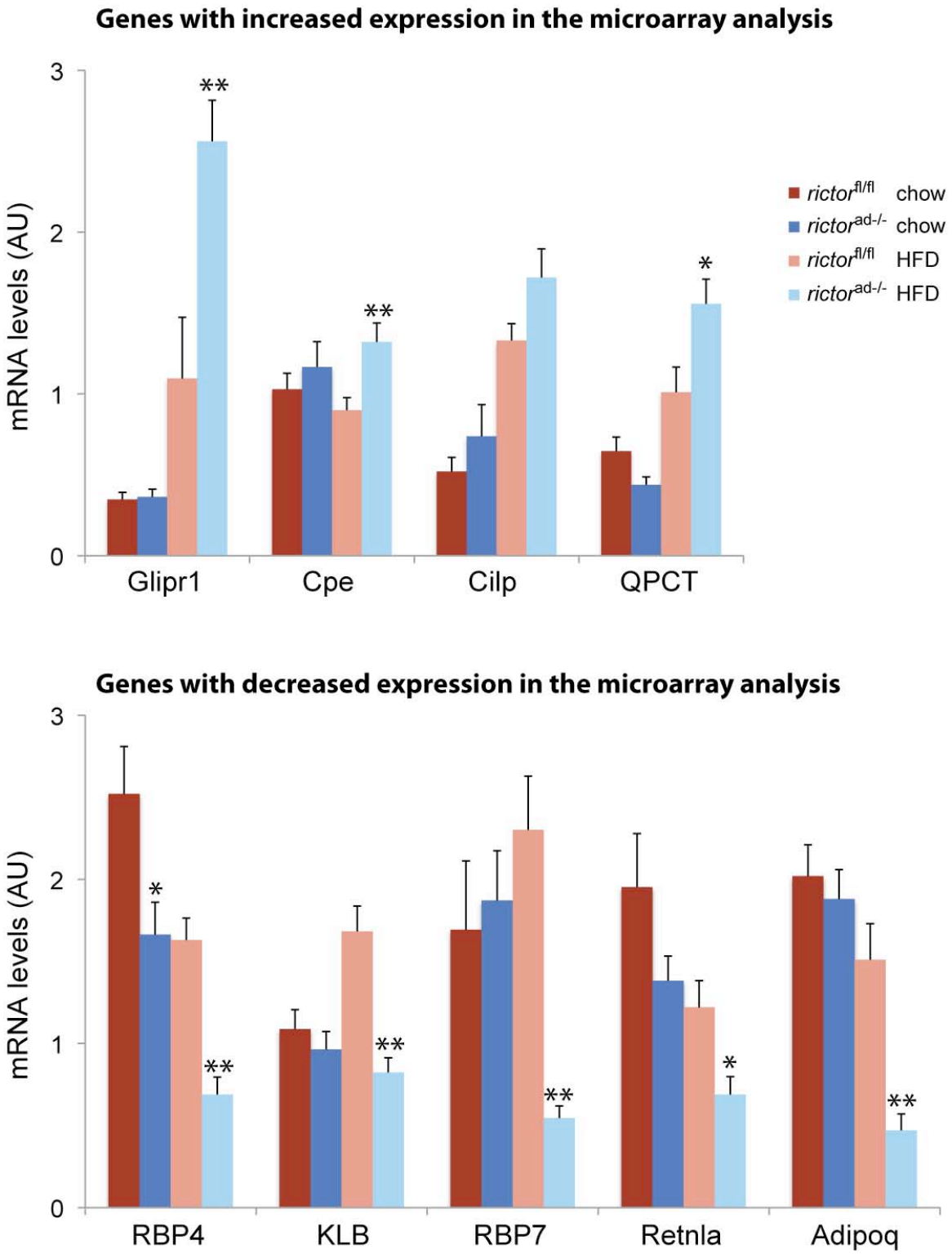

Figure II-S4: qPCR analysis of genes that revealed altered expression in the microarray analysis. *mRNA expression of indicated genes in adipose tissue of rictor$^{ad-/-}$ and rictor$^{fl/fl}$ mice fed a chow or high fat diet was determined by qPCR. Expression levels were normalized to Polr2a expression and are shown in arbitrary units (AU). The upper panel shows genes with increased expression in adipose tissue of rictor$^{ad-/-}$ mice, the lower panel shows genes with decreased expression in adipose tissue of rictor$^{ad-/-}$ mice. Values are represented as mean ± s.e.m. *P<0.05; **P<0.01 (n= 8-10). P-values refer to rictor$^{ad-/-}$ vs. rictor$^{fl/fl}$ on the individual diets.*

Supplementary Methods

Microarray

Tissue was homogenized in 1ml Trizol Reagent (Invitrogen) using a Mixer Mill MM 301 (Retsch) in the presence of 3 stainless steel beads. Isolated total RNA was furtherpurified on RNA Clean & Concentrator-5 columns (Zymo Research).

Total RNA preparations were analyzed using an Agilent 2100 bioanalyzer.

cDNA Target was synthesized, fragmented, biotin-labeled using the WT Target Labeling and Control Reagents (Affymetrix) starting from 270 ng total RNA according to the procedure described in the GeneChip Whole Transcript Sense Target Labeling Assay Manual, Version 4 (Affymetrix). A Nano-drop was used to determine all RNA and DNA concentrations. On average 33 μg of cRNA from each reaction was obtained. For each sample 10μg was used to generate cDNA. On average 7.2 μg of cDNA from each reaction was obtained. For each sample 5.5 μg of cDNA was fragmented and the resulting fragments of approximately 40-70 nucleotides were monitored with the Bioanalyzer using the RNA Nano 6000 Chip. All synthesis reactions were carried out in 0.5ml tubes using a PCR maching to ensure the highest possible degree of temperature control.

The hybridization cocktail (80ml) containing fragmented biotin-labeled target DNA at a final concentration of 25 ng/ml was transferred into Affymetrix Gene Chip Mouse Gene 1.0 ST Arrays (Affymetrix) and incubated at 45°C on a rotator in a hybridization oven 640 (Affymetrix) for 17h at 60 rpm. The arrays were washed and stained on a Fluidics Station 450 by using the Hybridization Wash and Stain Kit using the Fluidics Procedure FS450_0007. The GeneChips were processed with an Affymetrix GeneChip® Scanner 3700 7G. DAT image files of the microarrays were generated using Affymetrix GeneChip Command Console. Data were initially analyzed using XRAY software (Biotique) and later with the IPA (Ingenuity Pathways Analysis) Software (Ingenuity Systems). The IPA software allows the identification of biological networks, global functions and functional pathways of a particular dataset. The dataset representing genes with altered expression profile derived from the microarray analysis was imported into the IPA tool. The basis of the IPA program consists of the Ingenuity Pathway Knowledge Base, which is derived from known functions and interactions of genes published in the literature. Each gene product is assigned to functional categories. Some genes may participate in multiple functions and therefore some redundancy exists in gene number.

qPCR

Total RNA was isolated from frozen tissues using TriZOL reagent (Invitrogen). 3μg total RNA was reverse transcribed using Superscript II reverse transcriptase (Invitrogen) and random nonamers. qPCR was performed using the power SYBR green mix (Applied Biosystems) and normalized to Polr2a expression. The following primers were used: Polr2a sense 5'-AATCCGCATCATGAACAGTG-3', Polr2a antisense 5'-CAGCATGTTGGACTCAATGC-3'; Glipr sense 5'-AACCGAGCATTCTATCAG-3', Glipr antisense 5'-GAAGCCATCCAGACTATC-3'; Cpe sense 5'-GTGCTTTCTGCCAATCTG-3', Cpe antisense 5'-CTGCTGTCATCGTCATTC-3'; Cilp sense 5'-ATTGGCTCTATGAAATATCTCTG-3', Cilp antisense 5'-AGGCTGGACTCTTCTCAC-3'; QPCT sense 5'-ACGACTTGAGACCATTGC-3', QPCT antisense 5'-AGGACCGATAGCCATAGG-3'; RBP4 sense 5'-GCAAGACAACATCATCGC-3', RBP4 antisense 5'-GAGAAAGGAGGCTACACC-3'; KLB sense 5'-ATGCCACATACTGCTTCC-3', KLB antisense 5'-GTAGTTATGCCACACTTTCG-3'; RBP7 sense 5'-GTTACCTGGGAGAATGAC-3', RBP7 antisense 5'-TGTTGCTGGAGATGTATC-3'; Retnla sense 5'-CCTCCACTGTAACGAAGACTCTC-3', Retnla antisense 5'-GCAAAGCCACAAGCACACC-3'

Part 2: mTORC2 is required for cell migration

The following part describes the role of mTORC2 in cell migration. In collaboration with my colleague Vittoria Zinzalla we have analyzed the role of mTORC2 in cell migration in two cell lines. The first cell line is a mouse embryonic fibroblast (MEF) cell line with an inducible knockout of rictor. The second cell line is a 3T3-NIH fibroblast cell line with an inducible overexpression of activated H-Ras, which will result in transformation of these cells.
In this work, I have mainly generated and characterized the inducible MEF cell lines, while Vittoria Zinzalla has performed the experiments in the inducible H-Ras fibroblast cell line.

Manuscript in preparation

Cybulski N., Zinzalla V., Hall M.H. H-Ras transformed cells require mTOR complex 2 for cell migration

H-Ras transformed cells require mTOR complex 2 for cell migration

Nadine Cybulski[1], Vittoria Zinzalla[1], Michael N. Hall

Biozentrum, University of Basel, CH-4056 Basel, Switzerland

Running title: Loss of mTOR complex 2 decreases cell migration

Key words: mTORC2, Ras, Rho GTPases, signal transduction, cell lines

[1]These two authors contributed equally to this work.

Correspondence: Michael Hall, Klingelbergstrasse 70, CH-4056 Basel, Switzerland
E-mail: m.hall@unibas.ch, Tel: 0041 61 267 2150, Fax: 0041 61 267 21 49

Abstract

mTOR complex 2 is an essential kinase complex that is activated by growth factors and phosphorylates the kinases Akt and SGK1 at their hydrophobic motifs to fully activate them. mTORC2 is composed of mLST8, mSin1, rictor and the serine/threonine kinase mTOR. Upregulation of the mTOR signaling pathway is a common event in many tumors. However, most cancer studies addressed the role of mTOR dysregulation using the drug rapamycin, which specifically inhibits mTOR that functions in mTOR complex 1. Therefore, less is known about the role of mTORC2 in cancer biology. Here, we have generated a new mouse embryonic fibroblast cell line bearing an inducible knockout of the mTORC2 essential component *rictor* (iRicKO). Initial characterization of the cell line revealed that loss of *rictor* results in reduced cell proliferation. Furthermore, we show that loss of *rictor* increases mTORC1 assembly and S6K phosphorylation and thereby leads to increased cell size. To further investigate the role of mTORC2 in actin-dependent processes we analyzed cell motility and found reduced cell migration upon induction of *rictor* knockout. This reduced migratory behavior is due to impaired activity of the RhoGTPase family members Rac1, Cdc42, and RhoA. In addition, we also show that mTORC2 is upregulated and its activity is required for cell motility in H-Ras-transformed fibroblasts. Therefore, we provide evidence for the role of mTORC2 in cell migration of normal and oncogenic cell lines suggesting an important function of mTORC2 in the development of cancer and metastasis.

Introduction

The mammalian Target of Rapamycin (mTOR) is an evolutionary highly conserved serine/threonine kinase that is centrally involved in the control of cell growth, proliferation and metabolism (Wullschleger et al., 2006). mTOR is involved in several human diseases, including cardiovascular diseases, obesity, and diabetes, and it is estimated that 70% of human cancers are associated with malfunctions of the mTOR signaling pathway.

mTOR functions in one of two distinct multiprotein complexes named mTOR complex 1 (mTORC1) and mTORC2 (Jacinto et al., 2004; Loewith et al., 2002; Sarbassov et al., 2004). mTORC1 contains mTOR, mLST8 and raptor and is sensitive to the immunosuppressant and anti-cancer drug rapamycin. mTORC1 is activated by nutrients, such as amino acids, growth factors, such as insulin, and responds to the cellular energy

status. The most extensively studied function of mTORC1 is the regulation of translation via phosphorylation of S6 kinase and 4E-binding protein 1 (4E-BP1), but also autophagy, mitochondrial metabolism and transcription are regulated by mTORC1 (Soulard and Hall, 2007). mTORC2 contains mTOR, rictor, mLST8 and mSin1 and is resistant to direct rapamycin inhibition. Growth factors can increase mTORC2 activity, but the underlying mechanism is yet unknown. mTORC2 plays a fundamental role in controlling the activity of Akt/PKB and SGK1; it phosphorylates both kinases at their hydrophobic motif site - Akt at Ser473 and SGK1 at Ser422 (Garcia-Martinez and Alessi, 2008; Hresko and Mueckler, 2005; Sarbassov et al., 2005).

mTORC2 plays an important role in the regulation of actin cytoskeleton dynamics (Jacinto et al., 2004; Sarbassov et al., 2004). Knockdown of any component of mTORC2, including mTOR, mLST8, rictor and mSin1, causes a similar alteration of cell morphology and cell adhesion. In addition, mTORC2 regulates protein kinase C α (PKCα) activity by regulating its phosphorylation and stability (Facchinetti et al., 2008; Ikenoue et al., 2008). PKCα plays an important role in cytoskeleton organization (Larsson, 2006). However, the molecular mechanism by which mTORC2 controls actin cytoskeleton dynamics is not understood. It was shown that cell movement and chemotaxis highly depend on TORC2 in *Dictyostelium*, a powerful model organism to study these two mechanisms (Kamimura et al., 2008; Lee et al., 2005). Loss of any component of TORC2 results in loss of speed, cell polarity and directionality, overall affecting chemotaxis. Furthermore, it was shown that in *Dictyostelium* cytosolic Ras GTPases can activate TORC2 thereby leading to the activation of the PKBs, followed by several phosphorylation events on signaling proteins that regulate directed cell movement. In this study, we have analyzed the role of mTORC2 in controlling cell migration in the inducible *rictor* knockout MEF cell line. Our data suggest that mTORC2 promotes cell migration by maintaining the reciprocal balance between the RhoGTPases.

Migration of tumor cells is a prerequisite for cancer cell invasion and metastases and the underlying signaling mechanisms are complex. The role of the Ras signaling pathway in tumor initiation is well established, but whether and how it contributes to invasion and metastasis is not well understood (Campbell and Der, 2004; Furge et al., 2001). Given the more aggressive and lethal phenotype for metastatic tumors, it is necessary to gain further knowledge on the signaling mechanisms that lead to tumor cell migration and subsequently to invasion and metastases. A better understanding of these molecular mechanisms can lead to new approaches in the design of more effective therapies. *Ras*-oncogenes are mutated in 30% of all human cancers leading to constitutively activated Ras GTPases that are insensitive to GAP stimulation (Barbacid, 1987; Bos, 1989). One way how H-Ras, one of the *ras* genes, can regulate tumor metastasis is by increasing cell migration (Kim et al., 2003b; Moon et al., 2000). However, the signaling molecules implicated in these processes

have not been fully characterized. In this study, we have analyzed the role of mTORC2 in oncogenic H-Ras-mediated cell migration. Our findings suggest that H-Ras activates mTORC2, as detected by increased phosphorylation of Akt at Ser473, and that this complex is an important signaling intermediary in H-Ras-mediated cell migration.

Results

Generation of inducible raptor and rictor knockout MEF cell lines

While the function of mTORC1 can be easily studied by rapamycin treatment, we lack an mTORC2 specific inhibitor and hence we rely on genetic manipulation to study the function of mTORC2. To circumvent the rapamycin insensitivity of mTORC2 and obtain further insights into the TOR signaling branch mediated by mTORC2, we took advantage of the Cre/LoxP technology to generate inducible knockout mouse embryonic fibroblasts (MEFs) deficient for either the mTORC1-specific component *raptor* or the mTORC2-specific component *rictor.* In contrast to a constitutive knockout MEF cell line the inducible system allows a very tight and temporal regulation of recombination and thereby resulting in a very efficient knockout. Furthermore, it allows us to study immediate changes upon loss of mTOR complex integrity and circumvents the possibility of cell adaptation. Primary MEFs were isolated from mice homozygously floxed for *raptor* or *rictor,* respectively (Bentzinger et al., 2008; Polak et al., 2008). After immortalization with the simian virus 40 (SV40) large T antigen cells were infected with retroviruses carrying a tamoxifen-inducible Cre recombinase (CreERT2) and selected for stable integration (Fig. III-1A). CreERT2 is a fusion protein of a mutated estrogen receptor to the Cre recombinase, which remains in an inactive form within the cell (Feil et al., 1996; Leone et al., 2003). Only upon addition of the synthetic estrogen receptor ligand 4-hydroxytamoxifen (4-OHT) CreERT2 is activated, thereby allowing temporal control of gene recombination that leads to the knockout of the gene of interest. The resulting MEF cell lines bearing an inducible *raptor* or *rictor* knockout were named iRapKO and iRicKO, respectively.

Time course analysis of 4-OHT addition to the cell lines revealed that rictor or raptor proteins were no more detectable after 3 days of 4-OHT treatment (Fig III-1B). Therefore, for all subsequent experiments cells were pre-treated with 4-OHT for at least 3 days. Control cells without CreERT2 (control) were used to exclude any 4-OHT-induced effect that was not related to the induction of the knockout of rictor or raptor.

To verify that loss of either *raptor* or *rictor* in our cell system results in the expected changes within the mTOR signaling pathway, we analyzed the downstream targets of the

mTORC1 and mTORC2 signaling branches upon insulin stimulation. Loss of *rictor* results in a strong reduction of Akt Ser473 phosphorylation that also leads to a decrease in phosphorylation of FoxO1/3a, two Akt substrates, whose phosphorylation is affected when Akt is not phosphorylated at the hydrophobic motif (Guertin et al., 2006) (Fig III-1C). In agreement with previous findings loss of mTORC2 activity also leads to a decrease in PKCα protein levels (Facchinetti et al., 2008; Guertin et al., 2006; Jacinto et al., 2006). As expected, in 4-OHT-treated iRicKO cells mTORC1 activity and its downstream signaling remain unaffected upon insulin stimulation as observed by unchanged S6K phosphorylation. Furthermore, 4-OHT alone has no effect on the mTOR signaling pathway in control cells.

4-OHT treated iRapKO cells show a strong reduction in S6K Thr389 phosphorylation, as well as an increase in Akt Ser473 phosphorylation, confirming the specific loss of mTORC1 activity in iRapKO cells (Fig III-1D). The observed increase in Akt Ser473 phosphorylation is due to loss of the negative feedback loop that normally inhibits upstream signaling by the insulin pathway during prolonged stimulation of mTORC1 and S6K (Harrington et al., 2004; Shah et al., 2004; Um et al., 2004). Therefore, loss of mTORC1 or mTORC2 signaling in induced iRapKO or iRicKO cells, respectively, correlates well with findings from other cell systems where mTORC1 or mTORC2 activity was diminished. This allows us to use these cell lines to further study the functions of mTORC1 and mTORC2. In the following we have mainly continued on further characterizing the iRicKO cells.

Loss of rictor impairs cell proliferation

We determined whether loss of *rictor* in our cell system affects cell proliferation by comparing growth rates of untreated iRicKO cells and iRicKO cells pre-treated with 4-OHT for 3 days to induce *rictor* knockout. Equal number of cells were seeded and counted daily for 6 days. Non-induced iRicKO cells proliferated more rapidly than induced iRicKO cells (Fig. III-2A). 4-OHT alone had no effect on proliferation of control cells. Consistently, the population doubling (PD) of each group after 6 days confirmed the differences in growth rates shown by daily counts. PD for induced iRicKO cells was reduced by 30% as compared to untreated iRicKO cells, while untreated and 4-OHT-treated control cells showed exactly the same PD. To further examine the reduced proliferation rate in *rictor* knockout-induced iRicKO cells we analyzed the cell cycle distribution under normal growth conditions measuring the DNA content by flow cytometry. Loss of *rictor* resulted in an alteration in cell cycle distribution, with 45% of the cells arrested at G1/G0 phase while only 36% of untreated iRicKO cells were found in G1/G0 phase (Fig. III-2B). Furthermore, treatment with 4-OHT for 6 days, resembling a long-term loss of *rictor*, increased the ratio of cells arrested at G1/G0 phase (65%) even further. Therefore, *rictor* is required for normal cell proliferation.

Loss of rictor results in increased cell size and S6K phosphorylation.

While cell proliferation was impaired in *rictor* knockout-induced iRicKO cells due to an increase in G1/G0 arrest we furthermore found by FACS analysis that *rictor*-deficient iRicKO cells, under normal growth conditions, were increased in cell size as measured by the forward scatter distribution (Fig. III-2C). Increased cell size was apparent after 3 days of 4-OHT treatment and became even more obvious after 6 days of 4-OHT treatment. Increased cell size is indicative of increased cell growth that is mainly regulated by mTORC1 via S6K phosphorylation. Therefore, we closer analyzed S6K phosphorylation at the mTORC1 site Thr389 under normal growth conditions after loss of *rictor* in the iRicKO cells. 3 days after induction with 4-OHT there was a small but significant increase in basal S6K Thr389 phosphorylation, and this increase became even more apparent after 4 or 6 days of 4-OHT treatment (Fig. III-2C). The observed increase in S6K phosphorylation suggested an increase in mTORC1 activity. Since in *rictor*-deficient cells mTORC2 cannot be formed, we assumed that this could lead to an increase in mTORC1 assembly. To investigate this hypothesis we have treated iRicKO cells with or without 4-OHT for 6 days and subjected the cell extracts to immunoprecipitation with an anti-mTOR antibody. In untreated cells, raptor and rictor co-immunoprecipitated with mTOR, while in *rictor* deficient cells only raptor co-immunoprecipitated with mTOR. Furthermore, raptor binding to mTOR was clearly increased in 4-OHT treated cells compared to untreated cells (Fig. III-2D). Overall, we found that under normal growth conditions induction of *rictor* knockout increases mTORC1 assembly leading to increased S6K Thr389 phosphorylation and cell size.

Loss of rictor inhibits cell migration and affects RhoGTPase activity

Regulation of the actin cytoskeleton by mTORC2 has been described (Jacinto et al., 2004; Sarbassov et al., 2004); and, moreover, recent findings in *Dictyostelium* show the involvement of TORC2 in controlling cell polarity and chemotaxis (Kamimura et al., 2008; Lee et al., 2005). Therefore, we investigated the role of mTORC2 in directed cell migration in the iRicKO cells. We first treated the cells with 4-OHT for 3 days and then performed serum-induced transwell assays to determine cell motility. Induction of *rictor* knockout showed a significant decrease (app. 70%) in the number of migrating cells when stimulated with serum (Fig. III-3A). In contrast, 4-OHT did not impair serum-induced migration of control cells. This suggests that mTORC2 is involved in the regulation of cell motility.

The Rho family of GTPases, including Cdc42, Rac1 and RhoA are critical regulators of cell polarization and directional migration. The balance between the activity of these small GTPases determines the migratory behavior in fibroblasts (Fukata et al., 2003). Initial studies on the characterization of mTORC2 suggested the involvement of this complex in regulating the formation of active, GTP-bound Rac1 (Jacinto et al., 2004). Therefore, we

analyzed whether mTORC2 regulates serum-mediated cell migration in the iRicKO cells through signaling to the Rho family GTPases Cdc42, Rac1 and RhoA. After induction of *rictor* knockout with 4-OHT for 3 days we detected the activity of Cdc42, Rac1 and RhoA in serum-stimulated cells using pull down assays. Briefly, a fusion protein of glutathione-S-transferase (GST) and the CRIB domain of the Rac1/Cdc42 effector molecule PAK only allows binding of the activated, GTP-loaded Rac1/Cdc42. Similar, the Rho binding domain of the Rho effector Rhotekin fused to GST was used to pull down activated, GTP-bound RhoA. As expected, we observed that 4-OHT treatment alone did not affect Cdc42, Rac1 and RhoA activity in the control cells (Fig. III-3B). In contrast, *rictor* knockout significantly decreased the levels of GTP-bound Rac1 and Cdc42 after 5 min (Fig. III-3B) and 10 min (data not shown) of serum-stimulation, suggesting that mTORC2 is required for their activation. Since growth factor-induced Rac1 and Cdc42 activation has been shown to down-regulate RhoA in fibroblasts (Sander et al., 1999), we also analyzed RhoA activity by measuring the amount of GTP-bound RhoA after 5 min (Fig. III-3B) and 10 min (data not shown) of serum-stimulation. Induction of *rictor* knockout increased RhoA activity, while at the same time decreasing Cdc42 and Rac1 activity, suggesting that mTORC2 is required to inhibit RhoA in cells stimulated with serum. All together these data suggest that in the absence of mTORC2 the reciprocal balance between Cdc42/Rac1 and RhoA activities is lost, leading to an impaired migratory behavior in the MEFs.

mTORC2 activity is involved in oncogenic Ras induced cell migration.

The guanine nucleotide-binding protein Ras acts as a molecular switch connecting extracellular signals with a complex network of intracellular signal transduction pathways that mediate a variety of cellular responses including proliferation and differentiation (Karnoub and Weinberg, 2008). The three *Ras* proto-oncogenes, H-, N- and K-Ras, are amongst the most commonly mutated genes in all human cancers. In fact, mutational activation of Ras proteins promotes oncogenesis by disturbing a multitude of cellular processes, such as gene expression, cell cycle progression and cell proliferation, as well as cell survival and cell migration. Key steps in invasion and metastasis include alterations in cell adhesion, cell–matrix and cell–cell interactions, and the acquisition of an increased migratory phenotype. These cellular properties are regulated, in part, by Rho family GTPases and their control of actin organization. The aberrant activities of Rho GTPases have been implicated in contributing to a metastatic and invasive phenotype (Sahai and Marshall, 2002; Schmitz et al., 2000). The induction of cell migration through Ras has been shown to be critically dependent on Rho GTPase function (Zohn et al., 1998).

In the previous part we have shown that induction of *rictor* knockout inhibits cell migration and affects RhoGTPase activity. These data suggest a link between the Ras and mTORC2 signaling pathways in regulating cell migration behavior.

To investigate whether mTORC2 signaling is directly affected by Ras mutation, we analyzed Akt Ser473 phosphorylation in NIH3T3 fibroblasts harboring a tetracycline-inducible expression of a constitutively active mutant of H-Ras (NIH3T3/tet-on/H-RasG12R) (Park et al., 2006). The expression of H-RasG12R was detectable 6 h after addition of doxycycline and remained highly elevated for at least 72 h (Fig III-4A). The phosphorylation of the Ras downstream effector Erk1/2 (Thr202/Thr204), as well as the phosphorylation of Akt Ser473 were both increased within 6 h of doxycycline addition. In agreement with the role of oncogenic H-Ras in cell transformation (Park et al., 2006), the cells underwent morphological transformation between 2 and 3 days after addition of doxycycline (data not shown). To verify that mTORC2 is responsible for the phosphorylation of Akt at Ser473 after induction of oncogenic H-Ras, we analyzed the effect of *rictor* knockdown in NIH3T3tet-on/H-RasG12R cells pre-treated with doxycycline for 3 days. As shown in Fig. III-4B, siRNA-mediated knockdown of *rictor* strongly reduced the level of Akt Ser473 phosphorylation. These data establish that the increased Akt phosphorylation at Ser473 in cells expressing H-RasG12R depends on rictor and suggest that the mTORC2 signaling pathway is activated by the induction of oncogenic H-Ras.

Next, we investigated the role of mTORC2 in the control of cell migration in the inducible oncogenic H-Ras fibroblasts (NIH3T3tet-on/H-RasG12R) using two different cell motility assays. As shown by the wound healing assay, we found that in cells pre-treated with doxycycline for 3 days to induce oncogenic transformation, *rictor* knockdown significantly inhibited cell motility (Fig. III-5A). To confirm the inhibition of cell migration upon loss of mTORC2, we performed the Transwell assay. As expected, we observed that doxycycline treatment for 3 days increased serum-stimulated cell migration by 4 fold, which is in agreement with the role of oncogenic H-Ras in inducing cell migration. In contrast, a significant inhibition of cell migration was observed upon knockdown of *rictor* in oncogenic transformed cells (Fig. III-5B). Reduced expression of rictor and decreased phosphorylation of its substrate Akt at Ser473 in cells expressing siRNA was confirmed (Fig. III-5B).

As shown in Fig III-3B, induction of *rictor* knockout in the iRicKO cells inhibits cell migration and affects the activity of the RhoGTPases Rac1, Cdc42, and RhoA. Furthermore, properly activated RhoGTPases are required for the induction of cell migration through Ras. Since mTORC2 is required for the activation of cell migration by oncogenic H-Ras expression, this suggests that mTORC2 also regulates RhoGTPase activity in transformed NIH3T3tet-on/H-RasG12R cells. Therefore, we analyzed Rac1 activity in these cells upon *rictor* knockdown. In agreement with the findings in the iRicKO cells, knockdown of *rictor* in

NIH3T3tet-on/H-RasG12R cells pre-treated with doxycycline for 3 days caused a significant decrease in the level of GTP-bound Rac1 after 10 min of serum-stimulation (Fig. III-5C). Taken together, these data show that mTORC2 signaling plays an important role in the activation of RhoGTPases and cell migration by oncogenic H-Ras expression.

Discussion

Our data suggest that mTORC2 promotes cell migration by maintaining the reciprocal balance between Cdc42/Rac1 and RhoA activities in MEFs. Furthermore, we show that in fibroblasts transformed with oncogenic H-Ras the observed increases in Akt Ser473 phosphorylation and cell migration depend on mTORC2. To investigate the role of mTORC2 in cell migration we generated an inducible *rictor* knockout MEF cell line (iRicKO). Initial characterization of these cells under normal growth conditions revealed that upon loss of *rictor*, iRicKO cells showed decreased proliferation but increased cell size. The observed increase in cell size correlated with elevated S6K Thr389 phosphorylation and mTORC1 assembly. Currently, the mechanisms that regulate the formation of individual TORCs are unknown. Recent data suggest that under steady-state conditions, rictor and raptor associate with mTOR at near stoichiometric levels and that the ratios of rictor or raptor bound to mTOR seem to be inversely related in different cell lines (Sarbassov et al., 2005). However, in previous studies siRNA-mediated knockdown of rictor did not seem to significantly influence the amount of raptor subsequently associated with mTOR (Sarbassov et al., 2006). Our data, using the inducible system, are consistent with a balance between the two complexes: under normal growth conditions the induction of *rictor* knockout releases mTOR from mTORC2 and makes mTOR available to interact with raptor, thereby enhancing mTORC1 activity and cell growth. Therefore, our inducible knockout system appears to be more appropriate to study dynamic changes in mTOR signaling upon loss of *rictor*, as compared to cells with constitutive knockout of *rictor* or knockdown-mediated reduction in rictor protein levels.

Using the iRicKO cells we could show that loss of rictor inhibits cell migration and affects RhoGTPase activity. Consistent with our data, previous reports have shown that mTORC2 regulates the actin cytoskeleton through the GTPase Rac1 (Hernandez-Negrete et al., 2007; Jacinto et al., 2004). Furthermore, a recent study has identified the regulation of Rac1 activity by mTORC2 as an important mediator of PGE_2 – induced endothelial cell migration (Dada et al., 2008). In this study, we identified the molecular mechanism involved in mTORC2-mediated cell migration. Loss of rictor leads to a decrease in Cdc42/Rac1

activity and a simultaneous increase in RhoA activity upon serum stimulation. One of the major determinants of cell motility in fibroblasts is the correct reciprocal balance between Cdc42/Rac1 and Rho activities (Sander et al., 1999), and we have demonstrated that mTORC2 is required for the correct balance between the increased Cdc42/Rac1 activity and consequent RhoA inhibition. Consequently, the loss of this balance determines the impaired migration behavior in our *rictor*-deficient MEFs.

To investigate a potential role of mTORC2-dependent cell migration in cancer cells we went on to show that mTORC2 is indeed required for cell migration in fibroblasts transformed with oncogenic H-Ras. Ras interacts with and regulates multiple downstream effectors that stimulate diverse cytoplasmic signaling activities required for induction of cell migration. One of the most commonly studied signal transduction routes downstream of oncogenic Ras activation is the PI3K pathway (Rodriguez-Viciana et al., 1997). However, the PI3K-dependent molecular mechanism that leads to increased cell motility is not well understood. It was shown that PI3K can activate Rac GEFs to promote the activation of the small GTPase Rac1, leading to increased cell migration (Han et al., 1998; Nimnual et al., 1998). Our data also show that mTORC2, whose activity has been shown to be PI3K-dependent (O'Reilly et al., 2006), is required in oncogenic H-Ras mediated activation of cell motility and that RhoGTPases are affected in the absence of mTORC2. H-Ras mediated activation of cell motility is only partially rescued by rictor knockdown. This could be explained since H-Ras also activates the other complex of mTOR, mTORC1, as reported previously (Shaw and Cantley, 2006). In fact, our unpublished data and findings by others support a role for mTORC1 in cell migration that was shown to be dependent on protein synthesis via the 4E-BP1/eIF4E and S6K pathways (Liu et al., 2006). Overall, we suggest that mTORC2 can play an important role in the control of Ras-mediated tumor invasion and metastasis through the control of cell migration. Consistent with our findings in the inducible oncogenic H-Ras expressing cell line, recent reports have emphasized the role of mTORC2 in cell motility in tumors. Increased mTORC2 activity promotes glioma migration and invasiveness and rictor is required for elevated levels of phosphorylated Akt Ser473, which correlated with increased anchorage-independent growth and migration (Masri et al., 2007). Moreover, a recent study by Qiao et al. showed that mTORC2 activity regulates the metastatic potential of a series of human breast cancer cell lines that derived from successive biopsies from a single patient (Qiao et al., 2007).

Overall, our findings point out the importance of mTORC2 activity in cell migration, in particular in oncogenic H-Ras-transformed cells. We could show that mTORC2 is an important mediator of the Ras signaling pathway and is required at least for some of its oncogenic functions. The high frequency of cancers with elevated Ras signaling, as well as the generally lethal phenotype resulting from cancer spreading and metastases, emphasizes

the importance of continuously improving the design of more effective therapies. The role of mTORC2 in cancer only starts to be solved and mTORC2 could evolve into a potential drug target in the treatment of tumor invasion and metastasis.

Materials and Methods

Cell culture and transfections

NIH3T3tet-on/H-RasG12R cells were obtained from Young Yil Bahk (Park et al., 2006). The expression of H-Ras was induced by treatment of the cells with doxycycline (2μg/ml) for the indicated periods of time. All cell lines used were cultured in Dulbecco's-modified Eagle medium (DMEM, 4500mg/l glucose) supplemented with 10% fetal bovine serum (FBS). For experiments where cells were deprived of serum, cells were washed with phosphate-buffered saline, and incubated in serum-free DMEM. For restimulation experiments, cells were serum-starved for 3 hours and then treated with DMEM containing 100 mM insulin for 30 minutes. Cells were harvested with lysis buffer that contained 50 mM Tris pH 8.0, 150 mM NaCl, 0.5 mM EDTA, 1% (v/v) Triton-X-100, supplemented with protease inhibitor cocktail (Roche). Lysates were incubated for 30 minutes at 4°C, then cleared by a spin at 1000 g for 5 minutes. Supernatants were collected and used for immunoblots. Transfections with rictor and control siRNA were performed as described (Jacinto et al., 2004).

Generation of iRicKO and iRapKO, inducible Rictor and Raptor knock out MEF cell lines.

Mouse embryonic fibroblasts (MEFs) were isolated from either *rictor*^{loxP} or *raptor*^{loxP} mouse embryos at E12.5 and grown in DMEM supplemented with 10% FBS. 60mm dishes with primary cells were transfected with 2mg of a plasmid expressing simian virus 40 (SV40) large T antigen (kindly provided by Dr. David Ron; New York University School of Medicine. New York, USA). Immortalized MEFs were infected for 48h with retroviruses carrying a tamoxifen-inducible Cre recombinase (CreERT2) in the presence of 5mg/mL polybrene (Sigma). MEFs with stable integration of CreERT2 were subsequently selected in the presence of 3mg/mL puromycin (Sigma). The resulting cell lines allowing inducible Rictor or Raptor knock out were named iRicKO and iRapKO, respectively. Immortalized MEFs that were not infected were used as controls. Cells were treated for at least 3 days in the presence of 1mM 4-hydroxytamoxifen (4-OHT; Sigma) to induce Rictor or Raptor knockout.

Cloning and retroviral production

Retroviruses were produced by transfection of the ecotropic Phoenix packaging cell line with pMSCV vector. The CreERT2 fragment was cloned from pCDNA3-CreERT2 (kind gift from Dr. Patrick Matthias; Friedrich-Miescher-Institute, Basel, Switzerland) into pMSCVpuro using EcoR1 restriction sites.

Immunoblotting

Protein extracts were resolved on SDS-PAGE and transferred to nitrocellulose membranes (Whatman). Immunoblots were performed using the following antibodies: rictor, raptor, Akt pS473, FoxO3a pT32/FoxO1 pT24, FoxO3, PKCα, S6K, S6K pT389, S6, S6 pS235/236 (Cell Signaling); RhoA, H-Ras, PKCα pS657, ERK1/2, ERK1/2 pT202/Y204 (Santa Cruz); actin (Chemicon); Cdc42 (Pierce) and Rac1(Upstate).

Immunoprecipitation

mTOR immunoprecipitations were performed as described previously (Jacinto et al., 2004).

Cell proliferation assay and flow cytometry

50'000 cells that were either pre-treated or not with tamoxifen for 3 days were plated in duplicate in 60 mm dishes and cultured for up to 6 days under normal growing conditions. Cells were counted daily to establish growth curves. The number of population doublings (PD) is calculated as follows: $PD=\ln(N_f/N_i)/\ln 2$, where N_f and N_i are final and initial cell numbers, respectively.

Cell cycle distribution and cell size were analysed by flow cytometry (Becton Dickinson FACS Calibur). MEFs were harvested and stained with propidium iodide (PI) and cells were analysed for cell cycle distribution. Cell size was determined by measuring the forward scatter distribution.

Wound healing assay

Cells were cultured in six-well plates to reach confluence and then serum-starved for 24h. Wounds were introduced to the confluent monolayer of cells with a plastic pipette tip to generate a cleared scratch. The medium was changed to remove any floating or damaged cells. The cells were incubated at 37°C, and cell movement into the wound area was photographed at different time points.

Transwell assay

Cell migration assays were performed using an 8-μm pore size Transwell system (Corning Inc., Corning, NY, USA). Briefly, overnight serum-starved cells were trypsinized and

resuspended in serum-free DMEM at a density of 5 x 10^5 cells/ml. The top chamber of the Transwell was loaded with 0.1ml of the cell suspension, while the bottom chamber was loaded with 0.6ml DMEM containing 10%FBS. After incubation at 37°C for 16h noninvasive cells on the upper surface of the membrane were removed with a cotton swab. Cells that invaded were fixed with 4% paraformaldehyde, stained with crystal violet, and photographed. For quantification, the membranes were detached and solubilized in 10% acetic acid, and the intensity of the colored solution was quantified by spectrophotometrical analysis at 595 nm.

Effector domain pulldown assays

Rho, Rac, and Cdc42 activity were determined by pull down assays as described elsewhere (del Pozo et al., 2000; Ren et al., 2000). The pull down assays were performed with glutathione-agarose immobilized GST-Rhotekin (for RhoA) or GST-PAK1 (for Cdc42 or Rac1) effector domain. Total lysates and bound proteins were analyzed by immunoblotting.

Acknowledgements

We thank Drs Patrick Matthias, David Ron, Young Y. Bahk and Miguel A. del Pozo for providing cell lines and constructs. We are also grateful to Christoph Moroni for critical reading of the manuscript. We acknowledge support from the Swiss National Science Foundation and the Canton of Basel.

Figures

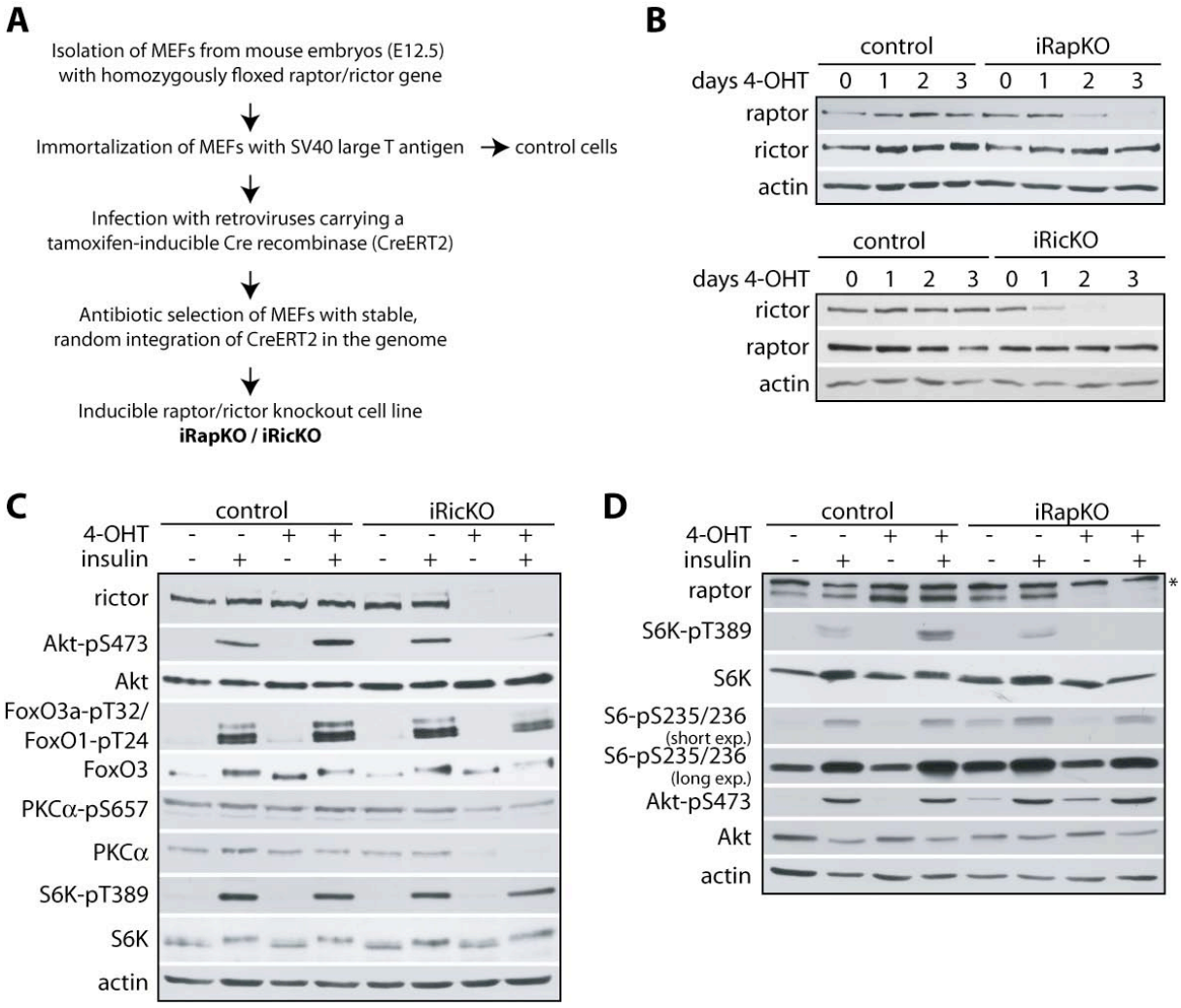

Fig. III-1. *Generation and initial characterization of iRapKO and iRicKO MEF cell lines. A, Scheme illustrating the generation of the inducible raptor and rictor knockout MEF cell lines, which were named iRapKO and iRicKO, respectively. B, Time course analysis of 4-OHT-dependent loss of raptor and rictor protein levels. Cells were treated up to 3 days with 4-OHT and protein levels were analysed by Immunoblot. C, Immunoblot analysis of the insulin stimulated mTOR signaling pathway after the induction of rictor knockout. Cells were serum starved only or starved and restimulated with insulin for 30 minutes. D, Immunoblot analysis of the insulin stimulated mTOR signaling pathway after the induction of raptor knockout. As C.*

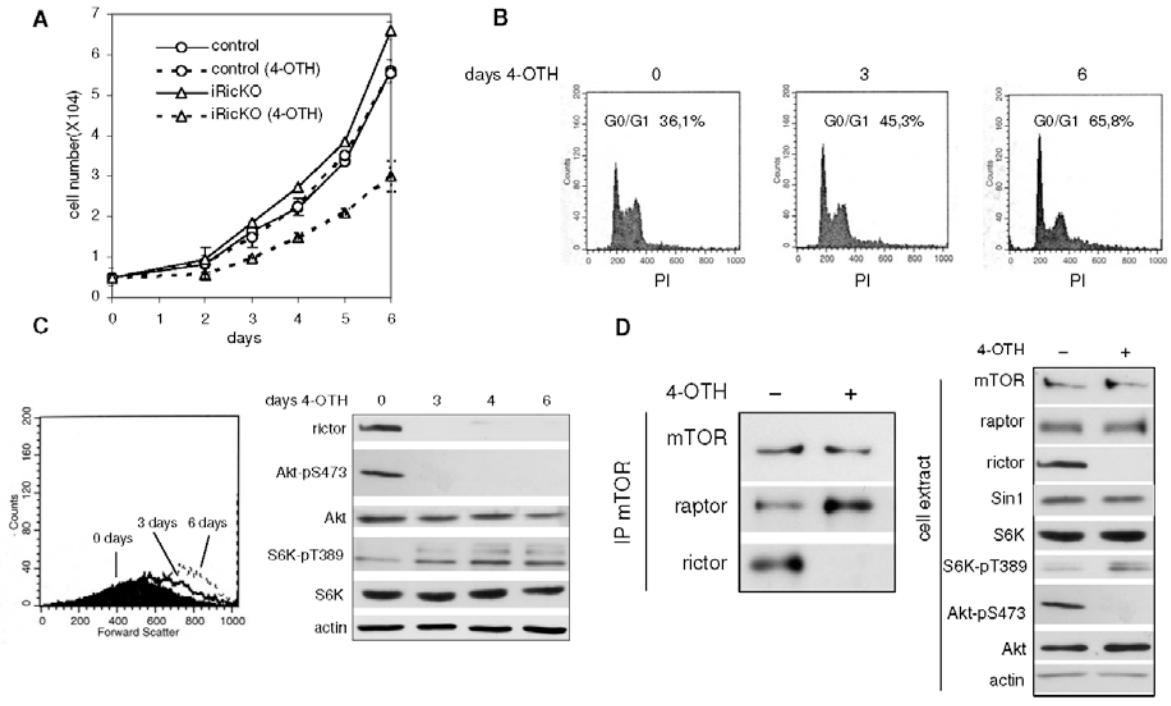

Fig. III-2. *Induction of rictor knockout impairs cell proliferation and increases cell size. A, Graphs representing growth curves of 4-OHT treated and untreated iRicKO and control cells. Cells were either pre-treated with 4-OHT for 3 days (dashed lines) or not (full lines) and then equal numbers of cells were seeded. iRicKO cells (triangle) and control cells (circle) were counted daily to establish the growth curves. B, Cell cycle distribution of untreated (day 0) and 4-OHT treated (day 3 and 6) iRicKO cells. Cells were stained with propidium iodide (PI) and cell cycle distribution was analysed by flow cytometry. Percentage of cells in G0/G1 phase is given for each graph. C, Cell size analysis of untreated (day 0) and 4-OHT treated (day 3 and 6) iRicKO cells. Cells were subjected to FACS analysis and cell size was determined by forward scatter distribution. D, Co-immunoprecipitation of raptor and rictor with mTOR. iRicKO cells were treated with (+) or without (-) 4-OHT for 6 days and cell extracts were subjected to IP by an anti mTOR antibody. Co-immunoprecipitated (IP mTOR) or total proteins (cell extract) were immunoblotted with specific antibodies to each of the TORC components and its signaling pathway. Data are representative of 2-3 independent experiments.*

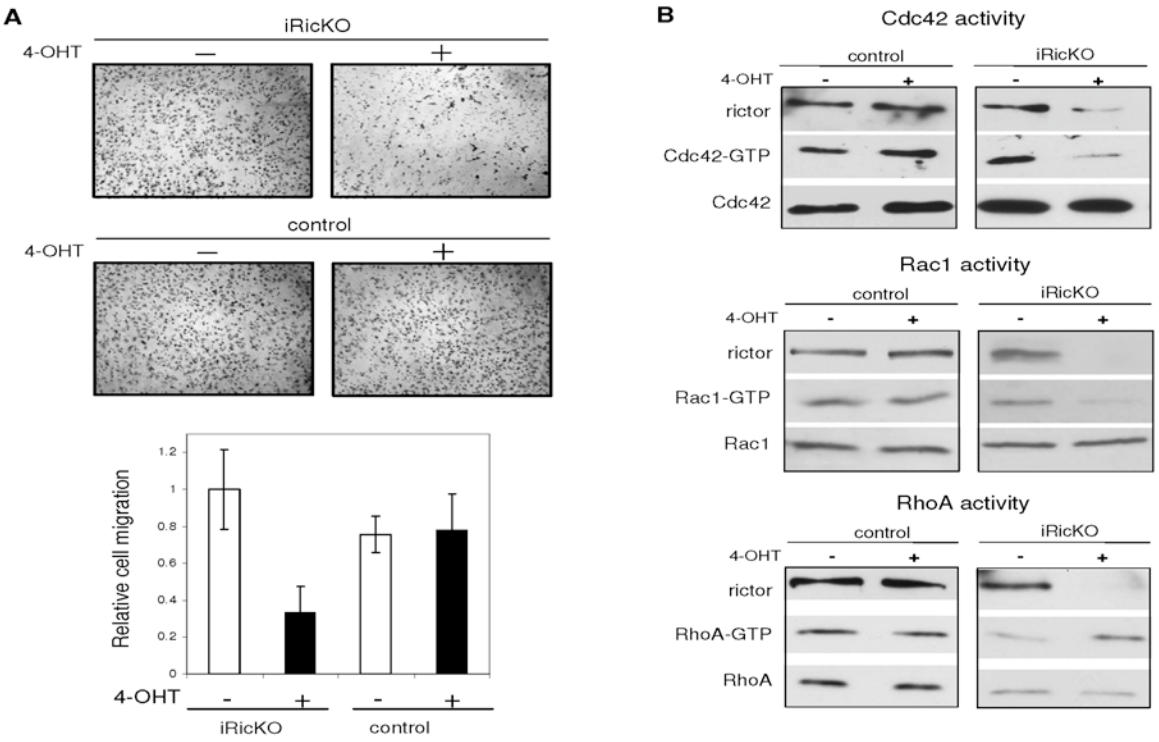

Fig. III-3. *Induction of rictor knockout decreases cell motility and affects RhoGTPase activity. A, Transwell assay of iRicKO and control cells pretreated with (+) or without (-) 4-OHT for 3 days. Equal numbers of serum starved cells were loaded on the top chamber of the transwell and allowed to migrate towards the serum (10%) containing medium in the bottom chamber for 16 h. The infiltrated membranes were stained with crystal violet and quantified. A representative image of stained filters is shown in the upper panel. B, RhoGTPase activity assays of iRicKO and control cells pretreated with (+) or without (-) 4-OHT for 3 days. GST-pull downs were performed on cell extracts from serum-starved cells that were re-stimulated for 5 minutes. To assess Cdc42/Rac1 and RhoA activation, GTP-loaded Cdc42/Rac1 and RhoA were isolated by pull-down with PAK-CRIB and Rhotekin-RBD fused to GST, respectively. Immunoblot analysis of rictor, total and GTP-bound Cdc42, Rac1 and RhoA is shown.*

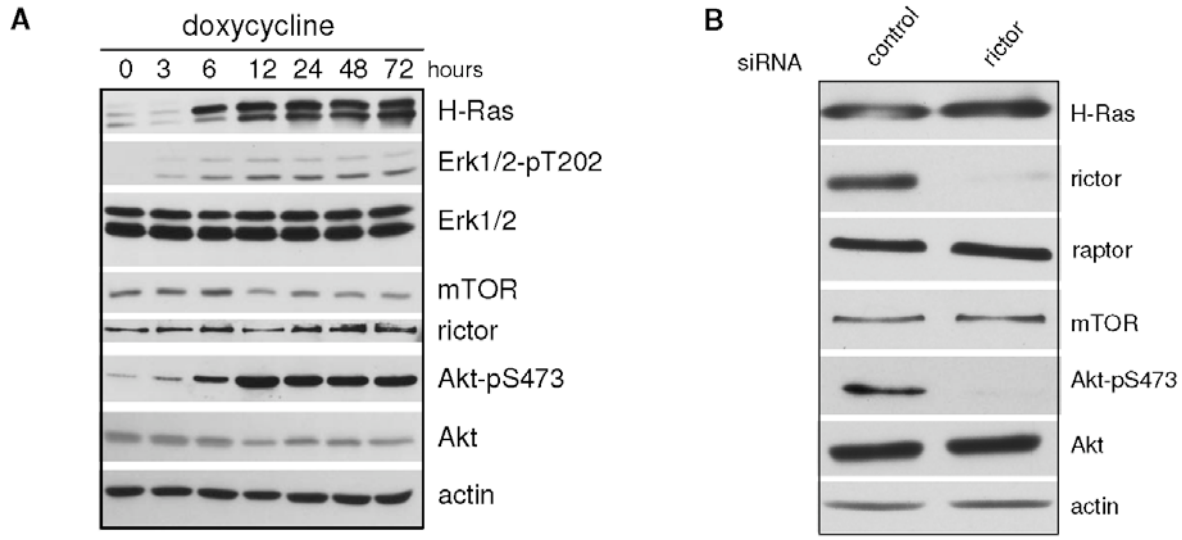

Fig. III-4. *mTORC2 activity is elevated in fibroblasts transformed with oncogenic Ras. A, Time course analysis of doxycycline-induced expression of H-RasG12R. NIH3T3 fibroblasts harbouring a tetracycline-inducible expression of a constitutively active mutant of H-Ras (NIH3T3/tet-on/H-RasG12R) were treated with doxycycline for the indicated time points. Indicated protein and phosphorylation levels were analysed by immunoblotting. B, Immunoblot analysis of NIH3T3/tet-on/H-RasG12R cells pre-treated with doxycycline for 3 days and subsequently treated with siRNA against rictor.*

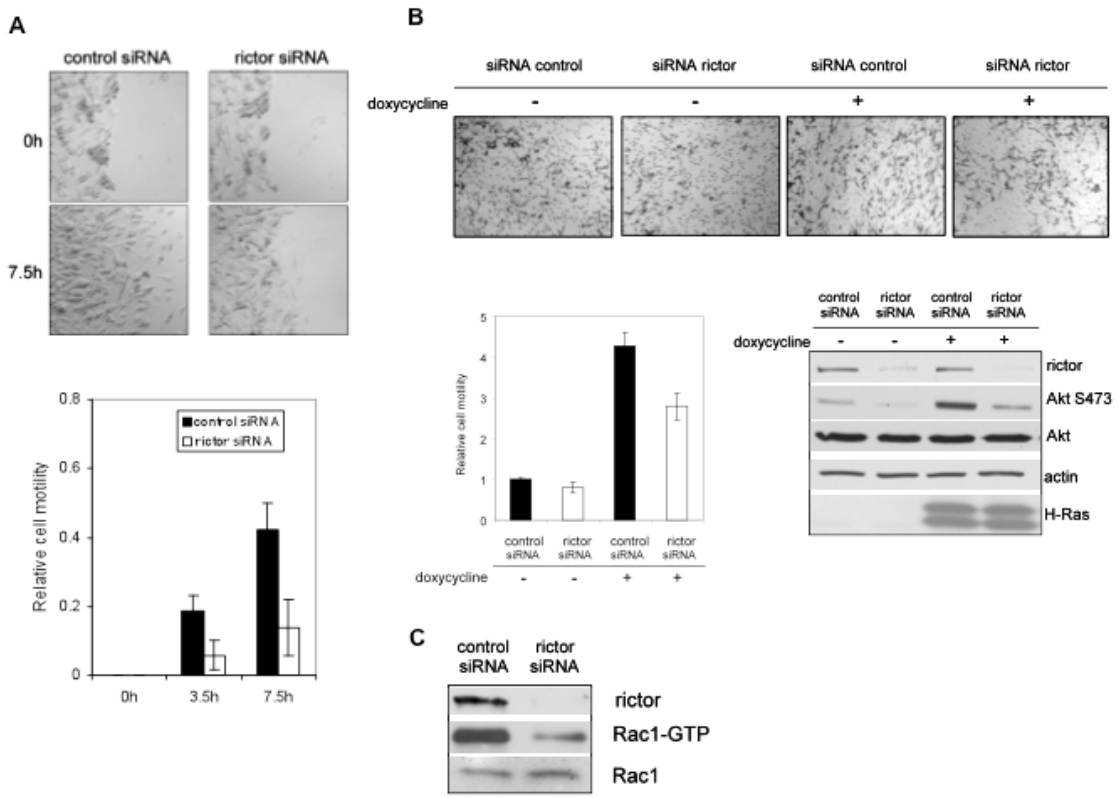

Fig. III-5. *mTORC2 activity is required for oncogenic Ras induced cell migration. A, Wound healing assay of transformed NIH3T3/tet-on/H-RasG12R treated with control or rictor siRNA. Representative images at 0 and 7.5 h time points (upper panel) after applying the wound and quantification of relative cell motility (lower panel). Bars are shown as mean ± SD. B, Transwell assay of transformed NIH3T3/tet-on/H-RasG12R treated with control or rictor siRNA. A representative image of stained filters is shown in the upper panel. The infiltrated membranes were stained with crystal violet and quantified (lower panel, left). Immunoblot anaysis is shown to confirm knockdown of rictor (lower panel, right). C, Rac1 activity assay of transformed NIH3T3/tet-on/H-RasG12R treated with control or rictor siRNA. GST-pull down was performed on cell extracts from serum-starved cells that were re-stimulated for 10 minutes. Immunoblot analysis of rictor, total and GTP-bound Rac1 is shown.*

Final conclusions & outlook

The goal of this thesis was to get a better understanding of the *in vivo* and *in vitro* functions of mTORC2.

The first part of this thesis focused on studying the *in vivo* function of mTORC2 in mice. Since a full body knockout of any mTORC2 component is embryonic lethal (Guertin et al., 2006; Jacinto et al., 2006; Shiota et al., 2006; Yang et al., 2006), we took advantage of the Cre/LoxP system that allows us to study mTORC2 function in individual tissues. In this work, we have focused on elucidating the role of mTORC2 in adipose tissue and described the phenotypic characterization of adipose-specific knockout mice of the mTORC2-specific component *rictor.* In the past years, adipose tissue has evolved as a highly metabolic tissue that plays an important role in regulating whole body energy metabolism. mTORC2 signaling is activated upon insulin stimulation and adipose tissue is one of the most insulin-sensitive tissues in the body, strongly suggesting a role for mTORC2 in this tissue.

We could show that mTORC2 in adipose tissue is important in controlling whole body metabolism and furthermore, we observed an unexpected role for adipose mTORC2 in controlling full body growth. The most surprising and striking phenotype was that *rictor*$^{ad-/-}$ mice were heavier than control *rictor*$^{fl/fl}$ mice due to an increase in lean mass. This phenotype was more pronounced on a HFD. Increased body size most likely results from increased serum levels of IGF1 in *rictor*$^{ad-/-}$ mice. Furthermore, *rictor*$^{ad-/-}$ mice were hyperinsulinemic, but glucose tolerant. Since IGF1 is mainly secreted from the liver, and insulin is secreted from the pancreas, our findings suggest the existence of an mTORC2-dependent adipose to liver/pancreas signaling axis that controls full body growth and metabolism.

In this work we did not yet succeed in identifying the signal that could derive from adipose tissue to regulate IGF1/insulin secretion from the liver/pancreas. In a first approach, we speculated that mTORC2 in adipose tissue may control expression of a secreted factor that in turn regulates the liver/pancreas. Therefore, we performed a global gene expression analysis on adipose tissue RNA from *rictor*$^{ad-/-}$ and *rictor*$^{fl/fl}$ mice. However, initial analysis of the data did not give any promising hit and a more profound and extended analysis of the data might be required. Furthermore, in the first approach, our search was limited to a secreted protein factor, but might need to be extended also to a non-protein factor such as a lipid, since lipids were shown to regulate systemic metabolism, as well. Dysregulation of lipid metabolism is a critical contributor to metabolic diseases (Ginsberg et al., 2006). For example, chronically elevated plasma free fatty acids (FFAs) from the adipose tissue are linked with the onset of peripheral insulin resistance and hepatic steatosis and have a role in the pathogenesis of type 2 diabetes (Boden and Shulman, 2002; Ginsberg et al., 2006).

More recently, a new class of hormones – lipokines – was identified in mice (Cao et al., 2008). Lipokines are adipose-derived lipid hormones that regulate systemic metabolism. Cao et al. identified C16:1n7-palmitoleate as a lipokine that improves insulin sensitivity in muscle and blocks fat accumulation in the liver. Whether mTORC2 in adipose tissue also regulates production and secretion of a lipokine remains to be determined. Interestingly, studies performed in yeast have shown that TORC2 regulates ceramide production (Aronova et al., 2008). It would be of interest to perform a lipidomic analysis of lipids in the blood or adipose tissue itself of *rictor*$^{ad-/-}$ mice and compare it to the lipid profile of *rictor*$^{fl/fl}$ mice.

The second part of this thesis focused on investigating new *in vitro* functions of mTORC2. Previous studies in yeast and mammals have shown that TORC2 is important for the regulation of actin cytoskeletal dynamics (Jacinto et al., 2004; Sarbassov et al., 2004; Schmidt et al., 1996). We have re-addressed this function of mTORC2 and studied its role in cell migration, a process that depends on a highly coordinated and dynamic actin cytoskeleton. We could show in fibroblasts that cell migration highly depends on mTORC2 and that mTORC2 regulates the activity of the main members of the RhoGTPase family, Rac1, Cdc42 and RhoA, which are critical regulators of the actin cytoskeleton. Cell migration is a central process during embryogenesis. However, developing mouse embryos lacking either one of the mTORC2 components *rictor* or *mLST8* only die around midgestation, which occurs around embryonic day E10.5, but develop normal during the early steps of embryonic development such as gastrulation, neurulation, and formation of the cardiovascular system (Guertin et al., 2006; Shiota et al., 2006). Since these morphogenetic processes involve coordinated and directional migration of cells, the observations in *rictor* and *mLST8*-deficient embryos rather suggest an mTORC2-independent regulation of cell migration during embryogenesis.

Cell migration is not only involved in physiological processes, such as embryogenesis, but also in pathophysiological processes, such as metastasis, which is the movement or spreading of cancer cells from one organ or tissue to another. In this study, we have also investigated the role of mTORC2-mediated cell migration in tumor cells using a transformed fibroblast cell line that expresses oncogenic H-Ras. Knockdown of *rictor* strongly affected cell migration in these cells and furthermore resulted in impaired activation of the RhoGTPase Rac1 upon serum stimulation, strongly suggesting a role for mTORC2 in tumor cell migration. Our *in vitro* results suggest that mTORC2 could be a potential target for the treatment of cancer and metastasis, however, further studies are now required to confirm that mTORC2-mediated cell migration plays an important role in the progression of metastases also *in vivo*.

To study cell migration in this work, we have generated an inducible *rictor* KO mouse embryonic fibroblast (MEF) cell line (iRicKO). In parallel, we have also generated an inducible *raptor* KO MEF cell line (iRapKO), and initial characterization of both is described in this work. The established cell lines are very powerful tools to study mTORC1 and mTORC2 signaling independently and are advantageous over other systems that also result in downregulation of mTORC signaling. The inducible knockout system is more efficient than a transient knockdown, which generally does not result in a complete loss of the protein. Furthermore, in contrast to a constitutive knockout MEF cell line, the inducible system allows a very tight and temporal regulation of recombination, resulting in a very efficient knockout, which allows to study immediate changes upon loss of mTOR complex integrity and circumvents the possibility of cell adaptation. In addition, isolation of constitutive knockout MEFs requires that the embryos can develop at least to E10.5. *raptor* or *mTOR* constitutive knockout MEFs do not exist, because *raptor*- or *mTOR*-deficient embryos die during early development at around E5.5- E7.0, which is too early for MEF isolation.

The inducible cell lines might be very helpful in studying global changes upon loss of either *raptor* or *rictor.* We have already performed a global gene expression analysis with iRicKO cells. However, only very few genes showed an altered expression, strongly suggesting that mTORC2 does not directly control gene transcription. The microarray analysis was performed on cells that were treated with tamoxifen for 3 days, resembling short-term loss of mTORC2. It is possible that a longer treatment, resembling a long-term loss of mTORC2, would influence expression of more genes, but these changes would be likely more indirect.

In addition to studying the mTORC1 and mTORC2-specific transcriptome, the inducible knockout MEFs could also be very helpful in studying the mTORC1 and mTORC2-specific phosphoproteome, which could lead to the identification of new downstream effectors of the mTOR signaling pathway.

References

Abraham, R.T. (2001). Cell cycle checkpoint signaling through the ATM and ATR kinases. Genes Dev *15*, 2177-2196.

Abraham, R.T. (2004). PI 3-kinase related kinases: 'big' players in stress-induced signaling pathways. DNA Repair *3*, 883-887.

Alessi, D.R., Kozlowski, M.T., Weng, Q.P., Morrice, N., and Avruch, J. (1998). 3-Phosphoinositide-dependent protein kinase 1 (PDK1) phosphorylates and activates the p70 S6 kinase in vivo and in vitro. Curr Biol *8*, 69-81.

Anderson, G.H., Veit, B., and Hanson, M.R. (2005). The Arabidopsis AtRaptor genes are essential for post-embryonic plant growth. BMC Biol *3*, 12.

Araki, T., Uesono, Y., Oguchi, T., and Toh, E.A. (2005). LAS24/KOG1, a component of the TOR complex 1 (TORC1), is needed for resistance to local anesthetic tetracaine and normal distribution of actin cytoskeleton in yeast. Genes Genet Syst *80*, 325-343.

Aronova, S., Wedaman, K., Aronov, P.A., Fontes, K., Ramos, K., Hammock, B.D., and Powers, T. (2008). Regulation of ceramide biosynthesis by TOR complex 2. Cell Metab *7*, 148-158.

Bachmann, R.A., Kim, J.H., Wu, A.L., Park, I.H., and Chen, J. (2006). A nuclear transport signal in mammalian target of rapamycin is critical for its cytoplasmic signaling to S6 kinase 1. J Biol Chem *281*, 7357-7363.

Barbacid, M. (1987). ras genes. Annu Rev Biochem *56*, 779-827.

Barquilla, A., Crespo, J.L., and Navarro, M. (2008). Rapamycin inhibits trypanosome cell growth by preventing TOR complex 2 formation. Proc Natl Acad Sci U S A *105*, 14579-14584.

Bays, H.E. (2009). "Sick fat," metabolic disease, and atherosclerosis. Am J Med *122*, S26-37.

Bentzinger, C.F., Romanino, K., Cloetta, D., Lin, S., Mascarenhas, J.B., Oliveri, F., Xia, J., Casanova, E., Costa, C.F., Brink, M.*, et al.* (2008). Skeletal muscle-specific ablation of raptor, but not of rictor, causes metabolic changes and results in muscle dystrophy. Cell Metab *8*, 411-424.

Bickle, M., Delley, P.A., Schmidt, A., and Hall, M.N. (1998). Cell wall integrity modulates RHO1 activity via the exchange factor ROM2. EMBO J *17*, 2235-2245.

Boden, G., and Shulman, G.I. (2002). Free fatty acids in obesity and type 2 diabetes: defining their role in the development of insulin resistance and beta-cell dysfunction. Eur J Clin Invest *32*, 14-23.

Bos, J.L. (1989). ras oncogenes in human cancer: a review. Cancer Res *49*, 4682-4689.

Brugarolas, J., Lei, K., Hurley, R.L., Manning, B.D., Reiling, J.H., Hafen, E., Witters, L.A., Ellisen, L.W., and Kaelin, W.G., Jr. (2004). Regulation of mTOR function in response to hypoxia by REDD1 and the TSC1/TSC2 tumor suppressor complex. Genes Dev *18*, 2893-2904.

Brunet, A., Park, J., Tran, H., Hu, L.S., Hemmings, B.A., and Greenberg, M.E. (2001). Protein kinase SGK mediates survival signals by phosphorylating the forkhead transcription factor FKHRL1 (FOXO3a). Mol Cell Biol *21*, 952-965.

Brunn, G.J., Hudson, C.C., Sekulic, A., Williams, J.M., Hosoi, H., Houghton, P.J., Lawrence, J.C., Jr., and Abraham, R.T. (1997). Phosphorylation of the translational repressor PHAS-I by the mammalian target of rapamycin. Science *277*, 99-101.

Burnett, P.E., Barrow, R.K., Cohen, N.A., Snyder, S.H., and Sabatini, D.M. (1998). RAFT1 phosphorylation of the translational regulators p70 S6 kinase and 4E-BP1. Proc Natl Acad Sci U S A *95*, 1432-1437.

Butler, A.A., and Le Roith, D. (2001). Control of growth by the somatropic axis: growth hormone and the insulin-like growth factors have related and independent roles. Annu Rev Physiol *63*, 141-164.

Byfield, M.P., Murray, J.T., and Backer, J.M. (2005). hVps34 is a nutrient-regulated lipid kinase required for activation of p70 S6 kinase. J Biol Chem *280*, 33076-33082.

Campbell, P.M., and Der, C.J. (2004). Oncogenic Ras and its role in tumor cell invasion and metastasis. Semin Cancer Biol *14*, 105-114.

Cannon, B., and Nedergaard, J. (2004). Brown adipose tissue: function and physiological significance. Physiol Rev *84*, 277-359.

Cao, H., Gerhold, K., Mayers, J.R., Wiest, M.M., Watkins, S.M., and Hotamisligil, G.S. (2008). Identification of a lipokine, a lipid hormone linking adipose tissue to systemic metabolism. Cell *134*, 933-944.

Cardenas, M.E., and Heitman, J. (1995). FKBP12-rapamycin target TOR2 is a vacuolar protein with an associated phosphatidylinositol-4 kinase activity. EMBO J *14*, 5892-5907.

Chen, E.J., and Kaiser, C.A. (2003). LST8 negatively regulates amino acid biosynthesis as a component of the TOR pathway. J Cell Biol *161*, 333-347.

Chen, L., Janetopoulos, C., Huang, Y.E., Iijima, M., Borleis, J., and Devreotes, P.N. (2003). Two phases of actin polymerization display different dependencies on PI(3,4,5)P3 accumulation and have unique roles during chemotaxis. Mol Biol Cell *14*, 5028-5037.

Chen, M.L., Xu, P.Z., Peng, X.D., Chen, W.S., Guzman, G., Yang, X., Di Cristofano, A., Pandolfi, P.P., and Hay, N. (2006). The deficiency of Akt1 is sufficient to suppress tumor development in Pten+/- mice. Genes Dev *20*, 1569-1574.

Cheng, S.W., Fryer, L.G., Carling, D., and Shepherd, P.R. (2004). Thr2446 is a novel mammalian target of rapamycin (mTOR) phosphorylation site regulated by nutrient status. J Biol Chem *279*, 15719-15722.

Chiang, G.G., and Abraham, R.T. (2005). Phosphorylation of mammalian target of rapamycin (mTOR) at Ser-2448 is mediated by p70S6 kinase. J Biol Chem *280*, 25485-25490.

Colombani, J., Raisin, S., Pantalacci, S., Radimerski, T., Montagne, J., and Leopold, P. (2003). A nutrient sensor mechanism controls Drosophila growth. Cell *114*, 739-749.

Copp, J., Manning, G., and Hunter, T. (2009). TORC-specific phosphorylation of mammalian target of rapamycin (mTOR): phospho-Ser2481 is a marker for intact mTOR signaling complex 2. Cancer Res *69*, 1821-1827.

Corradetti, M.N., Inoki, K., Bardeesy, N., DePinho, R.A., and Guan, K.L. (2004). Regulation of the TSC pathway by LKB1: evidence of a molecular link between tuberous sclerosis complex and Peutz-Jeghers syndrome. Genes Dev *18*, 1533-1538.

Cybulski, N., Polak, P., Auwerx, J., Ruegg, M.A., and Hall, M.N. (2009). mTOR complex 2 in adipose tissue negatively controls whole-body growth. Proc Natl Acad Sci U S A *106*, 9902-9907.

Dada, S., Demartines, N., and Dormond, O. (2008). mTORC2 regulates PGE2-mediated endothelial cell survival and migration. Biochem Biophys Res Commun *372*, 875-879.

del Pozo, M.A., Price, L.S., Alderson, N.B., Ren, X.D., and Schwartz, M.A. (2000). Adhesion to the extracellular matrix regulates the coupling of the small GTPase Rac to its effector PAK. EMBO J *19*, 2008-2014.

Deprost, D., Yao, L., Sormani, R., Moreau, M., Leterreux, G., Nicolai, M., Bedu, M., Robaglia, C., and Meyer, C. (2007). The Arabidopsis TOR kinase links plant growth, yield, stress resistance and mRNA translation. EMBO Rep *8*, 864-870.

Desai, B.N., Myers, B.R., and Schreiber, S.L. (2002). FKBP12-rapamycin-associated protein associates with mitochondria and senses osmotic stress via mitochondrial dysfunction. Proc Natl Acad Sci U S A *99*, 4319-4324.

DeYoung, M.P., Horak, P., Sofer, A., Sgroi, D., and Ellisen, L.W. (2008). Hypoxia regulates TSC1/2-mTOR signaling and tumor suppression through REDD1-mediated 14-3-3 shuttling. Genes Dev *22*, 239-251.

Diaz-Troya, S., Florencio, F.J., and Crespo, J.L. (2008). Target of rapamycin and LST8 proteins associate with membranes from the endoplasmic reticulum in the unicellular green alga Chlamydomonas reinhardtii. Eukaryot Cell *7*, 212-222.

Drenan, R.M., Liu, X., Bertram, P.G., and Zheng, X.F. (2004). FKBP12-rapamycin-associated protein or mammalian target of rapamycin (FRAP/mTOR) localization in the endoplasmic reticulum and the Golgi apparatus. J Biol Chem *279*, 772-778.

Duan, C., and Xu, Q. (2005). Roles of insulin-like growth factor (IGF) binding proteins in regulating IGF actions. Gen Comp Endocrinol *142*, 44-52.

Dupont, J., and Holzenberger, M. (2003). Biology of insulin-like growth factors in development. Birth Defects Res C Embryo Today *69*, 257-271.

Facchinetti, V., Ouyang, W., Wei, H., Soto, N., Lazorchak, A., Gould, C., Lowry, C., Newton, A.C., Mao, Y., Miao, R.Q.*, et al.* (2008). The mammalian target of rapamycin complex 2 controls folding and stability of Akt and protein kinase C. EMBO J *27*, 1932-1943.

Fadri, M., Daquinag, A., Wang, S., Xue, T., and Kunz, J. (2005). The pleckstrin homology domain proteins Slm1 and Slm2 are required for actin cytoskeleton organization in yeast and bind phosphatidylinositol-4,5-bisphosphate and TORC2. Mol Biol Cell *16*, 1883-1900.

Fang, Y., Park, I.H., Wu, A.L., Du, G., Huang, P., Frohman, M.A., Walker, S.J., Brown, H.A., and Chen, J. (2003). PLD1 regulates mTOR signaling and mediates Cdc42 activation of S6K1. Curr Biol *13*, 2037-2044.
Fang, Y., Vilella-Bach, M., Bachmann, R., Flanigan, A., and Chen, J. (2001). Phosphatidic acid-mediated mitogenic activation of mTOR signaling. Science *294*, 1942-1945.

Feil, R., Brocard, J., Mascrez, B., LeMeur, M., Metzger, D., and Chambon, P. (1996). Ligand-activated site-specific recombination in mice. Proc Natl Acad Sci U S A *93*, 10887-10890.

Findlay, G.M., Yan, L., Procter, J., Mieulet, V., and Lamb, R.F. (2007). A MAP4 kinase related to Ste20 is a nutrient-sensitive regulator of mTOR signalling. Biochem J *403*, 13-20.

Fonseca, B.D., Smith, E.M., Lee, V.H., MacKintosh, C., and Proud, C.G. (2007). PRAS40 is a target for mammalian target of rapamycin complex 1 and is required for signaling downstream of this complex. J Biol Chem *282*, 24514-24524.

Franz, C.M., Jones, G.E., and Ridley, A.J. (2002). Cell migration in development and disease. Dev Cell *2*, 153-158.

Frias, M.A., Thoreen, C.C., Jaffe, J.D., Schroder, W., Sculley, T., Carr, S.A., and Sabatini, D.M. (2006). mSin1 is necessary for Akt/PKB phosphorylation, and its isoforms define three distinct mTORC2s. Curr Biol *16*, 1865-1870.

Friedman, J.M. (2009). Leptin at 14 y of age: an ongoing story. Am J Clin Nutr *89*, 973S-979S.

Fukata, M., Nakagawa, M., and Kaibuchi, K. (2003). Roles of Rho-family GTPases in cell polarisation and directional migration. Curr Opin Cell Biol *15*, 590-597.

Furge, K.A., Kiewlich, D., Le, P., Vo, M.N., Faure, M., Howlett, A.R., Lipson, K.E., Woude, G.F., and Webb, C.P. (2001). Suppression of Ras-mediated tumorigenicity and metastasis through inhibition of the Met receptor tyrosine kinase. Proc Natl Acad Sci U S A *98*, 10722-10727.

Gangloff, Y.G., Mueller, M., Dann, S.G., Svoboda, P., Sticker, M., Spetz, J.F., Um, S.H., Brown, E.J., Cereghini, S., Thomas, G.*, et al.* (2004). Disruption of the mouse mTOR gene leads to early postimplantation lethality and prohibits embryonic stem cell development. Mol Cell Biol *24*, 9508-9516.

Garami, A., Zwartkruis, F.J., Nobukuni, T., Joaquin, M., Roccio, M., Stocker, H., Kozma, S.C., Hafen, E., Bos, J.L., and Thomas, G. (2003). Insulin activation of Rheb, a mediator of mTOR/S6K/4E-BP signaling, is inhibited by TSC1 and 2. Mol Cell *11*, 1457-1466.

Garaulet, M., Hernandez-Morante, J.J., de Heredia, F.P., and Tebar, F.J. (2007). Adiponectin, the controversial hormone. Public Health Nutr *10*, 1145-1150.

Garcia-Martinez, J.M., and Alessi, D.R. (2008). mTOR complex 2 (mTORC2) controls hydrophobic motif phosphorylation and activation of serum- and glucocorticoid-induced protein kinase 1 (SGK1). Biochem J *416*, 375-385.

Gingras, A.C., Gygi, S.P., Raught, B., Polakiewicz, R.D., Abraham, R.T., Hoekstra, M.F., Aebersold, R., and Sonenberg, N. (1999). Regulation of 4E-BP1 phosphorylation: a novel two-step mechanism. Genes Dev *13*, 1422-1437.

Gingras, A.C., Raught, B., Gygi, S.P., Niedzwiecka, A., Miron, M., Burley, S.K., Polakiewicz, R.D., Wyslouch-Cieszynska, A., Aebersold, R., and Sonenberg, N. (2001). Hierarchical phosphorylation of the translation inhibitor 4E-BP1. Genes Dev *15*, 2852-2864.

Ginsberg, H.N., Zhang, Y.L., and Hernandez-Ono, A. (2006). Metabolic syndrome: focus on dyslipidemia. Obesity (Silver Spring) *14 Suppl 1*, 41S-49S.

Grahammer, F., Artunc, F., Sandulache, D., Rexhepaj, R., Friedrich, B., Risler, T., McCormick, J.A., Dawson, K., Wang, J., Pearce, D.*, et al.* (2006). Renal function of gene-targeted mice lacking both SGK1 and SGK3. Am J Physiol Regul Integr Comp Physiol *290*, R945-950.

Guertin, D.A., and Sabatini, D.M. (2007). Defining the role of mTOR in cancer. Cancer Cell *12*, 9-22.

Guertin, D.A., Stevens, D.M., Saitoh, M., Kinkel, S., Crosby, K., Sheen, J.H., Mullholland, D.J., Magnuson, M.A., Wu, H., and Sabatini, D.M. (2009). mTOR complex 2 is required for the development of prostate cancer induced by Pten loss in mice. Cancer Cell *15*, 148-159.

Guertin, D.A., Stevens, D.M., Thoreen, C.C., Burds, A.A., Kalaany, N.Y., Moffat, J., Brown, M., Fitzgerald, K.J., and Sabatini, D.M. (2006). Ablation in mice of the mTORC components raptor, rictor, or mLST8 reveals that mTORC2 is required for signaling to Akt-FOXO and PKCalpha, but not S6K1. Dev Cell *11*, 859-871.

Guilherme, A., Virbasius, J.V., Puri, V., and Czech, M.P. (2008). Adipocyte dysfunctions linking obesity to insulin resistance and type 2 diabetes. Nat Rev Mol Cell Biol *9*, 367-377.

Ha, S.H., Kim, D.H., Kim, I.S., Kim, J.H., Lee, M.N., Lee, H.J., Jang, S.K., Suh, P.G., and Ryu, S.H. (2006). PLD2 forms a functional complex with mTOR/raptor to transduce mitogenic signals. Cell Signal *18*, 2283-2291.

Hajer, G.R., van Haeften, T.W., and Visseren, F.L. (2008). Adipose tissue dysfunction in obesity, diabetes, and vascular diseases. Eur Heart J *29*, 2959-2971.

Hall, A. (1998). Rho GTPases and the actin cytoskeleton. Science *279*, 509-514.

Han, J., Luby-Phelps, K., Das, B., Shu, X., Xia, Y., Mosteller, R.D., Krishna, U.M., Falck, J.R., White, M.A., and Broek, D. (1998). Role of substrates and products of PI 3-kinase in regulating activation of Rac-related guanosine triphosphatases by Vav. Science *279*, 558-560.

Hara, K., Maruki, Y., Long, X., Yoshino, K., Oshiro, N., Hidayat, S., Tokunaga, C., Avruch, J., and Yonezawa, K. (2002). Raptor, a binding partner of target of rapamycin (TOR), mediates TOR action. Cell *110*, 177-189.

Hara, K., Yonezawa, K., Weng, Q.P., Kozlowski, M.T., Belham, C., and Avruch, J. (1998). Amino acid sufficiency and mTOR regulate p70 S6 kinase and eIF-4E BP1 through a common effector mechanism. J Biol Chem *273*, 14484-14494.

Harrington, L.S., Findlay, G.M., Gray, A., Tolkacheva, T., Wigfield, S., Rebholz, H., Barnett, J., Leslie, N.R., Cheng, S., Shepherd, P.R.*, et al.* (2004). The TSC1-2 tumor suppressor controls insulin-PI3K signaling via regulation of IRS proteins. J Cell Biol *166*, 213-223.

Haruta, T., Uno, T., Kawahara, J., Takano, A., Egawa, K., Sharma, P.M., Olefsky, J.M., and Kobayashi, M. (2000). A rapamycin-sensitive pathway down-regulates insulin signaling via

phosphorylation and proteasomal degradation of insulin receptor substrate-1. Mol Endocrinol *14*, 783-794.

Haugen, F., and Drevon, C.A. (2007). The interplay between nutrients and the adipose tissue. Proc Nutr Soc *66*, 171-182.

Hayashi, T., Hatanaka, M., Nagao, K., Nakaseko, Y., Kanoh, J., Kokubu, A., Ebe, M., and Yanagida, M. (2007). Rapamycin sensitivity of the Schizosaccharomyces pombe tor2 mutant and organization of two highly phosphorylated TOR complexes by specific and common subunits. Genes Cells *12*, 1357-1370.

He, W., Barak, Y., Hevener, A., Olson, P., Liao, D., Le, J., Nelson, M., Ong, E., Olefsky, J.M., and Evans, R.M. (2003). Adipose-specific peroxisome proliferator-activated receptor gamma knockout causes insulin resistance in fat and liver but not in muscle. Proc Natl Acad Sci U S A *100*, 15712-15717.

Heasman, S.J., and Ridley, A.J. (2008). Mammalian Rho GTPases: new insights into their functions from in vivo studies. Nat Rev Mol Cell Biol *9*, 690-701.

Heitman, J., Movva, N.R., and Hall, M.N. (1991). Targets for cell cycle arrest by the immunosuppressant rapamycin in yeast. Science *253*, 905-909.

Helliwell, S.B., Howald, I., Barbet, N., and Hall, M.N. (1998a). TOR2 is part of two related signaling pathways coordinating cell growth in Saccharomyces cerevisiae. Genetics *148*, 99-112.

Helliwell, S.B., Schmidt, A., Ohya, Y., and Hall, M.N. (1998b). The Rho1 effector Pkc1, but not Bni1, mediates signalling from Tor2 to the actin cytoskeleton. Curr Biol *8*, 1211-1214.

Hernandez-Negrete, I., Carretero-Ortega, J., Rosenfeldt, H., Hernandez-Garcia, R., Calderon-Salinas, J.V., Reyes-Cruz, G., Gutkind, J.S., and Vazquez-Prado, J. (2007). P-Rex1 links mammalian target of rapamycin signaling to Rac activation and cell migration. J Biol Chem *282*, 23708-23715.

Hietakangas, V., and Cohen, S.M. (2007). Re-evaluating AKT regulation: role of TOR complex 2 in tissue growth. Genes Dev *21*, 632-637.

Hoeller, O., and Kay, R.R. (2007). Chemotaxis in the absence of PIP3 gradients. Curr Biol *17*, 813-817.

Holz, M.K., and Blenis, J. (2005). Identification of S6 kinase 1 as a novel mammalian target of rapamycin (mTOR)-phosphorylating kinase. J Biol Chem *280*, 26089-26093.

Hresko, R.C., and Mueckler, M. (2005). mTOR.RICTOR is the Ser473 kinase for Akt/protein kinase B in 3T3-L1 adipocytes. J Biol Chem *280*, 40406-40416.

Huang, J., Dibble, C.C., Matsuzaki, M., and Manning, B.D. (2008). The TSC1-TSC2 complex is required for proper activation of mTOR complex 2. Mol Cell Biol *28*, 4104-4115.

Ikenoue, T., Inoki, K., Yang, Q., Zhou, X., and Guan, K.L. (2008). Essential function of TORC2 in PKC and Akt turn motif phosphorylation, maturation and signalling. EMBO J *27*, 1919-1931.

Inoki, K., Corradetti, M.N., and Guan, K.L. (2005). Dysregulation of the TSC-mTOR pathway in human disease. Nat Genet *37*, 19-24.

Inoki, K., Li, Y., Xu, T., and Guan, K.L. (2003a). Rheb GTPase is a direct target of TSC2 GAP activity and regulates mTOR signaling. Genes Dev *17*, 1829-1834.

Inoki, K., Li, Y., Zhu, T., Wu, J., and Guan, K.L. (2002). TSC2 is phosphorylated and inhibited by Akt and suppresses mTOR signalling. Nat Cell Biol *4*, 648-657.

Inoki, K., Ouyang, H., Zhu, T., Lindvall, C., Wang, Y., Zhang, X., Yang, Q., Bennett, C., Harada, Y., Stankunas, K.*, et al.* (2006). TSC2 integrates Wnt and energy signals via a coordinated phosphorylation by AMPK and GSK3 to regulate cell growth. Cell *126*, 955-968.

Inoki, K., Zhu, T., and Guan, K.L. (2003b). TSC2 mediates cellular energy response to control cell growth and survival. Cell *115*, 577-590.

Isotani, S., Hara, K., Tokunaga, C., Inoue, H., Avruch, J., and Yonezawa, K. (1999). Immunopurified mammalian target of rapamycin phosphorylates and activates p70 S6 kinase alpha in vitro. J Biol Chem *274*, 34493-34498.

Jacinto, E., Facchinetti, V., Liu, D., Soto, N., Wei, S., Jung, S.Y., Huang, Q., Qin, J., and Su, B. (2006). SIN1/MIP1 maintains rictor-mTOR complex integrity and regulates Akt phosphorylation and substrate specificity. Cell *127*, 125-137.

Jacinto, E., Loewith, R., Schmidt, A., Lin, S., Ruegg, M.A., Hall, A., and Hall, M.N. (2004). Mammalian TOR complex 2 controls the actin cytoskeleton and is rapamycin insensitive. Nat Cell Biol *6*, 1122-1128.

Jacinto, E., and Lorberg, A. (2008). TOR regulation of AGC kinases in yeast and mammals. Biochem J *410*, 19-37.

Jaffe, A.B., and Hall, A. (2005). Rho GTPases: biochemistry and biology. Annu Rev Cell Dev Biol *21*, 247-269.

Jones, K.T., Greer, E.R., Pearce, D., and Ashrafi, K. (2009). Rictor/TORC2 regulates Caenorhabditis elegans fat storage, body size, and development through sgk-1. PLoS Biol *7*, e60.

Kam, Y., and Exton, J.H. (2004). Role of phospholipase D1 in the regulation of mTOR activity by lysophosphatidic acid. FASEB J *18*, 311-319.

Kamada, Y., Fujioka, Y., Suzuki, N.N., Inagaki, F., Wullschleger, S., Loewith, R., Hall, M.N., and Ohsumi, Y. (2005). Tor2 directly phosphorylates the AGC kinase Ypk2 to regulate actin polarization. Mol Cell Biol *25*, 7239-7248.

Kamimura, Y., Xiong, Y., Iglesias, P.A., Hoeller, O., Bolourani, P., and Devreotes, P.N. (2008). PIP3-independent activation of TorC2 and PKB at the cell's leading edge mediates chemotaxis. Curr Biol *18*, 1034-1043.

Karnoub, A.E., and Weinberg, R.A. (2008). Ras oncogenes: split personalities. Nat Rev Mol Cell Biol *9*, 517-531.

Kawai, M., Nakashima, A., Ueno, M., Ushimaru, T., Aiba, K., Doi, H., and Uritani, M. (2001). Fission yeast tor1 functions in response to various stresses including nitrogen starvation, high osmolarity, and high temperature. Curr Genet *39*, 166-174.

Keith, C.T., and Schreiber, S.L. (1995). PIK-related kinases: DNA repair, recombination, and cell cycle checkpoints. Science *270*, 50-51.

Kershaw, E.E., and Flier, J.S. (2004). Adipose tissue as an endocrine organ. J Clin Endocrinol Metab *89*, 2548-2556.

Kim, D.H., Sarbassov, D.D., Ali, S.M., King, J.E., Latek, R.R., Erdjument-Bromage, H., Tempst, P., and Sabatini, D.M. (2002). mTOR interacts with raptor to form a nutrient-sensitive complex that signals to the cell growth machinery. Cell *110*, 163-175.

Kim, D.H., Sarbassov, D.D., Ali, S.M., Latek, R.R., Guntur, K.V., Erdjument-Bromage, H., Tempst, P., and Sabatini, D.M. (2003a). GbetaL, a positive regulator of the rapamycin-sensitive pathway required for the nutrient-sensitive interaction between raptor and mTOR. Mol Cell *11*, 895-904.

Kim, E., Goraksha-Hicks, P., Li, L., Neufeld, T.P., and Guan, K.L. (2008). Regulation of TORC1 by Rag GTPases in nutrient response. Nat Cell Biol *10*, 935-945.

Kim, M.S., Lee, E.J., Kim, H.R., and Moon, A. (2003b). p38 kinase is a key signaling molecule for H-Ras-induced cell motility and invasive phenotype in human breast epithelial cells. Cancer Res *63*, 5454-5461.

Kloting, N., Koch, L., Wunderlich, T., Kern, M., Ruschke, K., Krone, W., Bruning, J.C., and Bluher, M. (2008). Autocrine IGF-1 action in adipocytes controls systemic IGF-1 concentrations and growth. Diabetes *57*, 2074-2082.

Kumar, A., Harris, T.E., Keller, S.R., Choi, K.M., Magnuson, M.A., and Lawrence, J.C., Jr. (2008). Muscle-specific deletion of rictor impairs insulin-stimulated glucose transport and enhances Basal glycogen synthase activity. Mol Cell Biol *28*, 61-70.

Kunz, J., Henriquez, R., Schneider, U., Deuter-Reinhard, M., Movva, N.R., and Hall, M.N. (1993). Target of rapamycin in yeast, TOR2, is an essential phosphatidylinositol kinase homolog required for G1 progression. Cell *73*, 585-596.

Kunz, J., Schneider, U., Howald, I., Schmidt, A., and Hall, M.N. (2000). HEAT repeats mediate plasma membrane localization of Tor2p in yeast. J Biol Chem *275*, 37011-37020.

Ladwein, M., and Rottner, K. (2008). On the Rho'd: the regulation of membrane protrusions by Rho-GTPases. FEBS Lett *582*, 2066-2074.

Larsson, C. (2006). Protein kinase C and the regulation of the actin cytoskeleton. Cell Signal *18*, 276-284.

Lee, G., and Chung, J. (2007). Discrete functions of rictor and raptor in cell growth regulation in Drosophila. Biochem Biophys Res Commun *357*, 1154-1159.

Lee, S., Comer, F.I., Sasaki, A., McLeod, I.X., Duong, Y., Okumura, K., Yates, J.R., 3rd, Parent, C.A., and Firtel, R.A. (2005). TOR complex 2 integrates cell movement during chemotaxis and signal relay in Dictyostelium. Mol Biol Cell *16*, 4572-4583.

Leone, D.P., Genoud, S., Atanasoski, S., Grausenburger, R., Berger, P., Metzger, D., Macklin, W.B., Chambon, P., and Suter, U. (2003). Tamoxifen-inducible glia-specific Cre mice for somatic mutagenesis in oligodendrocytes and Schwann cells. Mol Cell Neurosci *22*, 430-440.

Liao, L., Dearth, R.K., Zhou, S., Britton, O.L., Lee, A.V., and Xu, J. (2006). Liver-specific overexpression of the insulin-like growth factor-I enhances somatic growth and partially prevents the effects of growth hormone deficiency. Endocrinology *147*, 3877-3888.

Lingohr, M.K., Buettner, R., and Rhodes, C.J. (2002). Pancreatic beta-cell growth and survival - a role in obesity-linked type 2 diabetes? Trends Mol Med *8*, 375-384.

Liu, L., Li, F., Cardelli, J.A., Martin, K.A., Blenis, J., and Huang, S. (2006). Rapamycin inhibits cell motility by suppression of mTOR-mediated S6K1 and 4E-BP1 pathways. Oncogene *25*, 7029-7040.

Loewith, R., Jacinto, E., Wullschleger, S., Lorberg, A., Crespo, J.L., Bonenfant, D., Oppliger, W., Jenoe, P., and Hall, M.N. (2002). Two TOR complexes, only one of which is rapamycin sensitive, have distinct roles in cell growth control. Mol Cell *10*, 457-468.

Long, X., Lin, Y., Ortiz-Vega, S., Yonezawa, K., and Avruch, J. (2005a). Rheb binds and regulates the mTOR kinase. Curr Biol *15*, 702-713.

Long, X., Ortiz-Vega, S., Lin, Y., and Avruch, J. (2005b). Rheb binding to mammalian target of rapamycin (mTOR) is regulated by amino acid sufficiency. J Biol Chem *280*, 23433-23436.

Long, X., Spycher, C., Han, Z.S., Rose, A.M., Muller, F., and Avruch, J. (2002). TOR deficiency in C. elegans causes developmental arrest and intestinal atrophy by inhibition of mRNA translation. Curr Biol *12*, 1448-1461.

Luo, G., Gruhler, A., Liu, Y., Jensen, O.N., and Dickson, R.C. (2008). The sphingolipid long-chain base-Pkh1/2-Ypk1/2 signaling pathway regulates eisosome assembly and turnover. J Biol Chem *283*, 10433-10444.

Mahfouz, M.M., Kim, S., Delauney, A.J., and Verma, D.P. (2006). Arabidopsis TARGET OF RAPAMYCIN interacts with RAPTOR, which regulates the activity of S6 kinase in response to osmotic stress signals. Plant Cell *18*, 477-490.

Manning, B.D., and Cantley, L.C. (2003). Rheb fills a GAP between TSC and TOR. Trends Biochem Sci *28*, 573-576.

Manning, B.D., Tee, A.R., Logsdon, M.N., Blenis, J., and Cantley, L.C. (2002). Identification of the tuberous sclerosis complex-2 tumor suppressor gene product tuberin as a target of the phosphoinositide 3-kinase/akt pathway. Mol Cell *10*, 151-162.

Masri, J., Bernath, A., Martin, J., Jo, O.D., Vartanian, R., Funk, A., and Gera, J. (2007). mTORC2 activity is elevated in gliomas and promotes growth and cell motility via overexpression of rictor. Cancer Res *67*, 11712-11720.

Matsuo, T., Kubo, Y., Watanabe, Y., and Yamamoto, M. (2003). Schizosaccharomyces pombe AGC family kinase Gad8p forms a conserved signaling module with TOR and PDK1-like kinases. EMBO J *22*, 3073-3083.

Matsuo, T., Otsubo, Y., Urano, J., Tamanoi, F., and Yamamoto, M. (2007). Loss of the TOR kinase Tor2 mimics nitrogen starvation and activates the sexual development pathway in fission yeast. Mol Cell Biol *27*, 3154-3164.

Mattila, P.K., and Lappalainen, P. (2008). Filopodia: molecular architecture and cellular functions. Nat Rev Mol Cell Biol *9*, 446-454.

Menand, B., Desnos, T., Nussaume, L., Berger, F., Bouchez, D., Meyer, C., and Robaglia, C. (2002). Expression and disruption of the Arabidopsis TOR (target of rapamycin) gene. Proc Natl Acad Sci U S A *99*, 6422-6427.

Moon, A., Kim, M.S., Kim, T.G., Kim, S.H., Kim, H.E., Chen, Y.Q., and Kim, H.R. (2000). H-ras, but not N-ras, induces an invasive phenotype in human breast epithelial cells: a role for MMP-2 in the H-ras-induced invasive phenotype. Int J Cancer *85*, 176-181.

Mora, A., Komander, D., van Aalten, D.M., and Alessi, D.R. (2004). PDK1, the master regulator of AGC kinase signal transduction. Semin Cell Dev Biol *15*, 161-170.

Mothe-Satney, I., Brunn, G.J., McMahon, L.P., Capaldo, C.T., Abraham, R.T., and Lawrence, J.C., Jr. (2000). Mammalian target of rapamycin-dependent phosphorylation of PHAS-I in four (S/T)P sites detected by phospho-specific antibodies. J Biol Chem *275*, 33836-33843.

Murakami, M., Ichisaka, T., Maeda, M., Oshiro, N., Hara, K., Edenhofer, F., Kiyama, H., Yonezawa, K., and Yamanaka, S. (2004). mTOR is essential for growth and proliferation in early mouse embryos and embryonic stem cells. Mol Cell Biol *24*, 6710-6718.

Nimnual, A.S., Yatsula, B.A., and Bar-Sagi, D. (1998). Coupling of Ras and Rac guanosine triphosphatases through the Ras exchanger Sos. Science *279*, 560-563.

Nobukuni, T., Joaquin, M., Roccio, M., Dann, S.G., Kim, S.Y., Gulati, P., Byfield, M.P., Backer, J.M., Natt, F., Bos, J.L.*, et al.* (2005). Amino acids mediate mTOR/raptor signaling through activation of class 3 phosphatidylinositol 3OH-kinase. Proc Natl Acad Sci U S A *102*, 14238-14243.

Nojima, H., Tokunaga, C., Eguchi, S., Oshiro, N., Hidayat, S., Yoshino, K., Hara, K., Tanaka, N., Avruch, J., and Yonezawa, K. (2003). The mammalian target of rapamycin (mTOR) partner, raptor, binds the mTOR substrates p70 S6 kinase and 4E-BP1 through their TOR signaling (TOS) motif. J Biol Chem *278*, 15461-15464.

O'Reilly, K.E., Rojo, F., She, Q.B., Solit, D., Mills, G.B., Smith, D., Lane, H., Hofmann, F., Hicklin, D.J., Ludwig, D.L.*, et al.* (2006). mTOR inhibition induces upstream receptor tyrosine kinase signaling and activates Akt. Cancer Res *66*, 1500-1508.

Oldham, S., Montagne, J., Radimerski, T., Thomas, G., and Hafen, E. (2000). Genetic and biochemical characterization of dTOR, the Drosophila homolog of the target of rapamycin. Genes Dev *14*, 2689-2694.

Oshiro, N., Takahashi, R., Yoshino, K., Tanimura, K., Nakashima, A., Eguchi, S., Miyamoto, T., Hara, K., Takehana, K., Avruch, J.*, et al.* (2007). The proline-rich Akt substrate of 40 kDa (PRAS40) is a physiological substrate of mammalian target of rapamycin complex 1. J Biol Chem *282*, 20329-20339.

Oshiro, N., Yoshino, K., Hidayat, S., Tokunaga, C., Hara, K., Eguchi, S., Avruch, J., and Yonezawa, K. (2004). Dissociation of raptor from mTOR is a mechanism of rapamycin-induced inhibition of mTOR function. Genes Cells *9*, 359-366.

Park, J.W., Kim, S., Lim, K.J., Simpson, R.J., Kim, Y.S., and Bahk, Y.Y. (2006). A proteomic approach for unraveling the oncogenic H-Ras protein networks in NIH/3T3 mouse embryonic fibroblast cells. Proteomics *6*, 1175-1186.

Partovian, C., Ju, R., Zhuang, Z.W., Martin, K.A., and Simons, M. (2008). Syndecan-4 regulates subcellular localization of mTOR Complex2 and Akt activation in a PKCalpha-dependent manner in endothelial cells. Mol Cell *32*, 140-149.

Pearce, L.R., Huang, X., Boudeau, J., Pawlowski, R., Wullschleger, S., Deak, M., Ibrahim, A.F., Gourlay, R., Magnuson, M.A., and Alessi, D.R. (2007). Identification of Protor as a novel Rictor-binding component of mTOR complex-2. Biochem J *405*, 513-522.

Pearson, R.B., Dennis, P.B., Han, J.W., Williamson, N.A., Kozma, S.C., Wettenhall, R.E., and Thomas, G. (1995). The principal target of rapamycin-induced p70s6k inactivation is a novel phosphorylation site within a conserved hydrophobic domain. EMBO J *14*, 5279-5287.

Peng, X.D., Xu, P.Z., Chen, M.L., Hahn-Windgassen, A., Skeen, J., Jacobs, J., Sundararajan, D., Chen, W.S., Crawford, S.E., Coleman, K.G.*, et al.* (2003). Dwarfism, impaired skin development, skeletal muscle atrophy, delayed bone development, and impeded adipogenesis in mice lacking Akt1 and Akt2. Genes Dev *17*, 1352-1365.

Perry, J., and Kleckner, N. (2003). The ATRs, ATMs, and TORs are giant HEAT repeat proteins. Cell *112*, 151-155.

Petersen, J., and Nurse, P. (2007). TOR signalling regulates mitotic commitment through the stress MAP kinase pathway and the Polo and Cdc2 kinases. Nat Cell Biol *9*, 1263-1272.

Peterson, R.T., Beal, P.A., Comb, M.J., and Schreiber, S.L. (2000). FKBP12-rapamycin-associated protein (FRAP) autophosphorylates at serine 2481 under translationally repressive conditions. J Biol Chem *275*, 7416-7423.

Polak, P., Cybulski, N., Feige, J.N., Auwerx, J., Ruegg, M.A., and Hall, M.N. (2008). Adipose-specific knockout of raptor results in lean mice with enhanced mitochondrial respiration. Cell Metab *8*, 399-410.

Polak, P., and Hall, M.N. (2009). mTOR and the control of whole body metabolism. Curr Opin Cell Biol *21*, 209-218.

Potter, C.J., Pedraza, L.G., and Xu, T. (2002). Akt regulates growth by directly phosphorylating Tsc2. Nat Cell Biol *4*, 658-665.

Pullen, N., Dennis, P.B., Andjelkovic, M., Dufner, A., Kozma, S.C., Hemmings, B.A., and Thomas, G. (1998). Phosphorylation and activation of p70s6k by PDK1. Science *279*, 707-710.

Qiao, M., Iglehart, J.D., and Pardee, A.B. (2007). Metastatic potential of 21T human breast cancer cells depends on Akt/protein kinase B activation. Cancer Res *67*, 5293-5299.

Quadro, L., Blaner, W.S., Salchow, D.J., Vogel, S., Piantedosi, R., Gouras, P., Freeman, S., Cosma, M.P., Colantuoni, V., and Gottesman, M.E. (1999). Impaired retinal function and vitamin A availability in mice lacking retinol-binding protein. EMBO J *18*, 4633-4644.

Reiling, J.H., and Hafen, E. (2004). The hypoxia-induced paralogs Scylla and Charybdis inhibit growth by down-regulating S6K activity upstream of TSC in Drosophila. Genes Dev *18*, 2879-2892.

Reinke, A., Anderson, S., McCaffery, J.M., Yates, J., 3rd, Aronova, S., Chu, S., Fairclough, S., Iverson, C., Wedaman, K.P., and Powers, T. (2004). TOR complex 1 includes a novel component, Tco89p (YPL180w), and cooperates with Ssd1p to maintain cellular integrity in Saccharomyces cerevisiae. J Biol Chem *279*, 14752-14762.

Ren, X.D., Kiosses, W.B., Sieg, D.J., Otey, C.A., Schlaepfer, D.D., and Schwartz, M.A. (2000). Focal adhesion kinase suppresses Rho activity to promote focal adhesion turnover. J Cell Sci *113 (Pt 20)*, 3673-3678.

Ridley, A.J., Schwartz, M.A., Burridge, K., Firtel, R.A., Ginsberg, M.H., Borisy, G., Parsons, J.T., and Horwitz, A.R. (2003). Cell migration: integrating signals from front to back. Science *302*, 1704-1709.

Rodriguez-Viciana, P., Warne, P.H., Khwaja, A., Marte, B.M., Pappin, D., Das, P., Waterfield, M.D., Ridley, A., and Downward, J. (1997). Role of phosphoinositide 3-OH kinase in cell transformation and control of the actin cytoskeleton by Ras. Cell *89*, 457-467.

Sahai, E., and Marshall, C.J. (2002). RHO-GTPases and cancer. Nat Rev Cancer *2*, 133-142.

Saitoh, M., Pullen, N., Brennan, P., Cantrell, D., Dennis, P.B., and Thomas, G. (2002). Regulation of an activated S6 kinase 1 variant reveals a novel mammalian target of rapamycin phosphorylation site. J Biol Chem *277*, 20104-20112.

Sancak, Y., Peterson, T.R., Shaul, Y.D., Lindquist, R.A., Thoreen, C.C., Bar-Peled, L., and Sabatini, D.M. (2008). The Rag GTPases bind raptor and mediate amino acid signaling to mTORC1. Science *320*, 1496-1501.

Sancak, Y., Thoreen, C.C., Peterson, T.R., Lindquist, R.A., Kang, S.A., Spooner, E., Carr, S.A., and Sabatini, D.M. (2007). PRAS40 is an insulin-regulated inhibitor of the mTORC1 protein kinase. Mol Cell *25*, 903-915.

Sander, E.E., ten Klooster, J.P., van Delft, S., van der Kammen, R.A., and Collard, J.G. (1999). Rac downregulates Rho activity: reciprocal balance between both GTPases determines cellular morphology and migratory behavior. J Cell Biol *147*, 1009-1022.

Sarbassov, D.D., Ali, S.M., Kim, D.H., Guertin, D.A., Latek, R.R., Erdjument-Bromage, H., Tempst, P., and Sabatini, D.M. (2004). Rictor, a novel binding partner of mTOR, defines a rapamycin-insensitive and raptor-independent pathway that regulates the cytoskeleton. Curr Biol *14*, 1296-1302.

Sarbassov, D.D., Ali, S.M., Sengupta, S., Sheen, J.H., Hsu, P.P., Bagley, A.F., Markhard, A.L., and Sabatini, D.M. (2006). Prolonged rapamycin treatment inhibits mTORC2 assembly and Akt/PKB. Mol Cell *22*, 159-168.

Sarbassov, D.D., Guertin, D.A., Ali, S.M., and Sabatini, D.M. (2005). Phosphorylation and regulation of Akt/PKB by the rictor-mTOR complex. Science *307*, 1098-1101.

Schalm, S.S., and Blenis, J. (2002). Identification of a conserved motif required for mTOR signaling. Curr Biol *12*, 632-639.

Schalm, S.S., Fingar, D.C., Sabatini, D.M., and Blenis, J. (2003). TOS motif-mediated raptor binding regulates 4E-BP1 multisite phosphorylation and function. Curr Biol *13*, 797-806.

Schmidt, A., Bickle, M., Beck, T., and Hall, M.N. (1997). The yeast phosphatidylinositol kinase homolog TOR2 activates RHO1 and RHO2 via the exchange factor ROM2. Cell *88*, 531-542.

Schmidt, A., Kunz, J., and Hall, M.N. (1996). TOR2 is required for organization of the actin cytoskeleton in yeast. Proc Natl Acad Sci U S A *93*, 13780-13785.

Schmitz, A.A., Govek, E.E., Bottner, B., and Van Aelst, L. (2000). Rho GTPases: signaling, migration, and invasion. Exp Cell Res *261*, 1-12.

Sekulic, A., Hudson, C.C., Homme, J.L., Yin, P., Otterness, D.M., Karnitz, L.M., and Abraham, R.T. (2000). A direct linkage between the phosphoinositide 3-kinase-AKT signaling pathway and the mammalian target of rapamycin in mitogen-stimulated and transformed cells. Cancer Res *60*, 3504-3513.

Shah, O.J., Wang, Z., and Hunter, T. (2004). Inappropriate activation of the TSC/Rheb/mTOR/S6K cassette induces IRS1/2 depletion, insulin resistance, and cell survival deficiencies. Curr Biol *14*, 1650-1656.

Shaw, R.J., Bardeesy, N., Manning, B.D., Lopez, L., Kosmatka, M., DePinho, R.A., and Cantley, L.C. (2004a). The LKB1 tumor suppressor negatively regulates mTOR signaling. Cancer Cell *6*, 91-99.

Shaw, R.J., and Cantley, L.C. (2006). Ras, PI(3)K and mTOR signalling controls tumour cell growth. Nature *441*, 424-430.

Shaw, R.J., Kosmatka, M., Bardeesy, N., Hurley, R.L., Witters, L.A., DePinho, R.A., and Cantley, L.C. (2004b). The tumor suppressor LKB1 kinase directly activates AMP-activated kinase and regulates apoptosis in response to energy stress. Proc Natl Acad Sci U S A *101*, 3329-3335.

Shi, Y., and Burn, P. (2004). Lipid metabolic enzymes: emerging drug targets for the treatment of obesity. Nat Rev Drug Discov *3*, 695-710.

Shiota, C., Woo, J.T., Lindner, J., Shelton, K.D., and Magnuson, M.A. (2006). Multiallelic disruption of the rictor gene in mice reveals that mTOR complex 2 is essential for fetal growth and viability. Dev Cell *11*, 583-589.

Smith, E.M., Finn, S.G., Tee, A.R., Browne, G.J., and Proud, C.G. (2005). The tuberous sclerosis protein TSC2 is not required for the regulation of the mammalian target of rapamycin by amino acids and certain cellular stresses. J Biol Chem *280*, 18717-18727.

Soukas, A.A., Kane, E.A., Carr, C.E., Melo, J.A., and Ruvkun, G. (2009). Rictor/TORC2 regulates fat metabolism, feeding, growth, and life span in Caenorhabditis elegans. Genes Dev *23*, 496-511.

Soulard, A., and Hall, M.N. (2007). SnapShot: mTOR signaling. Cell *129*, 434.

Sturgill, T.W., Cohen, A., Diefenbacher, M., Trautwein, M., Martin, D.E., and Hall, M.N. (2008). TOR1 and TOR2 have distinct locations in live cells. Eukaryot Cell *7*, 1819-1830.

Sun, Y., Fang, Y., Yoon, M.S., Zhang, C., Roccio, M., Zwartkruis, F.J., Armstrong, M., Brown, H.A., and Chen, J. (2008). Phospholipase D1 is an effector of Rheb in the mTOR pathway. Proc Natl Acad Sci U S A *105*, 8286-8291.

Tee, A.R., Manning, B.D., Roux, P.P., Cantley, L.C., and Blenis, J. (2003). Tuberous sclerosis complex gene products, Tuberin and Hamartin, control mTOR signaling by acting as a GTPase-activating protein complex toward Rheb. Curr Biol *13*, 1259-1268.

Thedieck, K., Polak, P., Kim, M.L., Molle, K.D., Cohen, A., Jeno, P., Arrieumerlou, C., and Hall, M.N. (2007). PRAS40 and PRR5-like protein are new mTOR interactors that regulate apoptosis. PLoS One *2*, e1217.

Tontonoz, P., Hu, E., and Spiegelman, B.M. (1994). Stimulation of adipogenesis in fibroblasts by PPAR gamma 2, a lipid-activated transcription factor. Cell *79*, 1147-1156.

Tremblay, F., Brule, S., Hee Um, S., Li, Y., Masuda, K., Roden, M., Sun, X.J., Krebs, M., Polakiewicz, R.D., Thomas, G.*, et al.* (2007). Identification of IRS-1 Ser-1101 as a target of S6K1 in nutrient- and obesity-induced insulin resistance. Proc Natl Acad Sci U S A *104*, 14056-14061.

Ueno, M., Carvalheira, J.B., Tambascia, R.C., Bezerra, R.M., Amaral, M.E., Carneiro, E.M., Folli, F., Franchini, K.G., and Saad, M.J. (2005). Regulation of insulin signalling by hyperinsulinaemia: role of IRS-1/2 serine phosphorylation and the mTOR/p70 S6K pathway. Diabetologia *48*, 506-518.

Um, S.H., Frigerio, F., Watanabe, M., Picard, F., Joaquin, M., Sticker, M., Fumagalli, S., Allegrini, P.R., Kozma, S.C., Auwerx, J.*, et al.* (2004). Absence of S6K1 protects against age- and diet-induced obesity while enhancing insulin sensitivity. Nature *431*, 200-205.

Vander Haar, E., Lee, S.I., Bandhakavi, S., Griffin, T.J., and Kim, D.H. (2007). Insulin signalling to mTOR mediated by the Akt/PKB substrate PRAS40. Nat Cell Biol *9*, 316-323.

Wang, L., Harris, T.E., Roth, R.A., and Lawrence, J.C., Jr. (2007). PRAS40 regulates mTORC1 kinase activity by functioning as a direct inhibitor of substrate binding. J Biol Chem *282*, 20036-20044.

Wang, P., Mariman, E., Renes, J., and Keijer, J. (2008). The secretory function of adipocytes in the physiology of white adipose tissue. J Cell Physiol *216*, 3-13.

Wedaman, K.P., Reinke, A., Anderson, S., Yates, J., 3rd, McCaffery, J.M., and Powers, T. (2003). Tor kinases are in distinct membrane-associated protein complexes in Saccharomyces cerevisiae. Mol Biol Cell *14*, 1204-1220.

Weisman, R., and Choder, M. (2001). The fission yeast TOR homolog, tor1+, is required for the response to starvation and other stresses via a conserved serine. J Biol Chem *276*, 7027-7032.

Weisman, R., Choder, M., and Koltin, Y. (1997). Rapamycin specifically interferes with the developmental response of fission yeast to starvation. J Bacteriol *179*, 6325-6334.

Weisman, R., Finkelstein, S., and Choder, M. (2001). Rapamycin blocks sexual development in fission yeast through inhibition of the cellular function of an FKBP12 homolog. J Biol Chem *276*, 24736-24742.

Weisman, R., Roitburg, I., Nahari, T., and Kupiec, M. (2005). Regulation of leucine uptake by tor1+ in Schizosaccharomyces pombe is sensitive to rapamycin. Genetics *169*, 539-550.

Woo, S.Y., Kim, D.H., Jun, C.B., Kim, Y.M., Haar, E.V., Lee, S.I., Hegg, J.W., Bandhakavi, S., and Griffin, T.J. (2007). PRR5, a novel component of mTOR complex 2, regulates platelet-derived growth factor receptor beta expression and signaling. J Biol Chem *282*, 25604-25612.

Wullschleger, S., Loewith, R., and Hall, M.N. (2006). TOR signaling in growth and metabolism. Cell *124*, 471-484.

Wullschleger, S., Loewith, R., Oppliger, W., and Hall, M.N. (2005). Molecular organization of target of rapamycin complex 2. J Biol Chem *280*, 30697-30704.

Yakar, S., Sun, H., Zhao, H., Pennisi, P., Toyoshima, Y., Setser, J., Stannard, B., Scavo, L., and Leroith, D. (2005). Metabolic effects of IGF-I deficiency: lessons from mouse models. Pediatr Endocrinol Rev *3*, 11-19.

Yang, Q., Inoki, K., Ikenoue, T., and Guan, K.L. (2006). Identification of Sin1 as an essential TORC2 component required for complex formation and kinase activity. Genes Dev *20*, 2820-2832.

Yang, Z.-Z., Tschopp, O., Di-Poi, N., Bruder, E., Baudry, A., Dummler, B., Wahli, W., and Hemmings, B.A. (2005). Dosage-Dependent Effects of Akt1/Protein Kinase B{alpha} (PKB{alpha}) and Akt3/PKB{gamma} on Thymus, Skin, and Cardiovascular and Nervous System Development in Mice. Mol Cell Biol *25*, 10407-10418.

Zhang, H.H., Lipovsky, A.I., Dibble, C.C., Sahin, M., and Manning, B.D. (2006). S6K1 regulates GSK3 under conditions of mTOR-dependent feedback inhibition of Akt. Mol Cell *24*, 185-197.

Zhang, Y., Gao, X., Saucedo, L.J., Ru, B., Edgar, B.A., and Pan, D. (2003). Rheb is a direct target of the tuberous sclerosis tumour suppressor proteins. Nat Cell Biol *5*, 578-581.

Zohn, I.E., Symons, M., Chrzanowska-Wodnicka, M., Westwick, J.K., and Der, C.J. (1998). Mas oncogene signaling and transformation require the small GTP-binding protein Rac. Mol Cell Biol *18*, 1225-1235.

Appendix: Adipose mTORC1 controls energy homeostasis

The following part describes the phenotypic characterization of an adipose-specific knockout of the mTORC1-specific component *raptor* in mice. In parallel to my main projects described above, I also collaborated with my colleague Pazit Polak to develop the following project and plan the required experiments. The experiments were mainly performed by Pazit Polak.

Published in Cell Metabolism 8, 399-410, November 2008

Polak P., Cybulski N., Feige J.N., Auwerx J., Rüegg M.A., Hall M.H. Adipose-Specific Knockout of *raptor* Results in Lean Mice with Enhanced Mitochondrial Respiration.

Cell Metabolism
Article

Adipose-Specific Knockout of *raptor* Results in Lean Mice with Enhanced Mitochondrial Respiration

Pazit Polak,[1,3] Nadine Cybulski,[1,3] Jerome N. Feige,[2] Johan Auwerx,[2] Markus A. Rüegg,[1] and Michael N. Hall[1,*]
[1]Biozentrum, University of Basel, Basel, CH-4056, Switzerland
[2]Institut de Génétique et de Biologie Moléculaire et Cellulaire, Institut Clinique de la Souris, CNRS/INSERM, Université Louis Pasteur 67404, Illkirch, France
[3]These authors contributed equally to this work
*Correspondence: m.hall@unibas.ch
DOI 10.1016/j.cmet.2008.09.003

SUMMARY

raptor is a specific and essential component of mammalian TOR complex 1 (mTORC1), a key regulator of cell growth and metabolism. To investigate a role of adipose mTORC1 in regulation of adipose and whole-body metabolism, we generated mice with an adipose-specific knockout of *raptor* (*raptor*$^{ad-/-}$). Compared to control littermates, *raptor*$^{ad-/-}$ mice had substantially less adipose tissue, were protected against diet-induced obesity and hypercholesterolemia, and exhibited improved insulin sensitivity. Leanness was in spite of reduced physical activity and unaffected caloric intake, lipolysis, and absorption of lipids from the food. White adipose tissue of *raptor*$^{ad-/-}$ mice displayed enhanced expression of genes encoding mitochondrial uncoupling proteins characteristic of brown fat. Leanness of the *raptor*$^{ad-/-}$ mice was attributed to elevated energy expenditure due to mitochondrial uncoupling. These results suggest that adipose mTORC1 is a regulator of adipose metabolism and, thereby, controls whole-body energy homeostasis.

INTRODUCTION

The protein kinase target of rapamycin (TOR) is a highly conserved, central controller of cell growth and metabolism (Corradetti and Guan, 2006; Guertin and Sabatini, 2007; Wullschleger et al., 2006). TOR is found in two functionally and structurally distinct multiprotein complexes termed TOR complex 1 (TORC1) and TORC2 (Jacinto et al., 2004; Loewith et al., 2002; Sarbassov et al., 2004). In mammals, mTORC1 consists of mTOR, raptor, PRAS40, and mLST8 and is sensitive to rapamycin (Vander Haar et al., 2007; Hara et al., 2002; Kim et al., 2002, 2003; Loewith et al., 2002). mTORC2 contains mTOR, rictor, mSIN1, and mLST8 (Frias et al., 2006; Jacinto et al., 2004, 2006; Sarbassov et al., 2004; Yang et al., 2006) and is not directly inhibited by rapamycin, although long-term rapamycin treatment can inhibit mTORC2 indirectly in certain cell types (Sarbassov et al., 2006). As a central controller of cell growth, TOR plays a key role in development and aging and is implicated in disorders such as cancer, cardiovascular disease, obesity, and diabetes (Guertin and Sabatini, 2007; Wullschleger et al., 2006).

mTORC1 controls many cellular processes that ultimately determine cell growth, including protein synthesis, ribosome biogenesis, nutrient transport, and autophagy. The two best-characterized substrates of mTORC1 are S6 kinase (S6K) and 4E-BP, via which mTORC1 controls protein synthesis (Beretta et al., 1996; Brunn et al., 1997; Burnett et al., 1998; Hay and Sonenberg, 2004). mTORC1 is controlled by metabolic cues, i.e., nutrients, cellular energy, and growth factors such as insulin or IGF (Wullschleger et al., 2006). Although mTORC1 is present in essentially all tissues, the findings that it is controlled by metabolic signals and is implicated in metabolic disorders suggest that it plays a particularly important role in metabolic tissues. Thus, we have focused on studying the role of the mTORC1 signaling pathway in a metabolic tissue, in particular, adipose tissue.

The traditional role of white adipose tissue (WAT) is as a long-term fat storage depot for the body. However, it is also an important endocrine organ that secretes hormones such as leptin, adiponectin, TNFα, and many others (Gimeno and Klaman, 2005; Kershaw and Flier, 2004; Shi and Burn, 2004) that regulate energy homeostasis, lipid metabolism, appetite, fertility, and immune and stress responses. An excess or deficiency of adipose tissue can lead to severe metabolic diseases such as type 2 diabetes, cardiovascular disorders, and cancer.

Adipose tissue also participates in the regulation of energy homeostasis through adaptive thermogenesis. This occurs via a type of adipose tissue known as brown adipose tissue (BAT), which oxidizes fatty acids and dissipates energy as heat. Heat production in BAT is achieved by short-circuiting, or uncoupling, the mitochondrial proton gradient that is generated by the respiratory chain. Uncoupling of the proton gradient from ATP production in BAT is mediated by the BAT-specific uncoupling protein 1 (UCP1). Two UCP1 homologs termed UCP2 and UCP3 are also expressed in BAT, but these proteins are expressed at very low levels and it is less clear whether they transfer protons and are, thus, indeed uncoupling proteins (Brand and Esteves, 2005). *Trans*-differentiation between WAT and BAT can be achieved, at least partly, via expression of specific transcription factors. For example, expression of the transcription factor PRDM16 (Seale et al., 2007), PGC1α (Puigserver et al., 1998), RIP140 (Christian et al., 2005; Kiskinis et al., 2007; Leonardsson et al., 2004), FOXC2 (Cederberg et al., 2001), p107 (Scime et al., 2005), or retinoblastoma (Hansen et al., 2004;

Cell Metabolism
Adipose mTORC1 Controls Energy Homeostasis

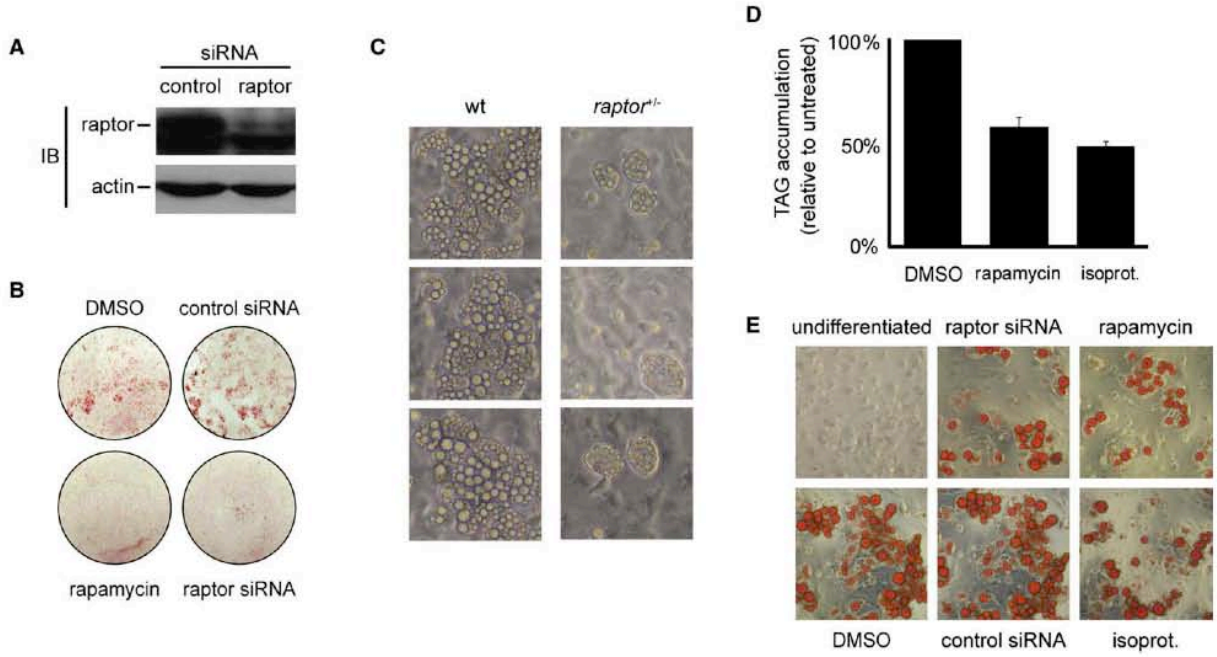

Figure 1. mTORC1 Is Required for Adipogenesis and Adipose Maintenance In Vitro

(A) Western blots showing the efficiency of raptor knockdown.

(B) 3T3-L1 preadipocytes were differentiated for 8 days and stained with oil red O. Rapamycin was added together with the differentiation mix and maintained during the differentiation period. siRNA-encoding viruses were added 2 days before differentiation.

(C) Representative pictures of differentiated MEFs were taken from three knockout embryos and three wild-type littermates.

(D) 3T3-L1 preadipocytes were differentiated and then treated with rapamycin or isoproterenol (isoprot.) or left untreated for another 6 days, and triglyceride (TAG) content was measured. Isoproterenol induces lipolysis and was used as a positive control. (n = 3, error bars represent SEM).

(E) 3T3-L1 preadipocytes were untreated or differentiated for 8 days. Differentiated cells were transduced with control or *raptor* siRNA-encoding viruses or treated with rapamycin or isoproterenol for another 6 days. Lipids were visualized by oil red O staining. siRNA-mediated raptor knockdown in differentiated 3T3-L1 cells was efficient, as determined by western blot (data not shown).

Scime et al., 2005) causes WAT cells to exhibit properties characteristic of brown fat.

Several studies have suggested that mTORC1 is essential for the differentiation and maintenance of adipocytes in vitro (Bell et al., 2000; Cho et al., 2004; El-Chaar et al., 2004; Gagnon et al., 2001; Kim and Chen, 2004; Yeh et al., 1995). To examine the role of mTORC1 in adipose tissue in vivo, we generated mice lacking the specific and essential mTORC1 component raptor. Since a nonconditional, full-body knockout of *raptor* in mice is embryonic lethal (Guertin et al., 2006), we generated conditional *raptor* knockout mice using the cre/loxP system. These mice were used to delete *raptor* specifically in adipose tissue. We demonstrate that adipose raptor controls adipocyte metabolism and, thereby, full-body energy homeostasis.

RESULTS

mTORC1 Is Required for Adipogenesis and Adipose Maintenance In Vitro

As shown previously, long-term rapamycin treatment prevents adipogenic differentiation of 3T3-L1 cells in culture (Bell et al., 2000; Cho et al., 2004; El-Chaar et al., 2004; Gagnon et al., 2001; Kim and Chen, 2004; Yeh et al., 1995). Since long-term rapamycin treatment can disrupt mTORC2 as well as inhibit mTORC1 (Sarbassov et al., 2006), we genetically knocked down raptor in undifferentiated 3T3-L1 preadipocytes to determine the role specifically of mTORC1 in adipogenesis (Figure 1A). The cells in which raptor was knocked down were then treated to induce adipogenesis and examined for lipid accumulation, by oil red O staining (Figure 1B). Inactivation of mTORC1 by either rapamycin treatment or knockdown of raptor prevented 3T3-L1 cells from differentiating into oil red O-staining cells, indicating that mTORC1 is indeed required for adipogenesis. To test further the requirement for mTORC1 in adipogenesis, we differentiated heterozygous *raptor*$^{+/-}$ mouse embryonic fibroblasts (MEFs) derived from mice lacking one copy of the *raptor* gene (see Supplemental Experimental Procedures). Heterozygous MEFs were used for this experiment because homozygous *raptor* knockout MEFs could not be obtained due to very early embryonic lethality, as observed previously (Guertin et al., 2006). The *raptor*$^{+/-}$ MEFs differentiated into adipocyte-like cells but with significantly reduced efficiency compared to MEFs from wild-type littermates (Figure 1C), providing further support for a role of mTORC1 in adipogenesis.

It has also been shown previously that culturing differentiated 3T3-L1 cells in the presence of rapamycin causes loss of fat, suggesting that mTORC1 is also required for maintenance of adipocytes (Kim and Chen, 2004). We confirmed this observation

Cell Metabolism
Adipose mTORC1 Controls Energy Homeostasis

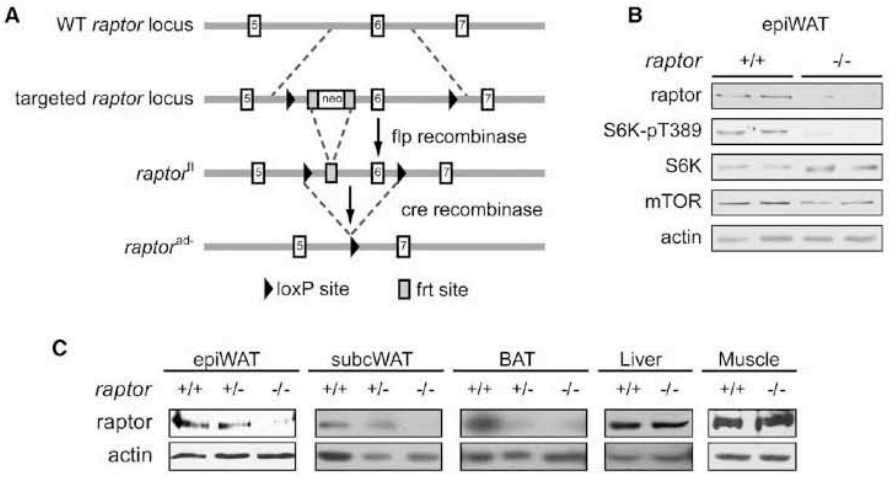

Figure 2. Generation and Validation of *raptor* Knockout

(A) Scheme describing the generation of *raptor* knockout.

(B) Western blot on epididymal WAT with raptor, S6K, mTOR, or actin antibodies as indicated, showing that the knockout was efficient.

(C) Western blots on epididymal WAT, inguinal WAT, BAT, liver, and soleus muscle with raptor or actin antibodies as indicated, showing that the knockout was specific to adipose tissue.

by measuring the triglyceride content of differentiated 3T3-L1 cells that were treated with rapamycin for 6 days after differentiation. Differentiated 3T3-L1 cells that were incubated with rapamycin for 6 days lost on average 46% of their triglyceride content (Figure 1D). Rapamycin treatment or siRNA-mediated raptor knockdown in differentiated 3T3-L1 adipocytes also caused loss of lipid stores as visualized by oil red O staining (Figure 1E). The above results confirm that mTORC1 is required for both establishment and maintenance of mature adipocytes in vitro.

Generation and Validation of Adipose-Specific *raptor* Knockout Mice

To elucidate the role of mTORC1 in adipose tissue, we utilized the cre/loxP system to generate mice in which raptor, an essential and specific component of mTORC1, is deleted exclusively in adipose tissue. A "floxed" *raptor* allele was created in embryonic stem cells of the 129S1/SvImJ mouse strain by introducing a loxP site into the introns flanking *raptor* exon 6, using a *neo* cassette (G418 resistance) flanked by frt sites as a selectable marker (Figure 2A). Stem cells in which homologous recombination had occurred were selected by G418 resistance, and recombination was confirmed by Southern blot analysis (data not shown). The targeted stem cells were injected into blastocysts of C57BL/6J mice to obtain chimeric floxed mice. After germline transmission, the mice were crossed to C57BL/6J mice expressing flp recombinase to remove the *neo* cassette. Progeny containing a floxed *raptor* allele lacking the *neo* cassette ($raptor^{fl/+}$) were further backcrossed to C57BL/6J mice. Mice used for all phenotyping experiments had been backcrossed four or five times. To knock out *raptor*, homozygous $raptor^{fl/fl}$ mice were crossed with transgenic mice expressing cre recombinase under control of the adipose-specific *fabp4/aP2* gene promoter ($aP2\text{-}cre^{Tg/0}$) (He et al., 2003). Resulting $raptor^{fl/+}$ $aP2\text{-}cre^{Tg/0}$ progeny were then crossed with $raptor^{fl/fl}$ mice to generate adipose-specific *raptor* knockout mice ($raptor^{ad-/-}$). Littermates lacking the *cre* gene ($raptor^{fl/fl}$) were used as controls.

Cre recombinase under control of the *aP2* promoter is expressed relatively late in adipogenesis (Tontonoz et al., 1994), leading to knockout of *raptor* only in mature adipocytes. Thus, the generated $raptor^{ad-/-}$ mice could be used to study the role of mTORC1 in the maintenance of mature adipocytes, but not in adipogenesis.

raptor protein and S6K phosphorylation (T389) were absent in white and brown adipose tissue, but not in other tissues, of $raptor^{ad-/-}$ mice (Figures 2B, 2C, and data not shown). We also examined, by RT-PCR, expression of the cre recombinase and confirmed that cre was expressed in white and brown adipose tissue, but not in macrophages, liver, muscle, kidney, intestine, pancreas, or spleen (data not shown). Thus, $raptor^{ad-/-}$ mice lack raptor and are defective for mTORC1 signaling specifically in adipose tissue.

$raptor^{ad-/-}$ mice were born at the expected Mendelian ratio. $raptor^{ad-/-}$ females showed reduced fertility, giving birth on average to 3.9 ± 0.5 pups per litter, as compared to 6.79 ± 0.6 and 6.8 ± 0.5 pups per litter for floxed females that did not express cre ($raptor^{fl/fl}$) and for wild-type C57BL/6J females, respectively. The time between litters was also slightly longer for $raptor^{ad-/-}$ females. $raptor^{ad-/-}$ males showed similar fertility to that of $raptor^{fl/fl}$ and C57BL/6J males.

$raptor^{ad-/-}$ Mice Are Lean and Resistant to Diet-Induced Obesity

As a first analysis of the effect of $raptor^{ad-/-}$ on adipose tissue, we monitored the weight of $raptor^{ad-/-}$ mice and littermate controls ($raptor^{fl/fl}$) over 13 weeks between the ages of 8 and 21 weeks. On a chow diet, $raptor^{ad-/-}$ mice weighed 18% less than $raptor^{fl/fl}$ mice (Figure 3A, left graph), but both gained weight at a similar rate. After 13 weeks, both the $raptor^{ad-/-}$ and $raptor^{fl/fl}$ mice had gained 33% of their initial weight. When challenged with a high-fat diet (HFD), $raptor^{ad-/-}$ mice initially gained weight more

Cell Metabolism
Adipose mTORC1 Controls Energy Homeostasis

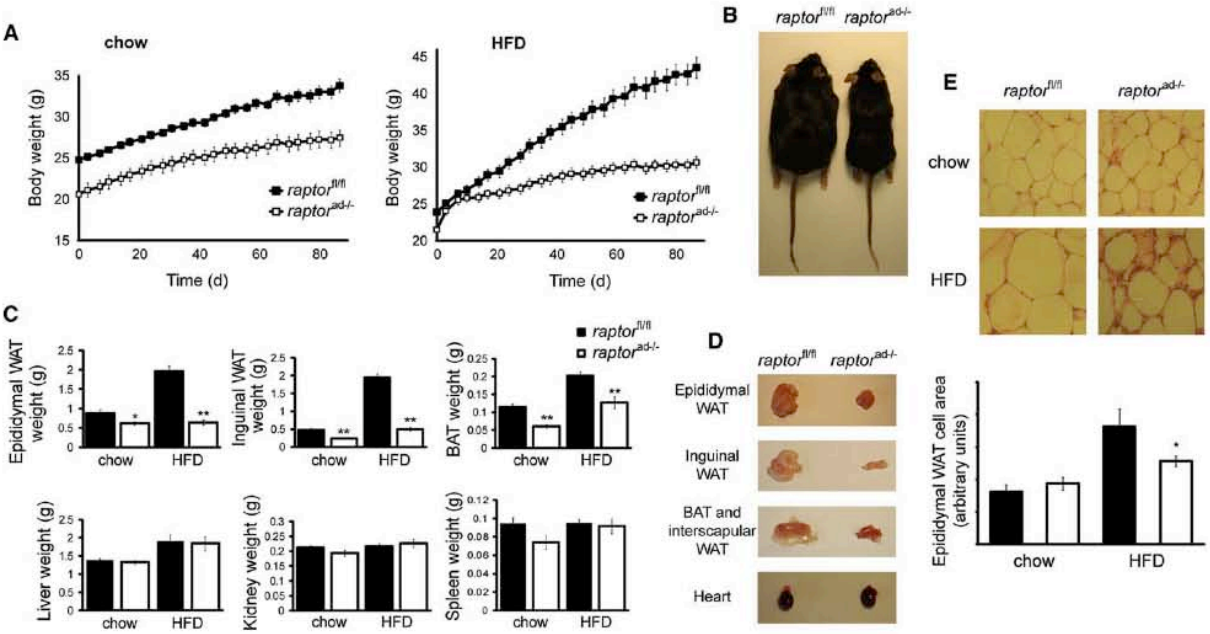

Figure 3. Knockout Mice Are Lean and Resistant to Diet-Induced Obesity

(A) Mice (8-week-old) were fed a chow or HFD for 13 weeks. Body weight was monitored biweekly (n = 15–20).

(B) Representative pictures of mice after 13 weeks on an HFD.

(C) Weight of epididymal WAT, inguinal WAT, BAT, liver, kidney, and heart was measured in 21-week-old mice (n = 13–18 for chow diet, n = 6–9 for HFD).

(D) Representative pictures of fat pads and heart from mice that were on an HFD for 13 weeks.

(E) (Top) Representative pictures of H&E staining of epididymal WAT sections from *raptor*$^{fl/fl}$ and *raptor*$^{ad-/-}$ mice fed a chow or HFD. (Bottom) Quantification of WAT cell circumference (n = 7–10). In all panels, error bars represent SEM.

rapidly than control *raptor*$^{fl/fl}$ mice (Figure 3A, right graph). However, while the control mice continued to gain weight throughout the time course of the experiment, *raptor*$^{ad-/-}$ mice gained little to no weight after the initial 2–3 week period on the HFD. After 13 weeks on the HFD, *raptor*$^{fl/fl}$ mice had gained 85% of their starting weight, whereas *raptor*$^{ad-/-}$ mice had gained only 41% of their starting weight (Figures 3A and 3B).

To determine the cause of the reduced body weight of *raptor*$^{ad-/-}$ mice, we examined individual fat pads and organs. The major fat pads of *raptor*$^{ad-/-}$ mice were significantly lighter and smaller than those of *raptor*$^{fl/fl}$ mice (Figures 3C and 3D). This difference in the fat pads was more pronounced for the mice on an HFD (Figures 3C and 3D). HFD-fed *raptor*$^{ad-/-}$ mice had 70% less WAT than similarly fed *raptor*$^{fl/fl}$ mice (Figure 3C). The knockout and control mice displayed no significant difference in the weight of lean organs, such as the liver, kidney, spleen, and heart, on either the chow or high-fat diet (Figures 3C and 3D), indicating that the effect of the knockout was specific to adipose tissue. This adipose-specific effect of the knockout was confirmed by DEXA scan analysis, which also showed that bone mass was unaltered in *raptor*$^{ad-/-}$ mice (data not shown). Thus, an adipose-specific knockout of mTORC1 results in leaner mice and confers resistance to diet-induced obesity.

raptor$^{ad-/-}$ Mice Have Smaller and Fewer WAT Cells

To determine whether the reduced amount of fat in *raptor*$^{ad-/-}$ mice is due to fewer fat cells and/or smaller fat cells, we measured the circumference of individual adipocytes in epididymal WAT of *raptor*$^{ad-/-}$ and *raptor*$^{fl/fl}$ mice (Figure 3E). The adipocytes from knockout and control mice on a chow diet were similar in size, suggesting that the lower amount of WAT in *raptor*$^{ad-/-}$ mice is due to fewer adipocytes. This finding was confirmed by FACS analysis, which showed that epididymal WAT of *raptor*$^{ad-/-}$ mice contained approximately three times fewer cells than WAT of *raptor*$^{fl/fl}$ mice (data not shown). Adipocytes from *raptor*$^{fl/fl}$ mice on a high-fat diet displayed an expected ~2-fold increase in size (Kubota et al., 1999; Lemonnier, 1972), whereas adipocytes from *raptor*$^{ad-/-}$ mice on an HFD displayed only a slight increase in size. Calculating and comparing the volumes of adipocytes from *raptor*$^{fl/fl}$ and *raptor*$^{ad-/-}$ mice on an HFD indicated that *raptor*$^{ad-/-}$ adipocytes were approximately half the size of the *raptor*$^{fl/fl}$ adipocytes. Although *raptor*$^{ad-/-}$ adipocytes were significantly smaller, this decrease was not sufficient to account for the observed overall reduction in adipose tissue (Figure 3C), indicating again that a *raptor* knockout also reduces adipocyte number. The reduced weight of a *raptor* knockout mouse is due to a combination of smaller and fewer WAT cells. There was no obvious morphological difference in BAT due to either diet or *raptor* knockout (data not shown), although the *raptor*$^{ad-/-}$ mice contained less overall BAT. Thus, mTORC1 is required to maintain adipose tissue.

raptor$^{ad-/-}$ Mice Have Better Metabolic Parameters

We next investigated the effect of the *raptor* knockout on whole-animal metabolism. First, we performed an IP glucose tolerance

Cell Metabolism
Adipose mTORC1 Controls Energy Homeostasis

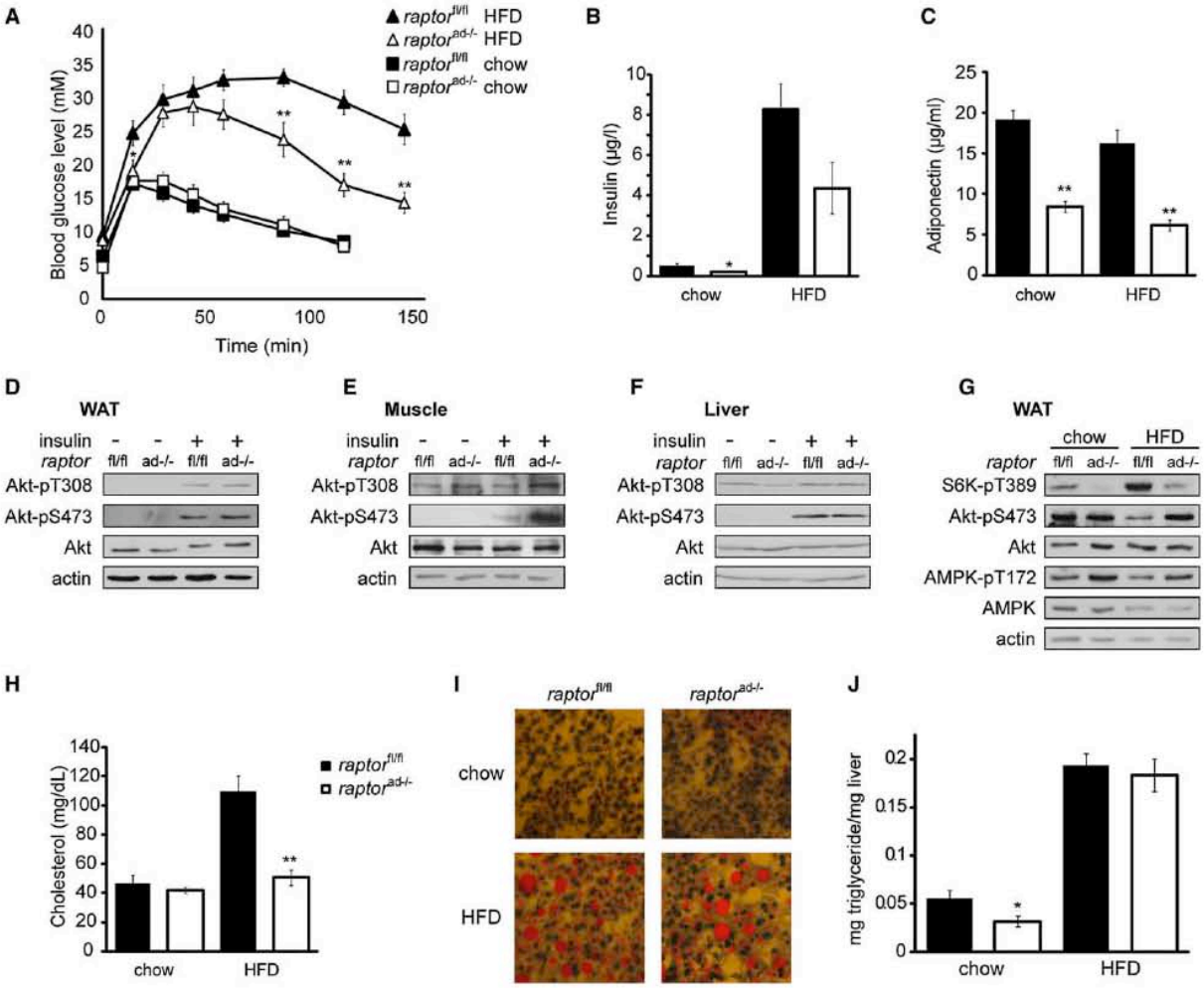

Figure 4. Metabolic Parameters

(A) IP glucose tolerance test (n = 7–10).

(B and C) Insulin and adiponectin plasma values (n = 10).

(D–G) Representative western blots on epididymal WAT, soleus muscle, or liver with the indicated antibodies (n = 5). A femto maximum sensitivity substrate (ECL) kit was used to detect basal levels of Akt-pS473 phosphorylation in Figure 4G.

(H) Cholesterol plasma values (n = 10).

(I) Representative pictures of oil red O and hematoxylin staining of liver sections from *raptor*$^{fl/fl}$ and *raptor*$^{ad-/-}$ mice fed a chow or HFD.

(J) Quantification of triglyceride content (n = 10). In all panels, error bars represent SEM.

test to determine the ability of the mice to clear glucose from the blood (Figure 4A). On a chow diet, the basal glucose level of the *raptor*$^{ad-/-}$ mice was lower than that of *raptor*$^{fl/fl}$ mice (4.72 ± 0.3 versus 6.36 ± 0.52 mM, respectively). Upon IP injection of glucose, the knockout mice had a normal glucose response and clearance rate. On the HFD, basal glucose levels were, as expected, higher than on the chow diet but slightly lower in *raptor*$^{ad-/-}$ mice compared to *raptor*$^{fl/fl}$ mice. HFD-fed *raptor*$^{ad-/-}$ and *raptor*$^{fl/fl}$ mice both exhibited reduced rates of glucose clearance. However, the glucose clearance rate of the *raptor*$^{ad-/-}$ mice was markedly better compared to the *raptor*$^{fl/fl}$ mice, indicating that the knockout mice were more glucose tolerant than control mice. We then determined plasma insulin levels. The fasting insulin levels were lower in *raptor*$^{ad-/-}$ mice compared to *raptor*$^{fl/fl}$ mice (Figure 4B). The lower insulin level combined with the observed lower basal glucose level and better glucose clearance rate suggest that *raptor*$^{ad-/-}$ mice are more insulin sensitive, despite lower adiponectin plasma levels (Figure 4C).

To determine whether insulin signaling is indeed enhanced in *raptor*$^{ad-/-}$ mice, we examined the effect of insulin stimulation on Akt phosphorylation (T308 and S473) in WAT, muscle, and liver of *raptor*$^{fl/fl}$ and *raptor*$^{ad-/-}$ mice. As expected, upon insulin stimulation, Akt was phosphorylated in all tissues (Figures 4D–4F). Akt phosphorylation was similar in WAT and liver of *raptor*$^{fl/fl}$ and *raptor*$^{ad-/-}$ mice, indicating that insulin signaling

Cell Metabolism
Adipose mTORC1 Controls Energy Homeostasis

is not enhanced in these tissues in *raptor*$^{ad-/-}$ mice. In contrast, Akt was hyperphosphorylated in muscle in *raptor*$^{ad-/-}$ mice compared to *raptor*$^{fl/fl}$ mice, indicating that insulin signaling is enhanced in muscle of *raptor*$^{ad-/-}$ mice. Thus, the lower basal glucose level and better glucose clearance rate of the knockout mice are likely due to improved insulin signaling and glucose uptake by muscle. In this context, it is important to note that muscle is the major insulin-stimulated glucose-consuming tissue.

Prolonged stimulation of mTORC1 and S6K inhibits upstream signaling by the insulin pathway (including Akt), thereby forming a negative feedback loop (Dowling et al., 2007; Harrington et al., 2004; Krebs et al., 2007; Shah et al., 2004; Tzatsos and Kandror, 2006; Ueno et al., 2005; Um et al., 2004). To investigate the effect of *raptor*$^{ad-/-}$ on this negative feedback loop, we examined Akt and S6K phosphorylation in WAT of HFD-fed *raptor*$^{ad-/-}$ and *raptor*$^{fl/fl}$ mice. HFD-fed control mice (*raptor*$^{fl/fl}$) exhibited S6K hyperphosphorylation and Akt hypophosphorylation, indicating that an HFD activates the negative feedback loop in WAT (Figure 4G). *raptor*$^{ad-/-}$ eliminated the HFD-induced negative feedback loop, as indicated by loss of S6K hyperphosphorylation and restoration of Akt phosphorylation (Figure 4G). Thus, the enhanced insulin sensitivity of the *raptor*$^{ad-/-}$ mice on HFD could also be due to loss of negative feedback in adipose tissue. In agreement with previous data (Aguilar et al., 2007), we also observed increased AMPK phosphorylation in WAT of *raptor*$^{ad-/-}$ mice compared to *raptor*$^{fl/fl}$ mice (Figure 4G), which could also contribute to higher insulin sensitivity. Taken together, the above results suggest that *raptor*$^{ad-/-}$ mice are more insulin sensitive due to enhanced insulin signaling in muscle and, on an HFD, in WAT.

Plasma levels of cholesterol showed a similar trend as observed for glucose tolerance (Figure 4H). Levels were similar for the *raptor*$^{ad-/-}$ and *raptor*$^{fl/fl}$ mice on the chow diet and were substantially increased for *raptor*$^{fl/fl}$ mice on the HFD. However, *raptor*$^{ad-/-}$ mice maintained normal cholesterol levels even on the HFD. The *raptor* knockout had no effect on plasma levels of triglycerides and free fatty acids on either the chow or high-fat diet (data not shown). Taken together, the above results suggest that inactivation of mTORC1 in adipose tissue improves whole-animal metabolism, in particular when mTORC1-deficient mice are challenged by an HFD.

As described above, the *raptor*$^{ad-/-}$ mice displayed reduced adiposity. Since an alteration in fat metabolism often results in aberrant accumulation of fat in the liver (steatosis), we examined the livers of the knockout and control mice by oil red O staining and quantification of liver triglyceride content (Figures 4I and 4J). On the chow diet, there was a small but significant reduction in the amount of triglycerides stored in livers of *raptor*$^{ad-/-}$ compared to *raptor*$^{fl/fl}$ mice. The HFD caused extensive and similar hepatic steatosis in *raptor*$^{ad-/-}$ and *raptor*$^{fl/fl}$ mice.

Food Intake or Absorption, Physical Activity, Adipose-Specific Lipolysis, or Expression of Fat Genes Do Not Account for the Leanness of *raptor*$^{ad-/-}$ Mice

What is the underlying mechanism that causes *raptor*$^{ad-/-}$ mice to be lean and resistant to diet-induced obesity? Adipose tissue is an endocrine organ that interacts with other metabolic organs to regulate behavior and whole-body metabolism. The observed leanness could, therefore, be due to the interaction of adipose

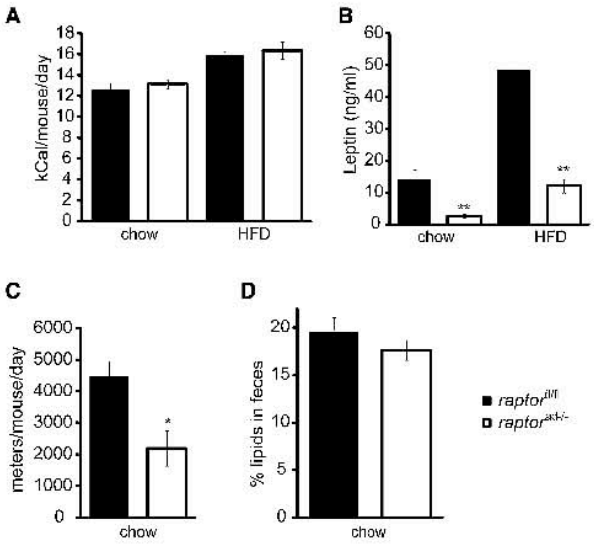

Figure 5. Food Intake, Leptin Levels, Voluntary Activity, and Fecal Lipid Content

(A) Mice (8-week-old) were fed a chow or HFD for 13 weeks. Food intake was measured biweekly (n = 15–20).

(B) Leptin plasma values (n = 10).

(C) Measurement of voluntary activity (n = 5–7).

(D) To measure lipid absorption in the digestive system, feces were collected over 24 hr, and fat was separated by methanol:chloroform extraction. Extracted lipids were weighed, and the percentage of feces fat (W/W) was calculated (n = 7–11). In all panels, error bars represent SEM.

tissue with other organs. To examine this possibility, we first measured feeding behavior. *raptor*$^{ad-/-}$ and *raptor*$^{fl/fl}$ mice consumed similar amounts of calories per day on both the chow and high-fat diets (Figure 5A). Similar food intake occurred despite markedly reduced plasma leptin levels in *raptor*$^{ad-/-}$ mice, suggesting enhanced leptin sensitivity (Figure 5B). The reduced leptin levels in *raptor*$^{ad-/-}$ mice are in agreement with the observed reduction in WAT mass (Figure 3C), as leptin levels correlate with WAT mass (Considine et al., 1996). Second, we investigated voluntary locomotor activity of *raptor*$^{ad-/-}$ and *raptor*$^{fl/fl}$ mice. Surprisingly, *raptor*$^{ad-/-}$ mice were less active than *raptor*$^{fl/fl}$ mice, as measured by activity on running wheels. On average, *raptor*$^{ad-/-}$ mice ran ~2000 m/day, whereas *raptor*$^{fl/fl}$ mice ran ~4500 m/day (Figure 5C). Third, we examined fecal lipid content to determine whether the observed leanness could be due to a defect in food absorption. There was no difference in the fecal lipid content of *raptor*$^{ad-/-}$ and *raptor*$^{fl/fl}$ mice (Figure 5D), indicating that *raptor*$^{ad-/-}$ mice did not have a defect in absorption of lipid from food. Thus, the leanness of *raptor*$^{ad-/-}$ mice is not due to decreased food intake, increased physical activity, or reduced lipid absorption.

An adipose maintenance defect could also be due to increased lipolysis or dedifferentiation resulting from decreased expression of adipose-specific fat storage genes. To test these possibilities, we first measured lipolysis in differentiated 3T3-L1 cells treated or untreated with rapamycin (Figure 6A) and in epididymal WAT pads of *raptor*$^{ad-/-}$ and *raptor*$^{fl/fl}$ mice (Figure 6B). In neither system did we detect a significant difference

Cell Metabolism
Adipose mTORC1 Controls Energy Homeostasis

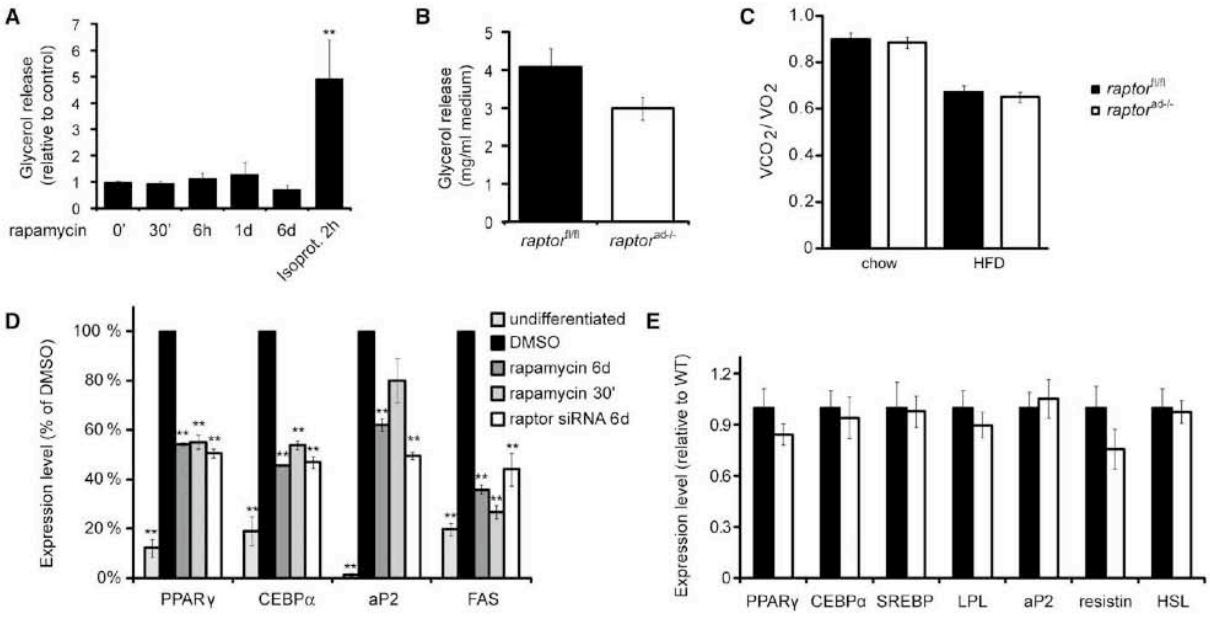

Figure 6. Lipolysis, Respiratory Exchange Ratio, and Gene Expression Analysis

(A) 3T3-L1 cells were differentiated and then treated or not with rapamycin for the indicated periods of time. Glycerol release was measured during the last 30 min (n = 4–6).

(B) Glycerol release was measured from epididymal WAT that was isolated and incubated in DMEM for 12 hr (n = 7).

(C) The respiratory exchange quotient was calculated as CO_2 production/O_2 consumption during indirect calorimetry measurements.

(D) 3T3-L1 cells were differentiated and then treated or not with rapamycin for the indicated periods of time. Gene expression levels were measured by qPCR on cDNA (n = 3–5). All genes were normalized to actin. $p \leq 0.01$ for all genes except *aP2* on day 6.

(E) Epididymal WAT was isolated, and gene expression levels were measured by qPCR on cDNA (n = 9 or 10). In all panels, error bars represent SEM.

in glycerol release from the cells upon inactivation of mTORC1. Finally, we determined the respiratory exchange ratio of *raptor*$^{ad-/-}$ and *raptor*$^{fl/fl}$ mice as a measure of the utilized energy source. As expected, HFD-fed mice had a lower ratio than chow-fed mice, indicating greater utilization of fat versus carbohydrates as an energy source. However, the *raptor*$^{ad-/-}$ and *raptor*$^{fl/fl}$ mice had a similar ratio (Figure 6C), indicating similar utilization of carbohydrates and fat as energy sources. These results suggest that the leanness of *raptor*$^{ad-/-}$ mice is not due to enhanced lipolysis.

We then analyzed the expression pattern of several well-known adipose-specific genes that mediate fat storage, in particular the genes encoding the transcription factors PPARγ, CEBPα, and SREBP and the genes encoding fatty acid-binding protein aP2, fatty acid synthase (FAS), lipoprotein lipase (LPL), resistin, and hormone-sensitive lipase (HSL). In 3T3-L1 cells, inhibition of mTORC1, either by rapamycin treatment or by *raptor* siRNA, caused a significant decrease in all genes examined (Figure 6D), suggesting that inactivation of mTORC1 causes mature adipocytes to "dedifferentiate" due to lack of expression of the genes necessary for lipid production and storage. These results are in agreement with a previous study that showed that the activity of PPARγ is reduced following rapamycin treatment (Kim and Chen, 2004). However, unexpectedly, similar expression levels were detected for the genes listed above in epididymal WAT derived from *raptor*$^{ad-/-}$ and *raptor*$^{fl/fl}$ mice (Figure 6E). This result suggests that, although inactivation of mTORC1 leads to a similar phenotype in cell culture and mice, i.e., loss of fat, the underlying molecular mechanism for this phenotype is probably more complex in vivo, where interactions between many different cell types and other external factors determine WAT metabolism. However, the leanness of *raptor*$^{ad-/-}$ mice appears not to be due to changes in expression of common lipid metabolizing genes.

Macrophage infiltration into WAT increases with obesity (Weisberg et al., 2003) and contributes to the secretion of inflammatory cytokines that are associated with changes in insulin sensitivity and other metabolic parameters (Weisberg et al., 2006; Xu et al., 2003). To determine the extent of macrophage infiltration into the epididymal WAT of *raptor*$^{ad-/-}$ and *raptor*$^{fl/fl}$ mice, we measured the expression level of *mac1*, a macrophage marker, in cDNA extracts made from WAT (including any infiltrated macrophages). As expected, *mac1* expression was increased in response to an HFD and the resulting obesity. However, there was little to no difference in *mac1* expression between *raptor*$^{ad-/-}$ and *raptor*$^{fl/fl}$ mice on either a chow or high-fat diet (data not shown). Thus, leanness was not due to a change in metabolism resulting from a difference in macrophage infiltration.

raptor$^{ad-/-}$ Mice Have Higher Energy Expenditure Due to an Increase in Uncoupled Respiration in WAT

Leanness of the *raptor*$^{ad-/-}$ mice could be due to increased energy expenditure. To investigate energy expenditure, we measured oxygen consumption by indirect calorimetry. *raptor*$^{ad-/-}$ mice displayed an increase in oxygen consumption as compared

Cell Metabolism
Adipose mTORC1 Controls Energy Homeostasis

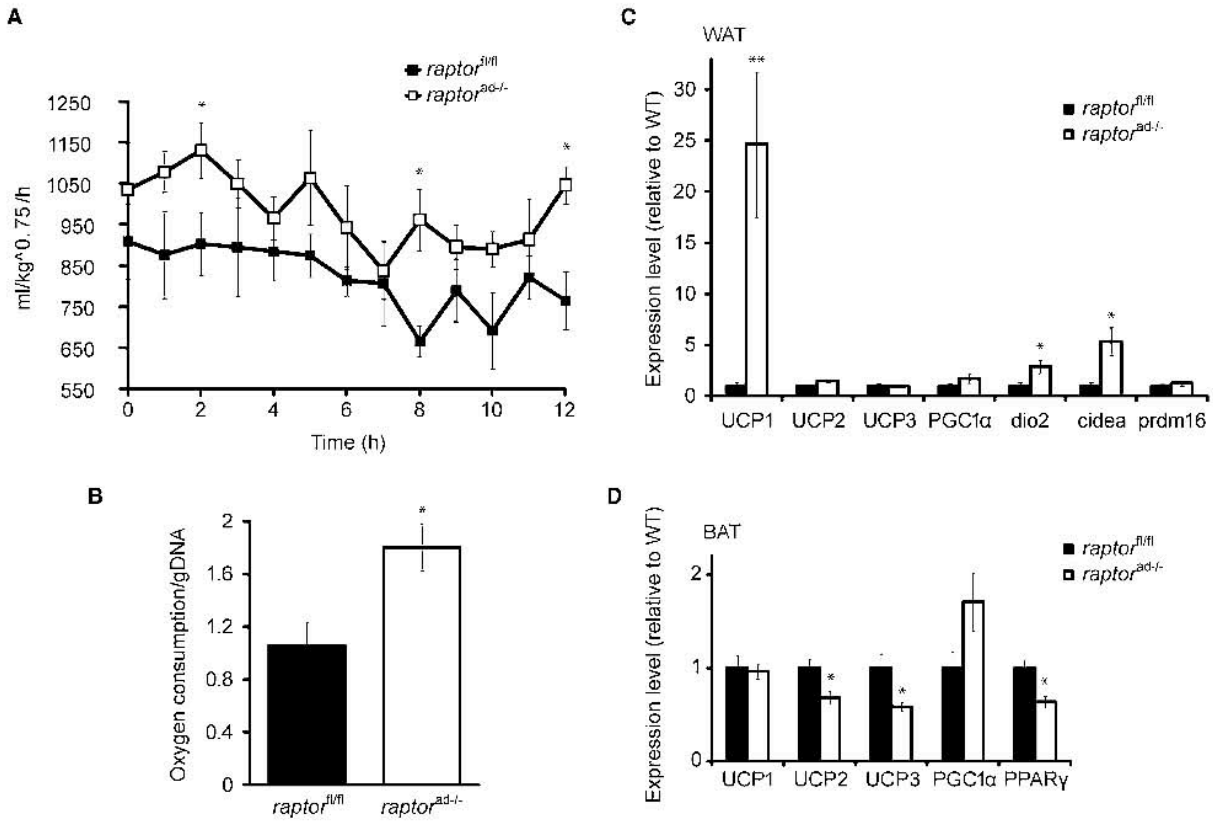

Figure 7. Energy Expenditure and Gene Expression in WAT and BAT

(A) O_2 consumption by 14-15 week old mice that remained on chow or HFD during the previous 5-6 weeks.

(B) O_2 consumption in primary white adipocytes isolated from *raptor*$^{fl/fl}$ or *raptor*$^{ad-/-}$ mice (n = 4), as measured with a Clark electrode. O_2 consumption was normalized to the amount of genomic DNA (gDNA).

(C and D) Epididymal WAT or BAT were isolated, and gene expression levels were measured by qPCR on cDNA (n = 9 or 10). In all panels, error bars represent SEM.

to *raptor*$^{fl/fl}$ mice (Figure 7A), suggesting that the knockout mice indeed expend more energy. We then analyzed, using a Clark electrode, the oxygen consumption by isolated white adipocytes derived from *raptor*$^{ad-/-}$ and *raptor*$^{fl/fl}$ mice. Adipocytes from *raptor*$^{ad-/-}$ mice displayed a significant increase in oxygen consumption compared to control adipocytes (Figure 7B). Thus, *raptor*$^{ad-/-}$ causes an increase in mitochondrial respiration in WAT.

Why is respiration increased in WAT of *raptor*$^{ad-/-}$ mice? The observed increase in oxygen consumption by isolated adipocytes, as described above, was abolished by the addition of ADP (data not shown). This effect of ADP, which stimulates coupled respiration and inhibits uncoupled respiration (Nicholls, 2001), suggested that the increase in oxygen consumption could be due to uncoupled mitochondrial respiration. To investigate this possibility further, we examined expression of mitochondrial uncoupling genes in WAT from *raptor*$^{ad-/-}$ and *raptor*$^{fl/fl}$ mice. We observed a strong increase (25-fold) in the expression of the *uncoupling protein 1* (*UCP1*) gene and, to a lesser extent, in expression of *UCP2* and other brown fat markers such as *type 2 deiodinase* (*dio2*) and *cidea* in WAT of *raptor*$^{ad-/-}$ mice (Figure 7C). Thus, the leanness of *raptor*$^{ad-/-}$ mice appears to be due to increased energy expenditure resulting from mitochondrial uncoupling in WAT. Surprisingly, we also detected a small increase (3-fold) in *UCP1* expression in skeletal muscle of *raptor*$^{ad-/-}$ mice. This increase might also contribute to the leanness of *raptor*$^{ad-/-}$ mice.

No difference in oxygen consumption was detected in brown adipocytes isolated from *raptor*$^{ad-/-}$ and *raptor*$^{fl/fl}$ mice (data not shown). In agreement with this finding, the level of *UCP1* expression in BAT was unaffected by *raptor* knockout (Figure 7D), although expression of *PPARγ*, as well as *UCP2* and *UCP3*, was reduced (Figure 7D). It remains to be determined why BAT mass is reduced in *raptor*$^{ad-/-}$ mice.

DISCUSSION

Here, we describe the generation and phenotypic characterization of conditional *raptor* knockout mice. Knockout of *raptor* specifically in adipose tissue (*raptor*$^{ad-/-}$) results in mice that are lean and resistant to diet-induced obesity. *raptor*$^{ad-/-}$ mice also exhibit an overall better metabolic profile than control

Cell Metabolism
Adipose mTORC1 Controls Energy Homeostasis

mice, including enhanced glucose tolerance and resistance to diet-induced hypercholesterolemia. Furthermore, we present evidence that the leanness of *raptor*$^{ad-/-}$ mice is due to elevated energy expenditure as a consequence of uncoupled mitochondria in white adipose tissue. These results suggest that mTORC1 in adipose tissue plays an important role in the control of both adipose metabolism and whole-body energy homeostasis.

Similar to adipose-specific *raptor* knockout, whole-body knockout of S6K1, which is positively regulated by mTORC1, results in lean mice that are resistant to diet-induced obesity due to increased energy expenditure (Pende et al., 2000; Um et al., 2004). Furthermore, *S6K1* knockout mice exhibit normal food intake despite lower leptin levels, smaller WAT cells, and enhanced insulin sensitivity. Conversely, knockout of 4E-BP1 and 4E-BP2, which are negatively regulated by mTORC1, results in increased obesity and hypersensitivity to diet-induced obesity due to lower energy expenditure (Le Bacquer et al., 2007). This remarkable correlation between adipose-specific knockout of mTORC1 and full-body knockout of its direct effectors S6K1 and 4E-BP1/2 suggests that at least part of the effects of the *S6K1* and *4E-BP1/2* knockouts are via adipose tissue. This, in turn, provides further evidence that mTORC1 signaling in adipose tissue plays a central role in controlling whole-animal metabolism.

raptor$^{ad-/-}$ mice have lower basal glucose levels, improved glucose clearance, and reduced plasma insulin levels compared to control *raptor*$^{fl/fl}$ mice, indicating that *raptor*$^{ad-/-}$ mice have enhanced insulin sensitivity. We find that this enhanced insulin sensitivity is due, at least in part, to increased insulin signaling in muscle and, on a high-fat diet, in adipose tissue. This underscores the role of adipose and, in particular, adipose mTORC1 in controlling whole-body energy homeostasis. The increased insulin signaling in adipose tissue is due to loss of the negative feedback loop within the mTORC1 pathway. It remains to be determined how mTORC1 signaling in adipose tissue controls insulin sensitivity in other tissues.

Previous studies on the role of mTORC1 in mitochondrial function have provided seemingly conflicting results. Observed changes in respiration by full-body S6K1 or 4E-BP1/2 knockout mice suggest, in line with our results, that mTORC1 negatively controls mitochondrial respiration (or uncoupling) (Le Bacquer et al., 2007; Um et al., 2004). In contrast, muscle-specific knockout of *raptor* results in decreased oxidative capacity and mitochondrial gene expression (Bentzinger et al., 2008 [this issue of *Cell Metabolism*]). Furthermore, rapamycin treatment or knockdown of mTOR or raptor in muscle cells or in *TSC* knockout MEFs decreases mitochondrial gene expression and oxygen consumption (Cunningham et al., 2007). These latter effects are via downregulation of PGC1α and the transcription factor YY1 and do not involve S6K1 or Akt (Cunningham et al., 2007; Schieke et al., 2006). Taken together, our data and the above findings suggest that mTORC1 controls mitochondrial respiration either negatively or positively depending on the mTORC1 effectors that might be found in a particular tissue.

Impaired TORC1 signaling in yeast, flies, and worms extends lifespan (Kaeberlein et al., 2005; Kapahi et al., 2004; Powers et al., 2006; Vellai et al., 2003). Inhibition of TOR signaling mimics nutrient deprivation, and the extension of lifespan by TOR inhibition might, thus, be equivalent to the extension of lifespan by dietary restriction. In this context, it is interesting to note that *raptor*$^{ad-/-}$ mice have improved metabolic parameters that could lead to extended lifespan. Furthermore, *raptor*$^{ad-/-}$ enhances respiration, and, at least as shown in budding yeast, impaired TORC1 signaling extends lifespan by increasing mitochondrial respiration among other effects (Bishop and Guarente, 2007; Bonawitz et al., 2007; Kaeberlein and Powers, 2007). It would be of interest to determine whether mTORC1 in mammals and, in particular, in adipose tissue controls lifespan.

Metformin is a widely prescribed antidiabetic drug that increases insulin sensitivity and lowers blood glucose and lipid levels. It functions through activation of the LKB1-AMPK pathway in liver (Shaw et al., 2005; Tzatsos and Kandror, 2006). Metformin also inactivates mTORC1 downstream of AMPK (Dowling et al., 2007; Gwinn et al., 2008; Shaw et al., 2004; Tzatsos and Kandror, 2006). Given that adipose-specific knockout of mTORC1 increases insulin sensitivity and lowers blood glucose and cholesterol levels, metformin might also exert part of its therapeutic effect via activation of AMPK and inhibition of mTORC1 in adipose tissue. It is also interesting to note that rapamycin treatment in humans and rats prevents weight gain (Rovira et al., 2008). Our results suggest that this effect might also be mediated via inhibition of mTORC1 in adipose tissue.

raptor$^{ad-/-}$ mice are lean due to a reduction in the size and number of adipocytes. A previous study in 3T3-L1 cells demonstrated that rapamycin blocks adipogenesis via inhibition of the key adipogenic transcription factor PPARγ (Kim and Chen, 2004). Kim and Chen (2004) also reported that rapamycin strongly inhibits PPARγ activity in differentiated 3T3-L1 and that incubation of differentiated 3T3-L1 with rapamycin induces loss of fat. Our results in 3T3-L1 cells support these findings (Figures 1 and 6D). However, surprisingly, *raptor*$^{ad-/-}$ mice are lean despite the absence of an effect on expression of PPARγ and PPARγ targets (Figure 6E, unpublished for PPARγ protein level). Thus, in animals, there must be a mechanism(s) in addition to mTORC1 signaling that maintains PPARγ. It remains to be determined what this mechanism might be. mTORC1-deficient mice lose fat due to increased *UCP1* expression leading to enhanced energy expenditure and not due to a PPARγ deficiency. Rapamycin treatment of differentiated 3T3-L1 cells did not lead to increased *UCP1* expression (data not shown), suggesting that the effect of *raptor* knockout on *UCP1* expression might not be cell autonomous.

Close examination of the weight curves shows that *raptor*$^{ad-/-}$ mice reached a maximal weight of ~30 g, regardless of being on a chow or high-fat diet (Figure 3A). This weight was reached at a slow, constant rate on the chow diet or very rapidly on the high-fat diet. This observed maximal weight suggests that there is a limit to the amount of fat that *raptor*$^{ad-/-}$ mice can accumulate. This is also supported by the findings that the size of individual adipocytes did not increase upon HFD and that the number of adipocytes was reduced in *raptor*$^{ad-/-}$ mice on both the chow and high-fat diet (Figure 3E). The reason for such a fixed limit on the amount of fat that *raptor*$^{ad-/-}$ mice can accumulate is unknown.

In conclusion, mTORC1 in adipose tissue regulates whole-body metabolism and energy homeostasis. Inhibition of mTORC1 results in metabolically healthier mice, with no apparent adverse effects. Thus, adipose mTORC1 is a potential target for antiobesity and antidiabetes drugs.

Cell Metabolism
Adipose mTORC1 Controls Energy Homeostasis

EXPERIMENTAL PROCEDURES

Materials

Adenoviruses encoding RNAi against raptor were created by cloning the previously described RNAi sequence and H1 promoter (Jacinto et al., 2004) from pSuper into pAd-DEST (Invitrogen). Empty pAd-DEST vector was used as control. For raptor knockdown, differentiated or undifferentiated 3T3-L1 were incubated with viruses for 2 days. Antibodies for raptor were from Bethyl. Antibodies for actin were from Chemicon. Antibodies for Akt, Akt pT308, Akt pS473, IRS1, AMPK, and AMPK pT172 were from Cell Signaling. Rapamycin was from LC Laboratories and was used at a concentration of 100 nM. Isoproterenol was from Sigma and was used at a concentration of 10 μM. Insulin, dexamethasone, and IBMX were from Sigma.

Supplemental Experimental Procedures can be found in the Supplemental Data available online.

SUPPLEMENTAL DATA

The Supplemental Data for this article include Supplemental Experimental Procedures and can be found with this article at http://www.cellmetabolism.org/S1550-4131(08)00287-8.

ACKNOWLEDGMENTS

We thank K. Beier and I. Ginez for assistance with histological analysis; T. Harach for assistance with the glucose tolerance test; A. Hein and P. Demougin for help with qPCR; J. Zoll, A.L. Lang, and B. Geny for valuable discussions and technical assistance with Clark electrode measurements; A. Löschmann for technical assistance with genotyping and histology; and T. Sorg, X. Warot, and M.F. Champy for contributions to generation and phenotyping of knockout mice. We thank K. Thomas and members of the Hall, Rüegg, and Auwerx groups for helpful discussions. We acknowledge support from the Roche Research Foundation (P.P.), FEBS (J.N.F.), and the Swiss National Science Foundation and the Canton of Basel (M.A.R. and M.N.H.). We declare that no competing interests exist.

Received: May 8, 2008
Revised: August 4, 2008
Accepted: September 9, 2008
Published: November 4, 2008

REFERENCES

Aguilar, V., Alliouachene, S., Sotiropoulos, A., Sobering, A., Athea, Y., Djouadi, F., Miraux, S., Thiaudiere, E., Foretz, M., Viollet, B., et al. (2007). S6 kinase deletion suppresses muscle growth adaptations to nutrient availability by activating AMP kinase. Cell Metab. *5*, 476–487.

Bell, A., Grunder, L., and Sorisky, A. (2000). Rapamycin inhibits human adipocyte differentiation in primary culture. Obes. Res. *8*, 249–254.

Bentzinger, C.F., Romanino, K., Cloetta, D., Lin, S., Mascarenhas, J.B., Oliveri, F., Xia, J., Casanova, E., Costa, C.F., Brink, M., Zorzato, F., Hall, M.N., and Ruegg, M.A. (2008). Skeletal muscle-specific ablation of raptor, but not of rictor, causes metabolic changes and results in muscle dystrophy. Cell Metabolism *8*, this issue, 411–424.

Beretta, L., Gingras, A.C., Svitkin, Y.V., Hall, M.N., and Sonenberg, N. (1996). Rapamycin blocks the phosphorylation of 4E–BP1 and inhibits cap-dependent initiation of translation. EMBO J. *15*, 658–664.

Bishop, N.A., and Guarente, L. (2007). Genetic links between diet and lifespan: shared mechanisms from yeast to humans. Nat. Rev. Genet. *8*, 835–844.

Bonawitz, N.D., Chatenay-Lapointe, M., Pan, Y., and Shadel, G.S. (2007). Reduced TOR signaling extends chronological life span via increased respiration and upregulation of mitochondrial gene expression. Cell Metab. *5*, 265–277.

Brand, M.D., and Esteves, T.C. (2005). Physiological functions of the mitochondrial uncoupling proteins UCP2 and UCP3. Cell Metab. *2*, 85–93.

Brunn, G.J., Hudson, C.C., Sekuli, A., Williams, J.M., Hosoi, H., Houghton, P.J., Lawrence, J.C., Jr., and Abraham, R.T. (1997). Phosphorylation of the translational repressor PHAS-I by the mammalian target of rapamycin. Science *277*, 99–101.

Burnett, P.E., Barrow, R.K., Cohen, N.A., Snyder, S.H., and Sabatini, D.M. (1998). RAFT1 phosphorylation of the translational regulators p70 S6 kinase and 4E–BP1. Proc. Natl. Acad. Sci. USA *95*, 1432–1437.

Cederberg, A., Gronning, L.M., Ahren, B., Tasken, K., Carlsson, P., and Enerback, S. (2001). FOXC2 is a winged helix gene that counteracts obesity, hypertriglyceridemia, and diet-induced insulin resistance. Cell *106*, 563–573.

Cho, H.J., Park, J., Lee, H.W., Lee, Y.S., and Kim, J.B. (2004). Regulation of adipocyte differentiation and insulin action with rapamycin. Biochem. Biophys. Res. Commun. *321*, 942–948.

Christian, M., Kiskinis, E., Debevec, D., Leonardsson, G., White, R., and Parker, M.G. (2005). RIP140-targeted repression of gene expression in adipocytes. Mol. Cell. Biol. *25*, 9383–9391.

Considine, R.V., Sinha, M.K., Heiman, M.L., Kriauciunas, A., Stephens, T.W., Nyce, M.R., Ohannesian, J.P., Marco, C.C., McKee, L.J., Bauer, T.L., and Caro, J.F. (1996). Serum immunoreactive-leptin concentrations in normal-weight and obese humans. N. Engl. J. Med. *334*, 292–295.

Corradetti, M.N., and Guan, K.L. (2006). Upstream of the mammalian target of rapamycin: do all roads pass through mTOR? Oncogene *25*, 6347–6360.

Cunningham, J.T., Rodgers, J.T., Arlow, D.H., Vazquez, F., Mootha, V.K., and Puigserver, P. (2007). mTOR controls mitochondrial oxidative function through a YY1-PGC-1[agr] transcriptional complex. Nature *450*, 736–740.

Dowling, R.J.O., Zakikhani, M., Fantus, I.G., Pollak, M., and Sonenberg, N. (2007). Metformin inhibits mammalian target of rapamycin dependent translation initiation in breast cancer cells. Cancer Res. *67*, 10804–10812.

El-Chaar, D., Gagnon, A., and Sorisky, A. (2004). Inhibition of insulin signaling and adipogenesis by rapamycin: effect on phosphorylation of p70 S6 kinase vs eIF4E–BP1. Int. J. Obes. Relat. Metab. Disord. *28*, 191–198.

Frias, M.A., Thoreen, C.C., Jaffe, J.D., Schroder, W., Sculley, T., Carr, S.A., and Sabatini, D.M. (2006). mSin1 is necessary for Akt/PKB phosphorylation, and its isoforms define three distinct mTORC2s. Curr. Biol. *16*, 1865–1870.

Gagnon, A., Lau, S., and Sorisky, A. (2001). Rapamycin-sensitive phase of 3T3–L1 preadipocyte differentiation after clonal expansion. J. Cell. Physiol. *189*, 14–22.

Gimeno, R.E., and Klaman, L.D. (2005). Adipose tissue as an active endocrine organ: recent advances. Curr. Opin. Pharmacol. *5*, 122–128.

Guertin, D.A., and Sabatini, D.M. (2007). Defining the role of mTOR in cancer. Cancer Cell *12*, 9–22.

Guertin, D.A., Stevens, D.M., Thoreen, C.C., Burds, A.A., Kalaany, N.Y., Moffat, J., Brown, M., Fitzgerald, K.J., and Sabatini, D.M. (2006). Ablation in mice of the mTORC components raptor, rictor, or mLST8 reveals that mTORC2 is required for signaling to Akt-FOXO and PKC[alpha], but not S6K1. Dev. Cell *11*, 859–871.

Gwinn, D.M., Shackelford, D.B., Egan, D.F., Mihaylova, M.M., Mery, A., Vasquez, D.S., Turk, B.E., and Shaw, R.J. (2008). AMPK phosphorylation of raptor mediates a metabolic checkpoint. Mol. Cell *30*, 214–226.

Hansen, J.B., Jorgensen, C., Petersen, R.K., Hallenborg, P., De Matteis, R., Boye, H.A., Petrovic, N., Enerback, S., Nedergaard, J., Cinti, S., te Riele, H., and Kristiansen, K. (2004). Retinoblastoma protein functions as a molecular switch determining white versus brown adipocyte differentiation. Proc. Natl. Acad. Sci. USA. *101*, 4112–4117.

Hara, K., Maruki, Y., Long, X., Yoshino, K., Oshiro, N., Hidayat, S., Tokunaga, C., Avruch, J., and Yonezawa, K. (2002). Raptor, a binding partner of target of rapamycin (TOR), mediates TOR action. Cell *110*, 177–189.

Harrington, L.S., Findlay, G.M., Gray, A., Tolkacheva, T., Wigfield, S., Rebholz, H., Barnett, J., Leslie, N.R., Cheng, S., Shepherd, P.R., et al. (2004). The TSC1–2 tumor suppressor controls insulin-PI3K signaling via regulation of IRS proteins. J. Cell Biol. *166*, 213–223.

Hay, N., and Sonenberg, N. (2004). Upstream and downstream of mTOR. Genes Dev. *18*, 1926–1945.

He, W., Barak, Y., Hevener, A., Olson, P., Liao, D., Le, J., Nelson, M., Ong, E., Olefsky, J.M., and Evans, R.M. (2003). Adipose-specific peroxisome

Cell Metabolism
Adipose mTORC1 Controls Energy Homeostasis

proliferator-activated receptor {gamma} knockout causes insulin resistance in fat and liver but not in muscle. Proc. Natl. Acad. Sci. USA *100*, 15712–15717.

Jacinto, E., Loewith, R., Schmidt, A., Lin, S., Ruegg, M.A., Hall, A., and Hall, M.N. (2004). Mammalian TOR complex 2 controls the actin cytoskeleton and is rapamycin insensitive. Nat. Cell Biol. *6*, 1122–1128.

Jacinto, E., Facchinetti, V., Liu, D., Soto, N., Wei, S., Jung, S.Y., Huang, Q., Qin, J., and Su, B. (2006). SIN1/MIP1 maintains rictor-mTOR complex integrity and regulates Akt phosphorylation and substrate specificity. Cell *127*, 125–137.

Kaeberlein, M., and Powers, R.W., III. (2007). Sir2 and calorie restriction in yeast: A skeptical perspective. Ageing Res. Rev. *6*, 128–140.

Kaeberlein, M., Powers, R.W., III, Steffen, K.K., Westman, E.A., Hu, D., Dang, N., Kerr, E.O., Kirkland, K.T., Fields, S., and Kennedy, B.K. (2005). Regulation of yeast replicative life span by TOR and Sch9 in response to nutrients. Science *310*, 1193–1196.

Kapahi, P., Zid, B.M., Harper, T., Koslover, D., Sapin, V., and Benzer, S. (2004). Regulation of lifespan in *Drosophila* by modulation of genes in the TOR signaling pathway. Curr. Biol. *14*, 885–890.

Kershaw, E.E., and Flier, J.S. (2004). Adipose tissue as an endocrine organ. J. Clin. Endocrinol. Metab. *89*, 2548–2556.

Kim, J.E., and Chen, J. (2004). Regulation of peroxisome proliferator-activated receptor-gamma activity by mammalian target of rapamycin and amino acids in adipogenesis. Diabetes *53*, 2748–2756.

Kim, D.H., Sarbassov, D.D., Ali, S.M., King, J.E., Latek, R.R., Erdjument-Bromage, H., Tempst, P., and Sabatini, D.M. (2002). mTOR interacts with raptor to form a nutrient-sensitive complex that signals to the cell growth machinery. Cell *110*, 163–175.

Kim, D.H., Sarbassov, D.D., Ali, S.M., Latek, R.R., Guntur, K.V., Erdjument-Bromage, H., Tempst, P., and Sabatini, D.M. (2003). GbetaL, a positive regulator of the rapamycin-sensitive pathway required for the nutrient-sensitive interaction between raptor and mTOR. Mol. Cell *11*, 895–904.

Kiskinis, E., Hallberg, M., Christian, M., Olofsson, M., Dilworth, S.M., White, R., and Parker, M.G. (2007). RIP140 directs histone and DNA methylation to silence Ucp1 expression in white adipocytes. EMBO J. *26*, 4831–4840.

Krebs, M., Brunmair, B., Brehm, A., Artwohl, M., Szendroedi, J., Nowotny, P., Roth, E., Furnsinn, C., Promintzer, M., Anderwald, C., et al. (2007). The mammalian target of rapamycin pathway regulates nutrient-sensitive glucose uptake in man. Diabetes *56*, 1600–1607.

Kubota, N., Terauchi, Y., Miki, H., Tamemoto, H., Yamauchi, T., Komeda, K., Satoh, S., Nakano, R., Ishii, C., Sugiyama, T., et al. (1999). PPAR[gamma] mediates high-fat diet-induced adipocyte hypertrophy and insulin resistance. Mol. Cell *4*, 597–609.

Le Bacquer, O., Petroulakis, E., Paglialunga, S., Poulin, F., Richard, D., Cianflone, K., and Sonenberg, N. (2007). Elevated sensitivity to diet-induced obesity and insulin resistance in mice lacking 4E–BP1 and 4E–BP2. J. Clin. Invest. *117*, 387–396.

Lemonnier, D. (1972). Effect of age, sex, and sites on the cellularity of the adipose tissue in mice and rats rendered obese by a high-fat diet. J. Clin. Invest. *51*, 2907–2915.

Leonardsson, G., Steel, J.H., Christian, M., Pocock, V., Milligan, S., Bell, J., So, P.-W., Medina-Gomez, G., Vidal-Puig, A., White, R., and Parker, M.G. (2004). Nuclear receptor corepressor RIP140 regulates fat accumulation. Proc. Natl. Acad. Sci. USA *101*, 8437–8442.

Loewith, R., Jacinto, E., Wullschleger, S., Lorberg, A., Crespo, J.L., Bonenfant, D., Oppliger, W., Jenoe, P., and Hall, M.N. (2002). Two TOR complexes, only one of which is rapamycin sensitive, have distinct roles in cell growth control. Mol. Cell *10*, 457–468.

Nicholls, D.G. (2001). A history of UCP1. Biochem. Soc. Trans. *29*, 751–755.

Pende, M., Kozma, S.C., Jaquet, M., Oorschot, V., Burcelin, R., Le Marchand-Brustel, Y., Klumperman, J., Thorens, B., and Thomas, G. (2000). Hypoinsulinaemia, glucose intolerance and diminished [beta]-cell size in S6K1-deficient mice. Nature *408*, 994–997.

Powers, R.W., III, Kaeberlein, M., Caldwell, S.D., Kennedy, B.K., and Fields, S. (2006). Extension of chronological life span in yeast by decreased TOR pathway signaling. Genes Dev. *20*, 174–184.

Puigserver, P., Wu, Z., Park, C.W., Graves, R., Wright, M., and Spiegelman, B.M. (1998). A cold-inducible coactivator of nuclear receptors linked to adaptive thermogenesis. Cell *92*, 829–839.

Rovira, J., Marcelo Arellano, E., Burke, J.T., Brault, Y., Moya-Rull, D., Banon-Maneus, E., Ramirez-Bajo, M.J., Gutierrez-Dalmau, A., Revuelta, I., Quintana, L.F., et al. (2008). Effect of mTOR inhibitor on body weight: from an experimental rat model to human transplant patients. Transpl. Int. *21*, 992–998.

Sarbassov, D.D., Ali, S.M., Kim, D.H., Guertin, D.A., Latek, R.R., Erdjument-Bromage, H., Tempst, P., and Sabatini, D.M. (2004). Rictor, a novel binding partner of mTOR, defines a rapamycin-insensitive and raptor-independent pathway that regulates the cytoskeleton. Curr. Biol. *14*, 1296–1302.

Sarbassov, D.D., Ali, S.M., Sengupta, S., Sheen, J.H., Hsu, P.P., Bagley, A.F., Markhard, A.L., and Sabatini, D.M. (2006). Prolonged rapamycin treatment inhibits mTORC2 assembly and Akt/PKB. Mol. Cell *22*, 159–168.

Schieke, S.M., Phillips, D., McCoy, J.P., Jr., Aponte, A.M., Shen, R.F., Balaban, R.S., and Finkel, T. (2006). The mammalian target of rapamycin (mTOR) pathway regulates mitochondrial oxygen consumption and oxidative capacity. J. Biol. Chem. *281*, 27643–27652.

Scime, A., Grenier, G., Huh, M.S., Gillespie, M.A., Bevilacqua, L., Harper, M.-E., and Rudnicki, M.A. (2005). Rb and p107 regulate preadipocyte differentiation into white versus brown fat through repression of PGC-1. Cell Metab. *2*, 283–295.

Seale, P., Kajimura, S., Yang, W., Chin, S., Rohas, L.M., Uldry, M., Tavernier, G., Langin, D., and Spiegelman, B.M. (2007). Transcriptional control of brown fat determination by PRDM16. Cell Metab. *6*, 38–54.

Shah, O.J., Wang, Z., and Hunter, T. (2004). Inappropriate activation of the TSC/Rheb/mTOR/S6K cassette induces IRS1/2 depletion, insulin resistance, and cell survival deficiencies. Curr. Biol. *14*, 1650–1656.

Shaw, R.J., Bardeesy, N., Manning, B.D., Lopez, L., Kosmatka, M., DePinho, R.A., and Cantley, L.C. (2004). The LKB1 tumor suppressor negatively regulates mTOR signaling. Cancer Cell *6*, 91–99.

Shaw, R.J., Lamia, K.A., Vasquez, D., Koo, S.-H., Bardeesy, N., DePinho, R.A., Montminy, M., and Cantley, L.C. (2005). The kinase LKB1 mediates glucose homeostasis in liver and therapeutic effects of metformin. Science *310*, 1642–1646.

Shi, Y., and Burn, P. (2004). Lipid metabolic enzymes: emerging drug targets for the treatment of obesity. Nat. Rev. Drug Discov. *3*, 695–710.

Tontonoz, P., Hu, E., and Spiegelman, B.M. (1994). Stimulation of adipogenesis in fibroblasts by PPAR[gamma]2, a lipid-activated transcription factor. Cell *79*, 1147–1156.

Tzatsos, A., and Kandror, K.V. (2006). Nutrients suppress phosphatidylinositol 3-kinase/Akt signaling via raptor-dependent mTOR-mediated insulin receptor substrate 1 phosphorylation. Mol. Cell. Biol. *26*, 63–76.

Ueno, M., Carvalheira, J.B., Tambascia, R.C., Bezerra, R.M., Amaral, M.E., Carneiro, E.M., Folli, F., Franchini, K.G., and Saad, M.J. (2005). Regulation of insulin signalling by hyperinsulinaemia: role of IRS-1/2 serine phosphorylation and the mTOR/p70 S6K pathway. Diabetologia *48*, 506–518.

Um, S.H., Frigerio, F., Watanabe, M., Picard, F., Joaquin, M., Sticker, M., Fumagalli, S., Allegrini, P.R., Kozma, S.C., Auwerx, J., and Thomas, G. (2004). Absence of S6K1 protects against age- and diet-induced obesity while enhancing insulin sensitivity. Nature *431*, 200–205.

Vander Haar, E., Lee, S.I., Bandhakavi, S., Griffin, T.J., and Kim, D.H. (2007). Insulin signalling to mTOR mediated by the Akt/PKB substrate PRAS40. Nat. Cell Biol. *9*, 316–323.

Vellai, T., Takacs-Vellai, K., Zhang, Y., Kovacs, A.L., Orosz, L., and Muller, F. (2003). Genetics: Influence of TOR kinase on lifespan in C. elegans. Nature *426*, 620.

Weisberg, S.P., McCann, D., Desai, M., Rosenbaum, M., Leibel, R.L., and Ferrante, A.W., Jr. (2003). Obesity is associated with macrophage accumulation in adipose tissue. J. Clin. Invest. *112*, 1796–1808.

Weisberg, S.P., Hunter, D., Huber, R., Lemieux, J., Slaymaker, S., Vaddi, K., Charo, I., Leibel, R.L., and Ferrante, A.W., Jr. (2006). CCR2 modulates inflammatory and metabolic effects of high-fat feeding. J. Clin. Invest. *116*, 115–124.

Wullschleger, S., Loewith, R., and Hall, M.N. (2006). TOR signaling in growth and metabolism. Cell *124*, 471–484.

Xu, H., Barnes, G.T., Yang, Q., Tan, G., Yang, D., Chou, C.J., Sole, J., Nichols, A., Ross, J.S., Tartaglia, L.A., and Chen, H. (2003). Chronic inflammation in fat plays a crucial role in the development of obesity-related insulin resistance. J. Clin. Invest. *112*, 1821–1830.

Yang, Q., Inoki, K., Ikenoue, T., and Guan, K.-L. (2006). Identification of Sin1 as an essential TORC2 component required for complex formation and kinase activity. Genes Dev. *20*, 2820–2832.

Yeh, W.C., Bierer, B.E., and McKnight, S.L. (1995). Rapamycin inhibits clonal expansion and adipogenic differentiation of 3T3–L1 cells. Proc. Natl. Acad. Sci. USA *92*, 11086–11090.

Acknowledgements

First of all, I am especially grateful to Mike Hall for giving me the opportunity to follow my PhD study in his lab as well as for his continuous support. Thank you for the interesting project and also for the challenge of doing mouse work in a yeast lab! I learnt a lot and hope that the work we established in the lab will be carried on in the future with the same excitement.

I am thankful to all present and past lab members who always provided an enjoyable and supportive atmosphere and were always available for helpful suggestions and discussions.

Special thanks go to Pazit Polak for our successful collaborations during the time we in this lab. I think we did a very good job in establishing the mouse research in the lab and it was definitely the result of a great teamwork. I enjoyed sharing the same office with you and being surrounded by your friendly craziness.

Thank you, Andrea Löschmann, for the great support in the mouse work and all the orders you had to do for me.

My thanks also go to Vittoria Zinzalla for the great collaboration and the good time I spent with you during the Cappuchino sessions, lunch breaks, or evening dinners while discussing science and other interesting topics.

I am also thankful to Wolfgang Oppliger. Whenever I needed help I knew I could ask you. I enjoyed the nice chats with you in swiss-german and the good times outside the lab when running in the Allschwiler surroundings.

Many thanks also go to Markus Rüegg for taking part in my thesis committee.

Furthermore, I would like to thank Prof. Konstantin Beier and Isabelle Ginez from the Anatomy Department for initially introducing us into histology and for allowing us to continuously use their microtome. Thanks to Taufiq Harach for showing for the first time how to inject and dissect mice. I am also thankful to Markus Rüegg and members of his lab, in particular Florian Bentzinger and Dimitri Clöetta, for helpful discussions and technical help with the mice. Further thanks go to Andreas Hein and Philippe Demougin for help with qPCRs. I am grateful for the helpful discussions with Johan Auwerx and members of his lab, in particular Marie Lagouge, who also provided great technical help. Many thanks also go to Renato Zedi and his team from the animal facility for excellent mouse husbandry.

I also want to thank the members from the Spang lab. I always enjoyed the times we spent together outside of the Biozentrum without having to discuss science. Thank you Melle, for the great friendship we could build up during the easy and difficult times of our PhDs.

Of course, I also want to thank all my friends from the outside world beyond the Biozentrum buildings. For all the great friendships and nice moments I could enjoy with you.

All my deep thanks go to my family. To my parents; you have supported me throughout my life, never doubted in my goals and always allowed and motivated me to follow my dreams. Thanks for all your love!

My very personal thanks go to Sven. For your patience, support, and motivation during my PhD and beyond – I could always count on you. But especially for being a wonderful part of my life. Simply for love!